

**Mechanisms of epithelial-to-mesenchymal transition in  
experimental and idiopathic pulmonary fibrosis**

Inaugural Dissertation  
submitted to the  
Faculty of Medicine  
in partial fulfillment of the requirements  
for the PhD-Degree  
of the Faculties of Veterinary Medicine and Medicine  
of the Justus Liebig University Giessen

by  
Jayachandran, Aparna  
of  
Kerala, India

Giessen 2008

From the Department of Medicine  
Director/Chairman: Prof. Dr. Werner Seeger  
of the Faculty of Medicine of the Justus Liebig University Giessen

First Supervisor and Committee Member: Prof. Dr. Oliver Eickelberg  
Second Supervisor and Committee Member: Prof. Dr. Erwin Bottinger  
Committee Members: Prof. Dr. Wolfgang Kummer  
Prof. Dr. Martin Bergmann

Date of Doctoral Defense: February 9<sup>th</sup>, 2009

# I Table of contents

<b>I</b>	<b>TABLE OF CONTENTS</b> .....	<b>I</b>
<b>II</b>	<b>LIST OF FIGURES</b> .....	<b>VI</b>
<b>III</b>	<b>LIST OF TABLES</b> .....	<b>VIII</b>
<b>IV</b>	<b>LIST OF ABBREVIATIONS</b> .....	<b>IX</b>
<b>V</b>	<b>SUMMARY</b> .....	<b>XII</b>
<b>VI</b>	<b>ZUSAMMENFASSUNG</b> .....	<b>XIV</b>
<b>1</b>	<b>INTRODUCTION</b> .....	<b>1</b>
<b>1.1</b>	<b>Idiopathic pulmonary fibrosis</b> .....	<b>1</b>
1.1.1	Characteristics of idiopathic pulmonary fibrosis.....	1
1.1.2	Histopathological changes in idiopathic pulmonary fibrosis.....	2
1.1.3	Pathogenesis of idiopathic pulmonary fibrosis.....	3
1.1.3.1	The inflammation fibrosis theory.....	3
1.1.3.2	Abnormal wound healing theory.....	4
1.1.4	Key effector cells in idiopathic pulmonary fibrosis.....	5
1.1.4.1	Alveolar epithelial cells in idiopathic pulmonary fibrosis.....	5
1.1.4.2	Fibroblasts in idiopathic pulmonary fibrosis.....	6
<b>1.2</b>	<b>Epithelial-to-mesenchymal transition</b> .....	<b>8</b>
1.2.1	Characteristics of epithelial and mesenchymal cells.....	8
1.2.2	Key cellular events during EMT.....	9
1.2.3	Role of EMT in embryos.....	10
1.2.4	Role of EMT in adults.....	10
1.2.4.1	EMT in wound healing.....	10
1.2.4.2	EMT in cancer.....	11
1.2.4.3	EMT in fibrosis.....	11

---

1.2.4.4 EMT in idiopathic pulmonary fibrosis .....	12
1.2.5 Inducers of EMT .....	13
1.2.5.1 TGF- $\beta$ is a major inducer of EMT .....	13
1.2.5.2 Sensing and propagating TGF- $\beta$ signals .....	14
1.2.5.3 Smad proteins .....	15
1.2.5.4 Role of TGF- $\beta$ in idiopathic pulmonary fibrosis .....	16
1.2.6 Transcriptional control of EMT .....	16
1.2.6.1 Role of SNAI in EMT .....	16
<b>2 AIMS OF THE STUDY .....</b>	<b>20</b>
<b>3 MATERIALS AND METHODS .....</b>	<b>21</b>
<b>3.1 Materials .....</b>	<b>21</b>
3.1.1 Equipment .....	21
3.1.2 Reagents .....	22
<b>3.2 Animal Tissues .....</b>	<b>25</b>
<b>3.3 Human Tissues .....</b>	<b>25</b>
<b>3.4 Methods .....</b>	<b>25</b>
3.4.1 Mammalian cell culture .....	25
3.4.1.1 A549 cells .....	25
3.4.1.2 Isolation of alveolar epithelial type II (AT2) cells .....	26
3.4.2 RNA isolation .....	27
3.4.2.1 RNA isolation from cultured cells .....	28
3.4.2.2 RNA isolation from lung homogenates .....	28
3.4.3 Determining RNA and DNA concentration .....	28
3.4.4 Reverse transcription reaction .....	28
3.4.5 Polymerase chain reaction .....	29
3.4.5.1 Semi-quantitative PCR .....	29
3.4.5.2 Real-time PCR .....	30
3.4.6 Protein isolation .....	32
3.4.6.1 Protein isolation from cell culture .....	32
3.4.6.2 Protein isolation from tissue .....	32
3.4.7 Gel electrophoresis .....	33

---

3.4.7.1 DNA gel electrophoresis .....	33
3.4.7.2 Protein gel electrophoresis .....	33
3.4.8 Western blot analysis .....	34
3.4.8.1 Western blotting .....	35
3.4.8.2 Protein visualization .....	35
3.4.9 Immunohistochemistry .....	36
3.4.10 Immunofluorescence .....	36
3.4.11 Laser-assisted microdissection .....	37
3.4.12 Cloning and transfection of human SNAI1 and SNAI2 .....	37
3.4.12.1 PCR product purification .....	37
3.4.12.2 Ligation of PCR products into pGEM-T Easy vector .....	37
3.4.12.3 Transformation and amplification of plasmids .....	38
3.4.12.4 Subcloning into mammalian expression vectors .....	38
3.4.12.5 Transfection of A549 cells .....	39
3.4.13 siRNA transfection .....	39
3.4.14 Migration assay .....	39
3.4.15 Experimental model of idiopathic pulmonary fibrosis .....	40
3.4.16 Experimental model of renal fibrosis .....	40
3.4.17 Statistical analysis of data .....	41
<b>4 RESULTS .....</b>	<b>42</b>
<b>4.1 Analysis of EMT <i>in vitro</i> .....</b>	<b>42</b>
4.1.1 Estimation of the purity of primary mouse AT2 cells .....	42
4.1.2 Expression of TGF- $\beta$ 1 signaling components in primary mouse AT2 cells .....	43
4.1.3 EMT marker localization in primary mouse AT2 cells .....	44
4.1.4 Mesenchymal marker expression in primary mouse AT2 cells .....	45
4.1.5 EMT marker gene expression in primary mouse AT2 cells .....	46
4.1.6 EMT marker gene expression in the human A549 cell line .....	47
4.1.7 SNAI1 and SNAI2 protein localization in A549 and primary mouse AT2 cells .....	48
<b>4.2 Analysis of EMT marker expression in an experimental model of pulmonary fibrosis .....</b>	<b>49</b>
4.2.1 EMT marker expression in bleomycin-induced pulmonary fibrosis .....	49
4.2.2 EMT marker expression in AT2 cells of bleomycin-treated mice .....	51
4.2.3 SNAI protein localization in lungs of bleomycin treated mice .....	52
<b>4.3 Analysis of EMT marker expression in lungs of patients with idiopathic pulmonary fibrosis .....</b>	<b>53</b>

---

4.3.1 Expression of EMT markers in idiopathic pulmonary fibrosis .....	53
4.3.2 SNAI gene expression in the lungs of patients with idiopathic pulmonary fibrosis .....	54
4.3.3 SNAI protein localization in lungs of patients with idiopathic pulmonary fibrosis .....	55
<b>4.4 Functional studies in A549 cells.....</b>	<b>56</b>
4.4.1 Effect of ectopically-expressed human SNAI1 on EMT marker gene expression in A549 cells.....	56
4.4.2 Effect of ectopically-expressed human SNAI2 on EMT marker gene expression in A549 cells.....	57
4.4.3 siRNA-mediated downregulation of SNAI1 and SNAI2 .....	59
4.4.4 Effect of siRNA-mediated downregulation of SNAI1 on EMT marker gene expression in A549 cells.....	60
4.4.5 Effect of siRNA-mediated downregulation of SNAI2 on EMT marker gene expression in A549 cells.....	61
4.4.6 Role of SNAI1 and SNAI2 in TGF- $\beta$ 1-induced cell migration .....	63
<b>4.5 Analysis of EMT in unilateral ureteral obstruction model of renal fibrosis .....</b>	<b>63</b>
4.5.1 EMT marker expression in a unilateral ureteral model of renal fibrosis.....	63
<b>5 DISCUSSION.....</b>	<b>66</b>
<b>5.1 Assessment of EMT in alveolar epithelial cells .....</b>	<b>66</b>
5.1.1 TGF- $\beta$ 1 as a potent inducer of EMT.....	66
5.1.2 Implication of SNAI in EMT of alveolar epithelial cells.....	67
5.1.2.1 Processes regulating SNAI nuclear localization.....	67
5.1.2.2 SNAI transcription factors in TGF- $\beta$ 1-induced EMT .....	68
<b>5.2 Evidence of EMT in bleomycin mouse model of pulmonary fibrosis.....</b>	<b>69</b>
<b>5.2.1 Implication of SNAI in bleomycin-induced lung fibrosis .....</b>	<b>70</b>
<b>5.3 Assessment of EMT marker expression in idiopathic pulmonary fibrosis .....</b>	<b>70</b>
5.3.1 Implication of SNAI in idiopathic pulmonary fibrosis .....	72
<b>5.4 Analysis of SNAI mediated transcriptional control of EMT in alveolar epithelial cells.....</b>	<b>73</b>
<b>5.5 EMT in a unilateral ureteral obstruction model of renal fibrosis .....</b>	<b>74</b>
<b>5.6 Conclusions and future perspectives .....</b>	<b>75</b>
<b>6 APPENDIX .....</b>	<b>77</b>

---

Table 6.1 Human RT-PCR primers.....	77
Table 6.2 Mouse RT-PCR primers.....	77
Table 6.3 Human real-time RT-PCR primers .....	78
Table 6.4 Mouse real-time RT-PCR primers .....	79
Table 6.5 Human siRNA sequences.....	79
Table 6.6 Primary antibodies used for western blotting (WB), immunohistochemistry (IHC) and immunofluorescence (IF).....	80
Table 6.7 Secondary antibodies used for western blotting, immunohistochemistry and immunofluorescence .....	80
<b>7 REFERENCES .....</b>	<b>82</b>
<b>8 DECLARATION .....</b>	<b>92</b>
<b>9 CURRICULUM VITAE.....</b>	<b>93</b>
<b>10 ACKNOWLEDGEMENTS.....</b>	<b>98</b>

---

## II List of figures

- Figure 1.1 Histopathological changes observed in IPF
- Figure 1.2 Hypothetical scheme of the main pathogenic events in IPF
- Figure 1.3 Alveolar epithelial transdifferentiation pathways
- Figure 1.4 Sources of myofibroblasts in IPF
- Figure 1.5 Morphological changes during EMT
- Figure 1.6 EMT in development and disease
- Figure 1.7 Schematic diagram of the TGF- $\beta$  signaling pathway from the cell membrane to the nucleus
- Figure 1.8 Comparative scheme of the main structural domains found in mammalian SNAI1 and SNAI2
- Figure 1.9 SNAI genes occupy a central position in triggering EMT in physiological and pathological situations
- Figure 4.1 Purity of primary alveolar epithelial type II (AT2) cells
- Figure 4.2 Expression of TGF- $\beta$ 1 signaling components in AT2 cells
- Figure 4.3 EMT marker localization and expression in primary AT2 cells
- Figure 4.4 Expression of mesenchymal marker  $\alpha$ -SMA in AT2 cells
- Figure 4.5 EMT marker gene expression in primary AT2 cells
- Figure 4.6 EMT marker gene expression in A549 cells
- Figure 4.7 SNAI localization in A549 and mouse AT2 cells
- Figure 4.8 Expression of EMT markers in total lung homogenates from bleomycin treated mice
- Figure 4.9 Expression of EMT markers in AT2 cells from the lungs of bleomycin treated mice
- Figure 4.10 Localization of SNAI in the lungs of bleomycin treated mice
- Figure 4.11 Expression of EMT markers in IPF
- Figure 4.12 Expression of SNAI genes in IPF
- Figure 4.13 Expression of SNAI protein in IPF



- 
- Figure 4.14 Effect of SNAI1 overexpression on EMT in A549 cells
- Figure 4.15 Effect of SNAI2 overexpression on EMT in A549 cells
- Figure 4.16 siRNA-mediated downregulation of SNAI1 and SNAI2 expression in A549 cells
- Figure 4.17 Effect of siRNA-mediated downregulation of SNAI1 expression on TGF- $\beta$ -mediated EMT
- Figure 4.18 Effect of siRNA-mediated downregulation of SNAI2 expression on TGF- $\beta$ -mediated EMT
- Figure 4.19 Effect of SNAI1 and SNAI2 on TGF- $\beta$ -induced cell migration
- Figure 4.20 Effect of BX471 on UUO-induced EMT marker expression

---

### III List of tables

Table 3.1	RT reaction master mix
Table 3.2	PCR reaction master mix
Table 3.3	PCR program
Table 3.4	Real-time PCR master mix
Table 3.5	Real-time PCR program
Table 3.6	Ligation mix
Table 6.1	Human semi-quantitative RT-PCR primers
Table 6.2	Mouse semi-quantitative RT-PCR primers
Table 6.3	Human real-time RT-PCR primers
Table 6.4	Mouse real-time RT-PCR primers
Table 6.5	siRNA sequences
Table 6.6	Primary antibodies used for western blotting (WB), immunohistochemistry (IHC) and immunofluorescence (IF)
Table 6.7	Secondary antibodies used for western blotting, immunohistochemistry and immunofluorescence

---

## IV List of abbreviations

ActR	Activin receptor
AEC	Alveolar epithelial cell
ALK	Activin receptor-like kinase
AMH	Anti-Müllerian hormone
ANOVA	Analysis of variance
APS	Ammonium persulfate
AT1	Alveolar type I
AT2	Alveolar type II
ATS	American Thoracic Society
BAL	Bronchoalveolar lavage
BMP	Bone morphogenetic protein
BMPR	Bone morphogenetic protein receptor
BSA	Bovine serum albumin
cDNA	Complementary deoxyribonucleic acid
CFA	Cystic fibrosing alveolitis
DAPI	4'6-Diamidino-2-phenylindole
DEPC	Diethylpyrocarbonate
DNA	Deoxyribonucleic acid
dNTP	Deoxynucleotide triphosphate
DMSO	Dimethyl sulfoxide
DTT	Dithiothreitol
ECM	Extracellular matrix
EDTA	Ethylendinitrilo-N, N, N', N', -tetra-acetic-acid
EGF	Epidermal growth factor
EMT	Epithelial-to-mesenchymal transition
ERK	Extracellular signal regulated kinase
FCS	Fetal calf serum

---

FGF	Fibroblast growth factor
FITC	Fluorescein isothiocyanate
GAPDH	Glyceraldehyde-3-phosphate dehydrogenase
Gfi	Growth factor independence protein
GS box	Glycine Serine box
HEPES	2-(4-(2-hydroxyethyl)-piperazinyl)-1-ethansulfonate
HRCT	High resolution computed tomography
HRP	Horse-radish peroxidase
IF	Immunofluorescence
IHC	Immunohistochemistry
IIP	Idiopathic interstitial pneumonia
IPF	Idiopathic pulmonary fibrosis
JNK	Jun N-terminal kinase
MAPK	Mitogen-activated protein kinase
MET	Mesenchymal-to-epithelial transition
MH	Mad homology
NES	Nuclear export signal
PAGE	Polyacrylamide gel electrophoresis
PBGD	Porphobilinogen deaminase
PBS	Phosphate-buffered saline
PCR	Polymerase chain reaction
PDGF	Platelet-derived growth factor
PI3K	Phosphoinositide 3-kinases
Pp2A	protein phosphatase 2A
ProSP-C	Pro-surfactant protein C
PVDF	Polyvinylidene difluoride
RNA	Ribonucleic acid
rpm	revolutions per minute
RT-PCR	Reverse transcriptase PCR
SD	Standard deviation
SDS	Sodium dodecyl sulfate

---

SDS-PAGE	SDS Polyacrylamide gel electrophoresis
SEM	Standard error of the mean
siRNA	Silencing RNA
SMA	Smooth muscle actin
SNAI	Snail
SNAI1	Snail homolog 1
SNAI2	Snail homolog 2
TAE	Tris-acetate-EDTA
T $\beta$ R	TGF- $\beta$ receptor
TEMED	<i>N,N,N',N'</i> -tetramethyl-ethane-1,2-diamine
TGF	Transforming growth factor
Tjp1	Tight junction protein 1
TNF- $\alpha$	Tumor necrosis factor- $\alpha$
UIP	Usual interstitial pneumonia
UO	Unilateral ureteral obstruction
WB	Western blotting

## V Summary

Idiopathic pulmonary fibrosis (IPF) is a fatal interstitial lung disease characterized by accumulation of activated myofibroblasts and excessive extracellular matrix deposition, in part mediated through enhanced TGF- $\beta$  signaling. TGF- $\beta$ 1 is a potent inducer of epithelial-to-mesenchymal transition (EMT), the reversible phenotypic switching of epithelial to fibroblast-like cells. Recently, EMT has been demonstrated in alveolar epithelial cells (AECs) and has been proposed as a causative factor in lung fibrosis, but its precise mediators and mechanisms in IPF remains to be resolved. During developmental and disease settings, the phenotypic conversion of the epithelium is under tight transcriptional control, however, the transcription factors eliciting EMT in IPF have yet to be identified. Putative roles for SNAI transcription factors as regulators of EMT during development and a wide variety of diseases including cancer and organ fibrosis have been documented.

This study is based on the hypothesis that in AECs, TGF- $\beta$ 1-induced SNAI transcription factors facilitate the acquisition of new morphology and motility, based on their ability to influence EMT marker gene expression. Thus, the objective of this study was to analyze the molecular mediators of TGF- $\beta$ 1-induced EMT *in vitro*, in human A549 and primary mouse AT2 cells, and to assess their contribution to the development of fibrosis in experimental and idiopathic pulmonary fibrosis *in vivo*.

Immunofluorescent costaining of Tjp1 and  $\alpha$ -SMA (an epithelial and mesenchymal marker, respectively) demonstrated TGF- $\beta$ 1-induced EMT in AECs. Furthermore, *in vitro*, TGF- $\beta$ 1 treatment increased the expression and nuclear accumulation of the zinc finger transcription factors SNAI1 (Snail) and SNAI2 (Slug), as assessed by RT-PCR and immunofluorescence. Ectopic expression of SNAI1 and SNAI2 proteins was sufficient to induce EMT in A549 cells, even in the absence of TGF- $\beta$ 1 stimulation. In contrast, the siRNA-mediated depletion of SNAI1 and SNAI2 attenuated TGF- $\beta$ 1-induced AEC migration and EMT in A549 cells. The detection of EMT *in vitro*, with an increase in SNAI transcription factors was substantiated *in vivo* in the bleomycin model of pulmonary fibrosis early in disease. *In vivo*, SNAI expression was elevated in

---

primary AECs isolated from fibrotic lungs, seven days after bleomycin challenge. An indication of occurrence of EMT with an increase in SNAI transcription factors was also corroborated in IPF patient lungs compared to control lungs. Furthermore, the occurrence of EMT, as well as the involvement of transcriptional control of SNAI factors was clarified in a unilateral ureteral obstruction (UUO) mouse model of renal fibrosis.

This study shows that (1) TGF- $\beta$ 1-induced EMT in alveolar epithelial cells is accompanied by elevated expression of SNAI transcription factors, (2) EMT in AECs is essentially controlled by SNAI transcription factors, as ectopic expression of SNAI1 and SNAI2 triggers EMT, whereas depletion of these factors abrogates TGF- $\beta$ 1-induced EMT, (3) increased expression of these zinc finger transcription factors are detected in an experimental model of lung fibrosis, with indication of the occurrence of EMT, (4) SNAI1 and SNAI2 upregulation have important implications for the development of IPF, (5) the detection of SNAI transcription factors early in EMT in a UUO model of renal fibrosis and the inhibition of EMT by leukocyte blocker treatment further emphasizes the significance of SNAI transcription factors in EMT as a causal factor in disease. Thus, reversal and/or inhibition of EMT may present a valid therapeutic option in lung fibrosis.

## VI Zusammenfassung

Die idiopathische pulmonale Fibrose (IPF) ist eine fatale interstitielle Lungenerkrankung, die durch Ansammlung von aktivierten Myofibroblasten und verstärkter extrazellulärer Matrixbildung gekennzeichnet ist. An diesem Vorgang ist der TGF- $\beta$  Signalweg beteiligt. Zudem induziert TGF- $\beta$ 1 die epitheliale-mesenchymale Transition (EMT), die reversible phänotypische Umwandlung von epithelialen zu fibroblasten-ähnlichen Zellen. Kürzlich konnte EMT in Alveolarepithelzellen in der Lungenfibrose gezeigt werden. Während des Entwicklungsprozesses und bei vielen Krankheiten, wie Krebs und Fibrose unterliegt die phänotypische Umwandlung des Epithels strengen Transkriptionsvorgängen. Die einzelnen Transkriptionsfaktoren, die EMT in IPF hervorrufen, sind noch zu identifizieren. Die vermeintliche Rolle von SNAI Transkriptionsfaktoren als EMT Regulatoren in anderen Erkrankungen wurde schon dokumentiert.

Die vorliegende Studie basiert auf der Hypothese, dass TGF- $\beta$ -induzierte SNAI Transkriptionsfaktoren in alveolaren Epithelzellen EMT-Markerexpression beeinflussen können und somit die Morphologie und Motilität der Zellen verändern können. Das Ziel dieser Arbeit war es, die molekularen Mechanismen von TGF- $\beta$ 1-induzierter EMT *in vitro*, in humanen A549 Zellen und primären murinen Alveolarepithelzellen zu untersuchen. Dabei galt es ihre Beteiligung bei der Entwicklung in experimenteller und idiopathischer pulmonaler Fibrose *in vivo* zu beurteilen.

Die TGF- $\beta$ 1-induzierte EMT in Alveolarepithelzellen wurde anhand epithelialer Proteinen (Tjp1) und mesenchymaler Proteinen ( $\alpha$ -SMA) durch Immunfluoreszenz nachgewiesen. Des weiteren wurde *in vitro*, nach Behandlung mit TGF- $\beta$ 1, eine erhöhte Expression und nukleäre Ansammlung der Zinkfingerproteine SNAI1 und SNAI2 mittels quantitative RT-PCR und Immunfluoreszenz ermittelt. Die ektopische Expression von SNAI1 und 2 war bereits ausreichend, um EMT in A549 Zellen zu induzieren; auch ohne TGF- $\beta$ 1 Stimulation. Im Gegensatz dazu, führte eine siRNA vermittelte Verringerung von SNAI1 und 2 zur Abschwächung einer TGF- $\beta$ 1 induzierten Migration von Alveolarepithelzellen und EMT in A549 Zellen. Der Nachweis von EMT *in vitro* mit



---

Anstieg an SNAI Transkriptionsfaktoren konnte *in vivo* im Bleomycinmodell der pulmonalen Fibrose belegt werden. Sieben Tage nach Bleomycin Exposition zeigten primäre Alveolarepithelzellen aus fibrotischen Lungen eine Erhöhung der SNAI Expression. Auch in IPF Lungen bestätigte sich dieses Ergebnis im Vergleich zu gesunden Lungen. Außerdem konnte EMT, sowie die Beteiligung von transkriptionskontrollierten SNAI Faktoren im Mausmodell der renalen Fibrose, einer unilateralen urethralen Obstruktion (UUO), nachgewiesen werden.

Zusammenfassend konnte gezeigt werden, dass die TGF- $\beta$ 1-induzierte EMT in Alveolarepithelzellen mit einer erhöhten Expression von SNAI Transkriptionsfaktoren einher geht. Die Überexpression von SNAI1 und 2 zeigte, dass diese Transkriptionsfaktoren den EMT-Prozeß im wesentlichen triggern, während eine Verringerung dieser Faktoren die TGF- $\beta$ 1-induzierte EMT aufhebt. Die Erhöhung dieser Zinkfingerproteine, mit dem Hinweis auf EMT, konnte zudem in einem experimentellen Modell der Lungenfibrose nachgewiesen werden. Diese Beobachtung bestätigte sich ebenfalls in humanen IPF-Proben. Der Nachweis von SNAI Transkriptionsfaktoren in EMT im renalen Fibrosemodell, der UUO, und die Hemmung von EMT durch Behandlung mit Leukozytenblockern, heben die Signifikanz dieser Faktoren als Ursache im Krankheitsmechanismus hervor. Eine Aufhebung und/oder Hemmung von EMT könnte somit eine Therapiemöglichkeit in der Behandlung der Lungenfibrose darstellen.

---

# 1 Introduction

## 1.1 Idiopathic pulmonary fibrosis

### 1.1.1 Characteristics of idiopathic pulmonary fibrosis

Idiopathic Pulmonary Fibrosis (IPF; also termed Cystic Fibrosing Alveolitis, CFA) is a chronically progressive, often fatal lung disease resulting in irreversible distortion of the lung architecture. The etiology of this disease still remains unknown. IPF has been classified as one of the seven types of Idiopathic Interstitial Pneumonia (IIP) and unlike the other forms of IIPs, IPF cannot be resolved by currently available treatment (W.D. Travis and T.E. King, Jr, 2002).

This disease has an insidious onset and occurs worldwide ( T.E. King, Jr , 2000). The prevalence of IPF is high in the male sex (male: female prevalence ration 1.4: 1.0) (N. Khalil, et al., 2004). The incidence of IPF is associated predominantly with increasing age and the majority of patients are over 60 years of age. Cigarette smoking, genetic factors, infectious agents, and environmental pollutants have been identified as some of the potential risk factors associated with this disease. The prognosis of IPF is poor with an overall median length of survival varying between 2.5 and 3.5 years after diagnosis (W.D. Travis and T.E. King, Jr, 2002).

Criteria for diagnosis of IPF are based on a combined consensus provided by the American Thoracic Society, European Respiratory Society, and the American College of Chest Physicians which encompasses clinical, radiological, and pathological information. Clinically, IPF is characterized by exertional dyspnea, nonproductive cough, inspiratory crackles termed velcro crackles, and digital clubbing. Worsening of pulmonary function is frequently encountered on physical examination. Bronchoalveolar lavage (BAL) fluid cellular analysis shows increased neutrophils and eosinophils. Severe pulmonary hypertension and *cor pulmonale* may be encountered late in the course of the disease (W.D. Travis and T.E. King, Jr, 2002, T.J. Gross, et al., 2001). Chest radiographs and High Resolution Computed Tomography (HRCT) scan suggest decreased lung volume, bilateral reticular opacities prominent in the lung periphery and lower lobes, areas of ground-glass appearance, septal thickening, subpleural honeycomb cysts and or traction

bronchiectasis (A.L. Katzenstein, et al., 1998). The appearance of histopathological patterns of Usual Interstitial Pneumonia (UIP) on surgical lung biopsy establishes the definitive pathological diagnosis of IPF and is associated with a poor prognosis (T.E. King, Jr., et al., 2001).

### 1.1.2 Histopathological changes in idiopathic pulmonary fibrosis

Pathological features that are routinely observed in IPF include alveolar epithelial cell damage, increased deposition of extracellular matrix (ECM) in the lung interstitium, enhanced fibroblast/myofibroblast proliferation and activation, and ultimately, distortion of normal lung architecture. The typical distribution of pathological changes is heterogeneous, with subpleural, basal, and predominantly peripheral distribution. The unique, typical histological features of IPF are termed UIP, which are increasingly used to distinguish IPF from other forms of IIP (W.D. Travis and T.E. King, Jr, 2002).

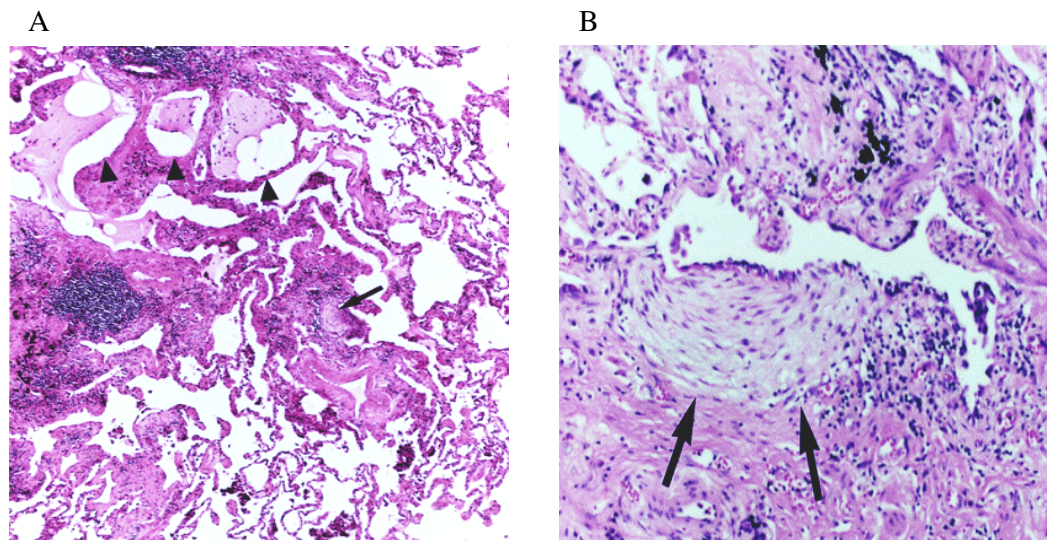


**Figure 1.1 Histopathological changes observed in IPF.** (A) Low magnification view of UIP, showing temporal heterogeneity, with dense collagen deposition on the left, and patchy areas containing normal alveolar septa present nearby (*right and bottom center*). A characteristic zone of microscopic honeycomb change (*arrowheads*) and a fibroblast focus (*arrow*) is seen in an area of fibrosis and inflammation in the center of the field. Hematoxylin and eosin; original magnification is  $\times 48$ . (B) Fibroblast focus in UIP (*arrows*) showing aggregate of spindle-shaped cells arranged in parallel beneath hyperplastic alveolar lining cells. Hematoxylin and eosin; original magnification is  $\times 300$  (A.L. Katzenstein, et al., 1998).

Low magnification power microscopy reveals temporal heterogeneity, a key feature of UIP (Figure 1.1). Temporal heterogeneity features areas of normal pulmonary parenchyma interspersed with interstitial inflammation, fibrosis, honeycombing changes, scattered fibroblast foci, and thickened alveolar septae lined by hyperplastic pneumocytes. Inflammation is usually mild to moderate, comprising primarily of lymphocytes and plasma cells, and occurs in areas of collagen deposition. Areas of honeycomb changes are composed of enlarged and distorted airspaces which are frequently lined by bronchiolar epithelium and filled with mucin (W.D. Travis and T.E. King, Jr, 2002).

The hallmark lesions of IPF are fibroblast foci, which are sites featuring activated myofibroblasts, synthesizing and depositing a collagen-rich ECM, and are located just beneath hyperplastic type II pneumocytes. Fibroblast foci are considered to be the earliest lesions in UIP and their presence is an important prognostic factor and their number has been shown to correlate with survival in IPF (T.E. King, Jr., et al., 2001, E.S. White, et al., 2003). High power magnification shows dense acellular collagen bundles with smooth muscle metaplasia. Alveolar epithelial injury with hyperplastic type II pneumocytes is often seen at areas of active fibrosis (E.S. White, et al., 2003) (Figure 1.1).

### 1.1.3 Pathogenesis of idiopathic pulmonary fibrosis

The precise mechanism that provokes IPF remains elusive. Much debate regarding the pathogenesis of IPF has recently been initiated, and the following theories have been postulated concerning current concepts in pathogenesis of IPF.

#### 1.1.3.1 The inflammation fibrosis theory

Initially, the classic concept that chronic inflammation triggered by an unrecognized stimulus being the primary cause of fibrosis was widely accepted (T.J. Gross, et al., 2001). Some of the premises for this long-prevailing belief were that local inflammation was a prominent feature in fibrotic lungs of all the IIPs and the BAL of IPF patients contained increased numbers of inflammatory cells (S. Harari, et al., 2005, M. Kelly, et al., 2003, T.E. King, Jr., et al., 2001, V.J. Thannickal, et al., 2004) However, studies with transgenic animals revealed that inflammatory response could be dissociated

from fibrosis (P.J. Sime, et al., 1997). Furthermore, clinical trials in IPF patients did not reveal any beneficial response to anti-inflammatory therapy (F. Chua, et al., 2005, J. Gauldie, et al., 2002, M. Selman, et al., 2001). These contradictory findings and the lack of compelling evidence failed to substantiate the inflammatory fibrosis hypothesis.

### 1.1.3.2 Abnormal wound healing theory

An alternate hypothesis regarding the pathogenesis of IPF has recently emerged. The new hypothesis is based on the notion that IPF is a disorder of inappropriate alveolar regeneration in response to repetitive epithelial injuries, rather than an inflammatory-driven disorder (M. Selman, et al., 2001).

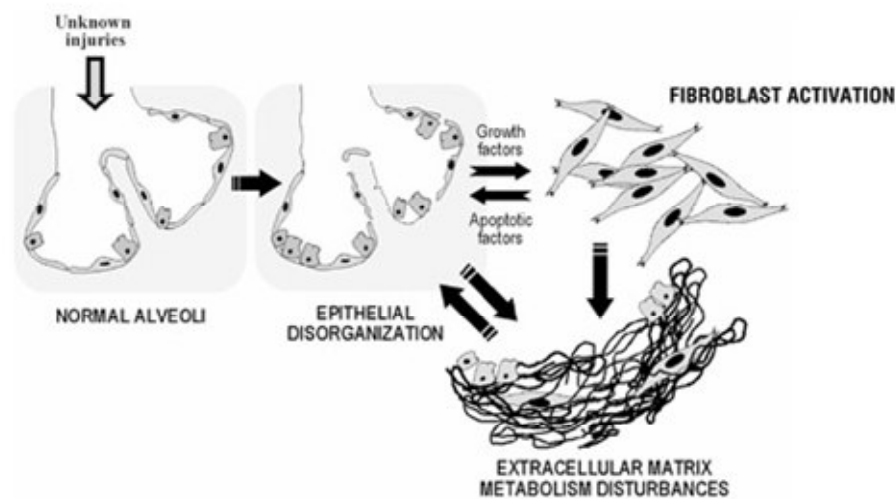


**Figure 1.2 Hypothetical scheme of the main pathogenic events in IPF.** Unknown insults provoke multiple microscopic foci of epithelial damage and stimulation. Activated alveolar epithelial cells release factors inducing fibroblast migration and proliferation. In the microenvironment of the lesion, myofibroblasts induce epithelial cell apoptosis and basement membrane disruption, thus contributing to abnormal re-epithelialization and perpetuation of a vicious circle (M. Selman, et al., 2001).

As illustrated in Figure 1.2, repeated episodes of acute injury to discrete peripheral areas of the lung by unidentified insult results in alveolar epithelial cell injury. This delays re-epithelialization and leads to denuded, disrupted basement membrane (E.S. White, et al., 2003). These cells subsequently produce exudates, which in turn promote fibroblast activation, proliferation, and migration into the wound. Fibroblasts may also secrete mediators that promote alveolar epithelial cell apoptosis. Formation of fibroblast foci featuring exaggerated mesenchymal cell proliferation leading to excessive ECM

deposition, which in turn distorts the normal lung structure with compromised gas exchange function and ultimately results in IPF (M. Selman, et al., 2001, M. Selman, et al., 2002).

The histological features of IPF suggest an inflammatory cause, but clinical findings and gene transfer studies in animal models support the concept of inflammation-independent fibrosis. However, some recent studies supports the role of acute and chronic inflammation in fibrosis and thus, a role for inflammation in IPF cannot be ruled out (G.W. Hunninghake, et al., 2003, F. Zuo, et al., 2002). The current view argues that the pathogenesis of IPF is complex and involves abnormalities in multiple pathways during both inflammation and wound healing (J. Gauldie, et al., 2002, R.M. Strieter, 2005).

### 1.1.4 Key effector cells in idiopathic pulmonary fibrosis

#### 1.1.4.1 Alveolar epithelial cells in idiopathic pulmonary fibrosis

In adults, the epithelial component of alveoli comprises type I and type II alveolar epithelial (AT1 and AT2) cells. The flattened AT1 pneumocytes cover more than 90% of the alveolar surface area of the peripheral lung, while the large, rounded AT2 pneumocytes cover 7% of the alveolar surface. AT1 and AT2 cells represent 8% and 16% of the total alveolar cells, respectively. AT1 cells interface with pulmonary capillaries and provide an intact surface of minimal thickness readily permeable to gases. The AT2 cells, which are often found in the corners of alveoli, are multifunctional cells that synthesize, store and secrete pulmonary surfactant, directionally transport sodium from apical to basolateral cell surfaces to minimize alveolar fluid, and participate in the immune response by producing molecules involved in innate host defence. AT2 cells are capable of undergoing mitosis and serve as progenitors of type I cells during homeostasis, as well as during lung injury. This differentiation is essential to re-establish a functional alveolar epithelium (M. Selman, et al., 2006).

AECs in IPF are morphologically abnormal, exhibiting heterogeneous phenotypes (M. Kasper, et al., 1996, A.L. Katzenstein, et al., 2002, M. Selman, et al., 2003). Numerous hyperplastic and hypertrophic AT2 pneumocytes, with abundant cytoplasm, large hyperchromatic nuclei, and prominent nucleoli are present in the fibrotic thickened alveolar septa. Large and elongated epithelial cells and, flattened and attenuated epithelial cells, overlying the fibroblastic foci are also observed.

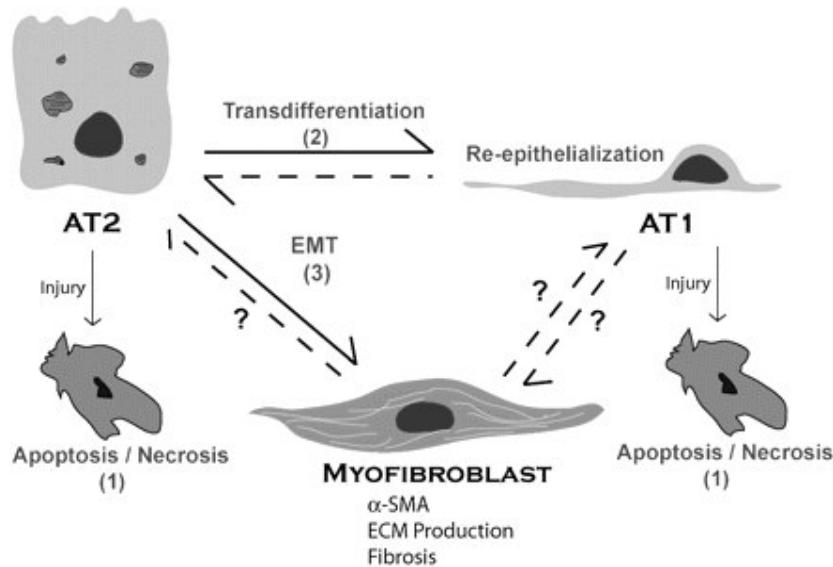


**Figure 1.3 Alveolar epithelial transdifferentiation pathways.** AECs demonstrate pluripotency. Under normal conditions, AT2 cells transdifferentiate into AT1 cells, and this process is reversible *in vitro*. Depending on the cellular environment and stimuli, AECs respond to injury by traveling down one of a number of pathways: apoptosis or necrosis (1); proliferation, transdifferentiation, and re-epithelialization (2); or EMT (3) to a myofibroblast phenotype, resulting in extracellular matrix (ECM) deposition, destruction of lung architecture, and fibrosis (B.C. Willis, et al., 2006).

The reasons and significance of these various phenotypic alternations in the AECs in IPF still remain unresolved. However, it is speculated that these phenotypic alterations in AECs may result from the initial injury and also that the differentiation of AT2 into AT1 pneumocytes is profoundly altered in IPF, which may be a key event culminating in fibrosis. Furthermore, these cells serve as the primary source of mediators such as TGF- $\beta$ , Platelet-derived growth factor (PDGF), Tumor necrosis factor- $\alpha$  (TNF- $\alpha$ ) that are capable of inducing fibroblast proliferation and activation, as well as, ECM accumulation in IPF (M. Selman, et al., 2006). As illustrated in Figure 1.3, according to the new paradigm, owing to the high plasticity of AECs and in part depending on the degree and nature of injury, AECs may contribute to diverse cellular pathways, such as, restoration of normal architecture by re-epithelialization, apoptosis or fibrogenesis (B.C. Willis, et al., 2006).

#### 1.1.4.2 Fibroblasts in idiopathic pulmonary fibrosis

Fibroblasts are dynamic cells that play crucial role in maintenance of matrix homoeostasis, and synthesis and degradation of a diverse group of extracellular

molecules. The maintenance of homeostasis is essential for the preservation of normal tissue function, which is lost in IPF. During IPF, fibroblasts exhibit an activated myofibroblasts phenotype. Myofibroblast accumulation, activation, and impaired apoptosis are key features of pathobiology of IPF. Myofibroblasts possess features intermediate between fibroblasts and smooth muscle cells. They are contractile, expressing  $\alpha$ -smooth muscle actin stress fibers and depositing excess ECM, resulting in structural remodeling that compromises lung function (E.S. White, et al., 2003). Despite the controversy surrounding IPF pathogenesis, it is well accepted that the interstitial fibroblast/myofibroblast represents the key effector cell responsible for the increased ECM deposition that is characteristic of IPF.

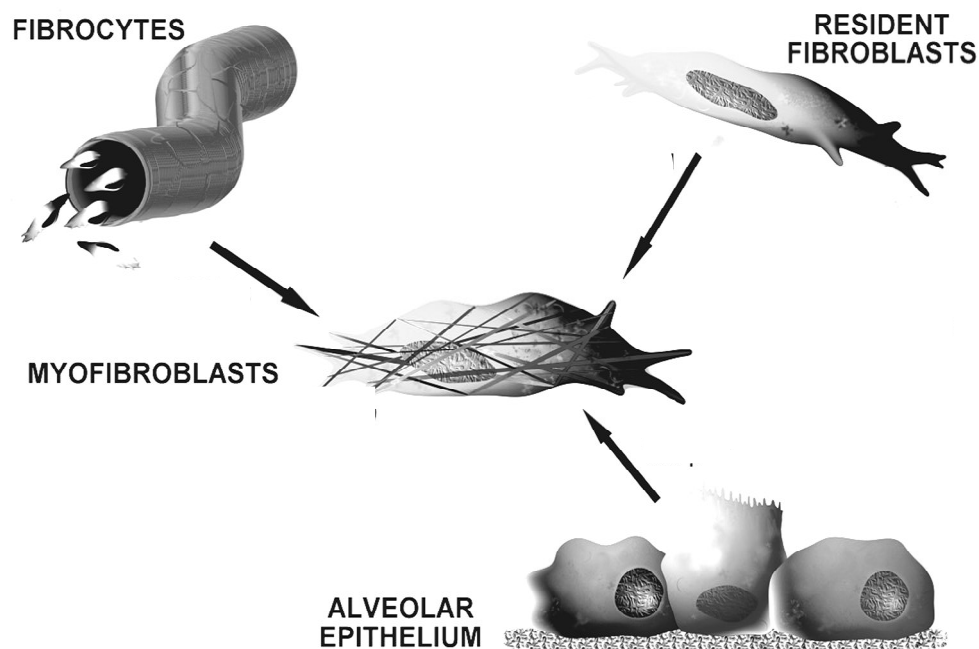


**Figure 1.4 Source of myofibroblasts in IPF.** Three prominent sources of myofibroblast have been proposed. Myofibroblasts can arise by proliferation of resident fibroblasts, from circulating fibrocytes, or from transitioning of alveolar epithelial cells (modified from C.J. Scotton, et al., 2007).

The number of  $\alpha$ -smooth muscle actin-positive, activated myofibroblasts is significantly increased in multiple forms of pulmonary fibrosis including IPF (B. Hinz, et al., 2007), but their origin remains to be elucidated. Currently, three major theories attempt to explain the accumulation of activated myofibroblasts in the lungs of IPF patients, depicted in Figure 1.4. First, it has been demonstrated that resident pulmonary



fibroblasts proliferate in response to fibrogenic cytokines and growth factors, thereby increasing the fibroblast pool via local fibroproliferation (S.H. Phan, 2002). Second, several recent studies have shown that bone marrow-derived circulating fibrocytes cells traffic to the lung during experimental lung fibrosis, and may serve as progenitors for interstitial fibroblasts (B.B. Moore, et al., 2006, R.J. Phillips, et al., 2004). Third, it was recently proposed that alveolar epithelial type II (AT2) cells are capable of undergoing epithelial-to-mesenchymal transition (EMT) (M. Selman, et al., 2006, B.C. Willis, et al., 2005).

## 1.2 Epithelial-to-mesenchymal transition

### 1.2.1 Characteristics of epithelial and mesenchymal cells

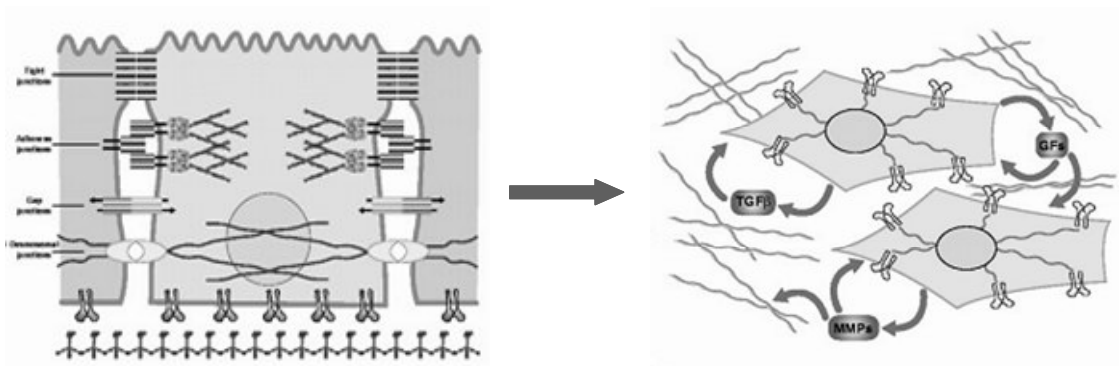


**Figure 1.5 Morphological changes during EMT.** During the process of EMT, well-differentiated epithelial cells revert to mesenchymal cells by loss of their highly polarized morphology, junctional complexes and undergo cytoskeletal rearrangement. They acquire a mesenchymal phenotype with invasive ability. The reversible switching of mesenchymal cells to epithelial cells is termed mesenchymal-to-epithelial transition (MET) (modified from D.C. Radisky, et al., 2005).

Epithelial and mesenchymal cells represent distinct lineages, each with a unique gene expression profile that imparts attributes specific to each cell type. Epithelial cells are polarized, closely adjoined by membrane associated specialized junctions such as adherens junctions, tight junctions, gap junctions and desmosomes. These cells attach to an underlying basement membrane or basal lamina. Several studies have identified specific epithelial markers, such as, E-cadherin, a prototypic epithelial adhesion molecule in adherens junction (H. Peinado, et al., 2004); Tjp1 and occludin, integral components of

tight junctions. Epithelial cells are polarized and often secrete glandular products from the apical surface and some also secrete ECM from the basal surface (J. Zavadil, et al., 2005).

By contrast, mesenchymal cells do not have apical-basolateral polarity, specialized membrane structures or basal lamina. They contact neighboring mesenchymal cells only focally. Mesenchymal cells display actin cytoskeleton aggregated in stress fibers, which endows these cells with migratory ability. Vimentin,  $\alpha$ -SMA, fibronectin, collagen precursors, talin,  $\alpha$ -actin and  $\beta$ -filamin are some of the phenotypic markers characteristic of mesenchymal cells (J.P. Thiery, 2003).

### 1.2.2 Key cellular events during EMT

Garry Greenburg and Elisabeth Hay recognized EMT as a distinct process in 1982 (G. Greenburg, et al., 1982). This multi-step event results in the phenotypic, reversible switching of epithelial to fibroblast-like or mesenchymal cells. The orchestrated series of events resulting in EMT include remodeling of epithelial cell-cell and cell-matrix adhesion contacts, reorganization of the actin cytoskeleton, and induction of mesenchymal gene expression. The cell morphology changes from a cuboidal to a fibroblastic shape. During EMT, epithelial cells lose apical basal polarity and acquire front-end back-end polarity. EMT endows the sedentary cell with the ability to become motile. They may start expressing gelatinase and the invasive activity allows them to pass through the underlying basement membrane. Epithelial marker expression gradually decreases while mesenchymal marker expression increases inversely, in cells adopting a mesenchymal phenotype. These changes in marker expression have been considered the hallmarks of EMT (P. Savagner, 2001). Numerous cellular changes are associated with EMT, but not all EMTs exhibit the whole range of changes (B. Boyer, et al., 2000). The precise spectrum of changes that occur during EMT is probably determined by the integration of extracellular signals the cell receives, although this is still unclear (J.P. Thiery, 2003). As depicted in Figure 1.6, EMT has emerged as a fundamental process during embryonic development. It has recently been recognized as a potential mechanism for cancer progression and fibrosis. EMT occurs during both physiological and pathological states (M.A. Huber, et al., 2005).

### 1.2.3 Role of EMT in embryos

EMT is an evolutionary conserved process, initially discovered and described in embryonic development and morphogenesis in multicellular organisms. In vertebrates, it facilitates the formation of a three-layered embryo by gastrulation. EMT is also pivotal for organogenetic processes and contributes to the formation of the neural crest, heart, musculoskeletal system, craniofacial structures and peripheral nervous system (M.A. Huber, et al., 2005, J.P. Thiery, 2003).

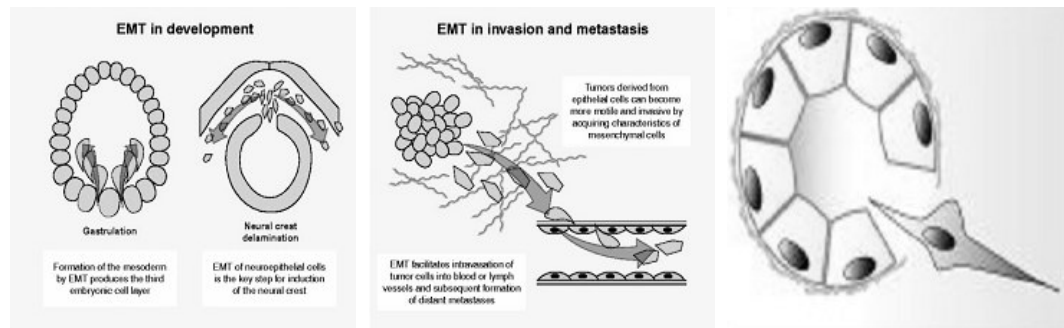


**Figure 1.6 EMT in development and disease.** EMT is an evolutionary-conserved process occurring during gastrulation and neural crest development. In adults, EMT contributes to cancer by facilitating invasion and metastasis, and also promotes fibrosis of epithelial organs such as the kidney, liver and lungs (modified from D.C. Radisky, et al., 2005; R. Kalluri, et al., 2003).

### 1.2.4 Role of EMT in adults

EMT is a highly controlled, spatio-temporally regulated process that does not occur under usual circumstances in adults (B. Boyer, et al., 2000). However, EMT has been reported to play an integral role in wound healing. The reactivation and inappropriate induction of developmental EMT in adults leads to a variety of pathogenic conditions. EMT has gained wide recognition as a mechanism that facilitates cancer progression and metastasis, as well as, the development of chronic degenerative fibrotic disorders of the epithelial organs namely kidney, liver and lung.

#### 1.2.4.1 EMT in wound healing

Following epithelial injury, EMT has been implicated in accelerating wound closure and healing process. Studies in keratinocytes have revealed the occurrence of EMT during skin wound healing (P. Savagner, et al., 2005). Contraction and re-

---

epithelialization are the main requisites of wound repair. The key cell types involved in this process are myofibroblasts and epithelial cells. Epithelial injury can be repaired through formation of granulation tissue, a provisional structure generated by ECM deposition, fibroblast proliferation, angiogenesis and immune cell influx. Myofibroblasts are the key cells involved in the creation of granulation tissue. An additional function of myofibroblasts is ECM contraction, through the formation of stress fibers containing  $\alpha$ -SMA. Normally, completion of injury repair is followed by degradation of the provisional ECM and apoptosis of the myofibroblasts, however, sustained myofibroblast activation stimulates dysfunctional repair mechanisms, leading to the accumulation of fibrotic ECM that is rich in collagens which coalesces into fibrous bundles resistant to degradation (V.J. Thannickal, et al., 2004).

#### **1.2.4.2 EMT in cancer**

Numerous observations in tissue culture models of epithelial cells, transgenic mouse tumour models and human tumour biopsies support the idea that EMT has a central role in tumor progression (M.A. Huber, et al., 2005). During progression to metastatic competence, carcinoma cells acquire mesenchymal gene expression patterns and properties. EMT also enables cells to evade apoptosis, and it is widely-accepted as a mechanism underlying metastasis. The changes in adhesive properties and the activation of proteolysis and motility are specifically associated with tumor invasiveness, and also enable tumor cells to metastasize and establish secondary tumors at distant sites (J.P. Thiery, 2003).

#### **1.2.4.3 EMT in fibrosis**

In adults, EMT is speculated to occur during wound healing, involving resident epithelial cells, in response to injury as an additional source of fibroblasts. The molecular basis of EMT with respect to fibrosis is starting to emerge (R. Kalluri, et al., 2003), and much that is known about the mechanisms underlying EMT has been gleaned from studies on embryogenesis and carcinogenesis. In organ fibrosis, enhanced fibroblast proliferation and activation is considered unfavorable, as it leads to an increase in fibrotic scar formation. EMT has been extensively studied in renal fibrosis. Recently, EMT has also been implicated in the fibrosis of various other organs including the lung, liver,

anterior sub capsular cataracts in humans (A.M. Hales, et al., 1994, S. Saika, et al., 2004, B.C. Willis, et al., 2005, M. Zeisberg, et al., 2007) .

The most convincing evidence for EMT as a source of myofibroblasts *in vivo* was derived from a study utilizing a model of gammaGT-LacZ transgenic mice, in which genetically-tagged proximal tubular epithelial cells gave rise to up to 36% of interstitial fibroblasts via EMT, following unilateral ureteral obstruction (UUO), a model of acute renal injury (M. Iwano, et al., 2002). Further evidence for the importance of EMT in the progression of chronic renal disease has been provided by the observation that MET, the reversal of EMT, results in resolution of fibrosis (M. Zeisberg, et al., 2005). These observations underscore the possible importance of EMT in the kidney fibrosis, and similar mechanisms may also apply to other epithelial organs like lung and liver, where tissue fibrosis eventually leads to impairment of organ function.

#### **1.2.4.4 EMT in idiopathic pulmonary fibrosis**

In the lung, AT2 cells are believed to serve as progenitors for repair of the alveolar epithelium following injury. They are capable of both self-renewal and of giving rise to AT1 cells (B.C. Willis, et al., 2007). Recently, *in vitro* studies have demonstrated that AT2 cells from both human (H. Kasai, et al., 2005) and murine (K.K. Kim, et al., 2006, B.C. Willis, et al., 2005) origins can transition into fibroblasts upon stimulation with TGF- $\beta$ 1, a potent inducer of EMT. Another study showed that epithelial cells contributed to the increase in fibroblasts *in vivo*, wherein triple transgenic mouse with lung epithelial cells tagged for  $\beta$ -galactosidase, were treated with TGF- $\beta$ 1 (K.K. Kim, et al., 2006). The co-localization of EMT markers was demonstrated in AT2 cells in lung biopsies from IPF patients (K.K. Kim, et al., 2006, B.C. Willis, et al., 2005). This also demonstrated the high plasticity of AT2 cells. The lung epithelial plasticity is an area of active research. Collectively, these studies strongly suggest that alveolar epithelial cells may serve as a possible source of fibroblasts in lung fibrosis. The extent to which this process contributes to fibrosis following injury in the lung is also a subject of active investigation.

### 1.2.5 Inducers of EMT

Several mechanisms are involved in initiating and executing EMT. EMT can be induced by a number of extracellular mediators individually or in combination. Several elicitors of EMT have been identified as ECM components, such as collagen as well as growth factors, including Epidermal growth factor (EGF), scatter factor or hepatocyte growth factor, Wnt ligands and members of the Fibroblast growth factor (FGF) and TGF- $\beta$  families (P. Savagner, 2001). In the majority of epithelial cell types and transgenic mouse tumour models, these mediators of EMT activate diverse signal transduction pathways, which have emerged as important for EMT. These pathways can be activated by specific signals, but are also controlled by crosstalk between each other. Induction of EMT appears to be highly tissue- and cell- type-specific, because factors that induce EMT under some circumstances can have quite different effects in others (J.P. Thiery, 2003).

#### 1.2.5.1 TGF- $\beta$ is a major inducer of EMT

Transforming growth factor (TGF)- $\beta$  represents a main inducer and regulator of EMT in multiple organ systems, during embryonic development, cancer progression, as well as organ fibrosis. TGF- $\beta$  signaling is typically associated with the induction and maintenance of EMT. Knowledge of the precise molecular mechanisms mediating TGF- $\beta$ - induced-EMT is beginning to emerge (M.A. Huber, et al., 2005).

TGF- $\beta$  was initially characterized after purification from human placenta in 1983 (C.A. Frolik, et al., 1983). Subsequently, more than 60 members of TGF- $\beta$  superfamily of growth factors have been identified. Members of the TGF- $\beta$  family are pleiotropic, as they exert extremely diverse biological effects on a large variety of cell types. TGF- $\beta$  and its family members control cell division, migration, adhesion, cell-fate determination and differentiation, and apoptosis. TGF- $\beta$  signaling is essential for embryonic development and adult tissue homeostasis (B. Schmierer, et al., 2007). The TGF- $\beta$  ligands consist of three highly homologous isoforms, TGF- $\beta$ 1, TGF- $\beta$ 2, and TGF- $\beta$ 3 (A.B. Roberts, 1998).

### 1.2.5.2 Sensing and propagating TGF- $\beta$ signals

Members of the TGF- $\beta$  superfamily initiate their cellular action through a family of transmembrane receptor-linked serine/threonine kinases. These receptors include a short cysteine-rich extracellular domain, a single transmembrane domain, and an intracellular serine/threonine kinase domain (J. Massague, 1996). Three functional classes of receptors can be distinguished: type I, type II, and type III. Seven type I receptors (ALKs 1–7), termed activin receptor-like kinases (ALKs) and five type II receptors (ActR-IIA, ActR-IIB, BMPRII, AMHR-II and T $\beta$ R-II) have been identified in vertebrates (P. ten Dijke, et al., 2004). The type III (T $\beta$ R-III) receptor recently was shown to enhance TGF- $\beta$  signaling (J. Massague, et al., 2006).

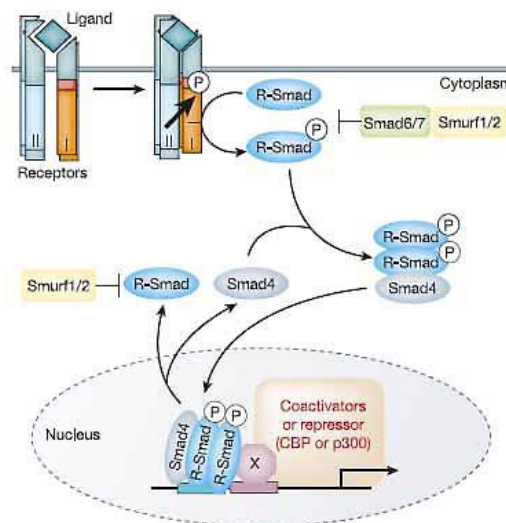


**Figure 1.7 Schematic diagram of the TGF- $\beta$  signaling pathway from the cell membrane to the nucleus.** The arrows indicate signal flow. At the cell surface, the ligand binds to the type I / type II receptor complex and induces phosphorylation of the GS segment (red) in the type I receptor. Consequently, R-Smads are phosphorylated, form a complex with Smad4 and this translocates into the nucleus to regulate transcription of target genes, assisted by either co-activators or co-repressors. R-Smads and Smad4 shuttle between the nucleus and the cytoplasm. Smurf1, Smurf2, Smad6, and Smad7 function as inhibitors of TGF- $\beta$  signaling (R. Derynck, et al., 2003).

In the absence of ligand, T $\beta$ R-I and T $\beta$ R-II are present as homodimers in the plasma membrane (L. Gilboa, et al., 1998). As illustrated in Figure 1.7, upon binding to TGF- $\beta$ , the T $\beta$ R-II receptor forms a heteromeric complex with the T $\beta$ R-I receptor,

---

resulting in the phosphorylation of conserved Gly/Ser-rich (GS box) in type I receptor and thereby activating T $\beta$ RI. T $\beta$ RI in turn propagates signals to intracellular signaling mediators known as Smads (J.L. Wrana, et al., 2000).

### 1.2.5.3 Smad proteins

Signaling from activated T $\beta$ RI to the nucleus occurs predominantly by phosphorylation of cytoplasmic protein mediators belonging to the Smad family. Smads can be divided into three classes based on their functional properties: the receptor-regulated Smads (Smad 1, 2, 3, 5, and 8), the common Smad (Smad4), and the antagonistic Smads (Smad 6 and 7). They all consist of conserved amino and carboxyl terminal Mad homology (MH) domains that are separated by a linker region. The N-terminal MH1 domain has DNA-binding activity, whereas the C-terminal MH2 domain has protein-binding and transactivation properties.

In the absence of phosphorylation, Smads are transcriptionally inert. The type I receptors for TGF- $\beta$ , activin, nodal and myostatin (ALKs 4, 5 and 7) phosphorylate Smads 2 and 3, whereas the Bone morphogenetic protein (BMP) and Anti-Müllerian hormone (AMH) type I receptors (ALKs 1, 2, 3 and 6), phosphorylate Smads 1, 5 and 8. The phosphorylated Smad then forms a heteromeric complex with Smad4, which in turn translocate into the nucleus and regulate the transcription of target genes, both positively and negatively. Smads constantly undergo cycles of receptor-mediated phosphorylation and phosphatase-mediated dephosphorylation, and thereby shuttle in and out of the nucleus. Smad 6 and 7 diverge structurally from other members of the Smad family and function as inhibitors of TGF- $\beta$  signaling (J. Massague, et al., 2006, P. ten Dijke, et al., 2004, F. Verrecchia, et al., 2007, O. Eickelberg, et al., 2007).

In addition to the Smad pathway, non-Smad signal transduction downstream of TGF- $\beta$  receptors has been proposed to occur in a cell-type-dependent manner. TGF- $\beta$  has been shown to activate other mediators such as the mitogen-activated protein kinases (MAPKs). Extracellular signal regulated kinase (ERK), Jun N-terminal kinase (JNK), p38, Phosphoinositide 3-kinases (PI3K), PP2A phosphatases and Rho family members (J. Massague, et al., 2006).



#### 1.2.5.4 Role of TGF- $\beta$ in idiopathic pulmonary fibrosis

There are a number of cytokines and growth factors that are found in IPF tissue however, whether each or all play a pathogenic role in progressive fibrosis is unknown, but TGF- $\beta$ 1 in particular is thought to have a pivotal role in fibrogenesis. This multifunctional cytokine is a key regulator of ECM assembly and remodeling, and is an integral component of fibrotic tissue in IPF (T.J. Broekelmann, et al., 1991, R.K. Coker, et al., 2001, K. Ask, et al., 2008). Elevated TGF- $\beta$ 1 expression was detected in IPF lung tissue in contrast to that of normal adult lungs. No differences in TGF- $\beta$ 2 and TGF- $\beta$ 3 isoform levels were noted (N. Khalil, et al., 1996).

A more direct evaluation of the impact of TGF- $\beta$ 1 involves the transient overexpression of active TGF- $\beta$ 1 in lungs of rodents, using adenoviral vector-mediated gene transfer. Within a few days of introducing the vector, spontaneously active TGF- $\beta$ 1 was expressed and there was evidence of tissue remodeling culminating in pulmonary fibrosis, without any pronounced inflammation. Fibroblastic foci were induced and myofibroblasts differentiation was evident (P.J. Sime, et al., 1997). Currently, TGF- $\beta$ 1 has been implicated as a major inducer of EMT in lung fibrosis.

### 1.2.6 Transcriptional control of EMT

Numerous pathways have been described *in vitro* that control phenotype transition. *In vivo* developmental studies suggest that EMT appears to be coordinated and is under the tight regulation of transcriptional control. An important component of EMT pathway involves activation of key transcription factors (M.A. Huber, et al., 2005, M.A. Nieto, 2002, H. Peinado, et al., 2003). Many of the EMT-responsive genes activated by these transcription factors encode proteins involved in the induction of EMT, and create feedback loops that may help sustain the mesenchymal phenotype (D.C. Radisky, 2005). Some models suggest several transcription factors may be key modulators of transitional event.

#### 1.2.6.1 Role of SNAI in EMT

Recent functional and localization experiments indicate that the SNAI family of transcription factors is key EMT contributor, which functions overall as epithelial phenotype repressor (P. Savagner, 2001). The Snail superfamily is divided into the SNAI

and Scratch families, with three members of the SNAI family having been described in vertebrates to date: SNAI1, SNAI2 and SNAI3 (A. Barrallo-Gimeno, et al., 2005). SNAI1 and SNAI2, also termed as Snail and Slug, respectively, are well-documented as elicitors of EMT in various systems. The role of SNAI3 still remains to be elucidated.

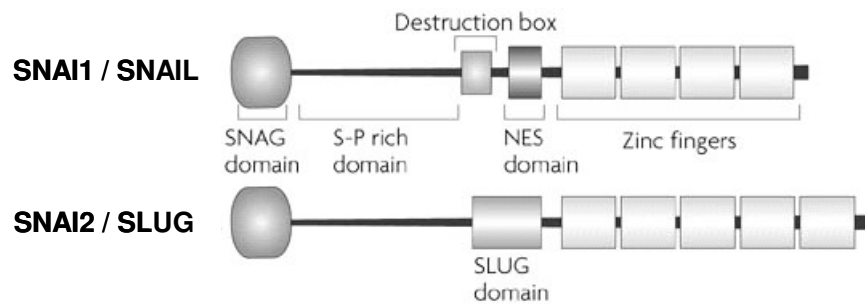


**Figure 1.8 Comparative scheme of the main structural domains found in mammalian SNAI1 and SNAI2.** SNAI transcription factors have a common organization: highly conserved C-terminal containing zinc fingers and a divergent N-terminal SNAG domain. The central region of SNAI1 protein has a serine-proline rich domain, and a regulatory domain with destruction and nuclear export signal boxes. SNAI2 protein contains a SLUG domain in this region (H. Peinado, et al., 2007).

Members of the SNAI family are zinc finger transcription factors that share a common structure: a highly conserved C-terminal region, containing four to six zinc fingers ( $C_2H_2$  type) and a divergent N-terminal region as shown in Figure 1.8. The zinc fingers function as the sequence-specific DNA-binding domains that recognize consensus E2-box type elements  $C/A(CAGGTG)$  (M.A. Nieto, 2002). SNAI factors are currently thought to be transcriptional repressors (K. Hemavathy, et al., 2000). Their repressor capacity is dependent on the SNAG domain in the N-terminal part of the protein, with seven to nine amino acids that are conserved between SNAI and growth factor independence (Gfi) proteins. The central region of the SNAI1 protein has a serine-proline-rich region that is highly divergent between SNAI members. SNAI2 proteins contain the so-called slug domain in this region, the function of which remains elusive (H. Peinado, et al., 2007).

By contrast, two different functional domains have been identified in the central region of SNAI1 proteins: a regulatory domain containing a nuclear export signal (NES) and a destruction box domain (B.P. Zhou, et al., 2004). The post-translational

modifications involving phosphorylation of proline/serine residues in both regions and potential modification of adjacent lysine residues has been implicated in the subcellular localization of SNAI1, protein stability and repressor activity.

The SNAI1 and SNAI2 genes are highly homologous and in certain circumstances can replace each other functionally. For instance, the consequences of SNAI2 knockdown in avian embryonic neural crest development can be rescued by transfection of SNAI1 (M. Sefton, et al., 1998). However, physiologically, they have distinct roles. SNAI1 is expressed during mesoderm formation, gastrulation and neural crest development, as well as in most developmental processes in which EMT is required. SNAI2 expression has been associated with mesoderm and migratory neural crest cells, as well as, in other tissues not always associated with EMT. SNAI1 is essential for mouse gastrulation, and SNAI1 and SNAI2 for neural crest development in frog and avian embryos, respectively (M.A. Nieto, 2002). However, they seem not to be essential for mouse neural crest formation, but are instead involved in left–right asymmetry (S.A. Murray, et al., 2006).

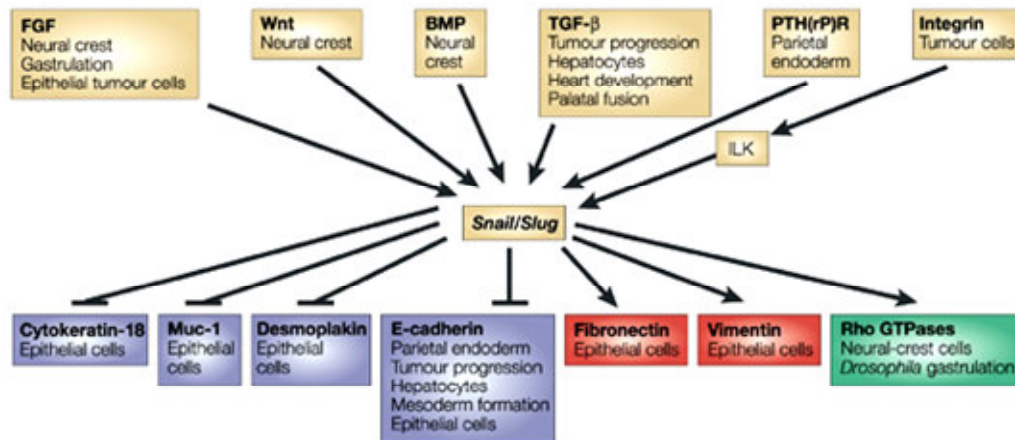


**Figure 1.9 Snail genes occupy a central position in triggering EMT in physiological and pathological situations.** Different signaling molecules have been implicated in the activation of SNAI genes in several processes that subsequently lead to EMT. SNAI genes, in turn, directly or indirectly regulate the expression of target genes (M.A. Nieto, et al., 2002).

The initial evidence that a zinc finger protein is involved in the control of EMT came from studies of SNAI2 in the chicken embryo. SNAI2 was expressed in chicken embryos in epiblast cells lining the primitive streak during gastrulation, as well as in neural crest cells just before they emerge from the neural tube, and later during their

migration phase. Treatment of developing embryos with antisense oligonucleotides from SNAI2 interferes with these two processes, suggesting a potential causal role for SNAI2 in the EMT process *in vivo* (P. Savagner, 2001).

As evident from *in vitro* and *in vivo* studies, SNAI transcription factors mediate repression of the epithelial phenotype. However, the mechanisms by which they induce mesenchymal genes remain largely unknown. It is also known that a plethora of molecules can induce SNAI during development (Figure 1.9). SNAI members are now thought to be involved in tumor progression, thus having potential clinical interest. The specific role of these different repressors in IPF remains to be elucidated.

---

## 2 Aims of the study

Recent studies have implicated the occurrence of (1) TGF- $\beta$ 1-mediated EMT in alveolar epithelial cells *in vitro* and *in vivo* in a triple transgenic mouse model, (2) EMT in transgenic mice treated with bleomycin and (3) EMT in lung biopsies from human IPF patients. The key molecular mediators regulating EMT are beginning to emerge. The contribution of SNAI transcription factors to the development and progression of IPF remains to be elucidated. Therefore, the expression of EMT markers and SNAI transcription factors were assessed in cell culture, in mouse model of bleomycin-induced pulmonary fibrosis and in lung samples from human IPF patients. EMT marker and SNAI expression were also determined in kidney samples from a UUO mouse model. In detail, the specific aims of this research were:

- 1) to assess the occurrence of EMT *in vitro* in the human A549 alveolar epithelial cell line and in primary mouse alveolar type II (AT2) cells, and to analyze whether TGF- $\beta$ 1 controls regulatory genes of EMT in these cells,
- 2) to analyze the TGF- $\beta$ 1-induced expression and localization patterns of SNAI transcription factors, SNAI1 and SNAI2 *in vitro*,
- 3) to determine the occurrence of EMT *in vivo*, in an experimental mouse model of pulmonary fibrosis, and to assess the regulation of SNAI transcription factors *in vivo*,
- 4) to assess the occurrence of EMT in human IPF lungs and to determine the expression pattern of SNAI transcription factors in context to the disease,
- 5) to demonstrate the role of SNAI transcription factors in EMT in alveolar epithelial cells by performing functional studies by ectopic expression, as well as silencing of SNAI factors in A549 cells,
- 6) to assess the occurrence of EMT *in vivo* in UUO model of neonatal renal fibrosis and also to analyze whether EMT and SNAI expression is attenuated in UUO animal model by treatment with leukocyte blocker BX471.

## 3 Materials and Methods

### 3.1 Materials

#### 3.1.1 Equipment

ABI PRISM 7500 Sequence Detection System	Applied Biosystems, USA
Cell Culture Incubator; Cytoperm2	Heraeus, Germany
Developing machine; X Omat 2000	Kodak, USA
Electrophoresis chamber	Bio-Rad, USA
Film cassette	Sigma-Aldrich, Germany
Filter Tip FT: 10, 20, 100, 200, 1000	Greiner Bio-One, Germany
Filter units 0.22 µm syringe-driven	Millipore, USA
Fluorescence microscope; LEICA AS MDW	Leica, Germany
Freezer -20 °C	Bosch, Germany
Freezer -40 °C	Kryotec, Germany
Freezer -80 °C	Heraeus, Germany
Fridge +4 °C	Bosch, Germany
Gel blotting paper 70 × 100 mm	Bioscience, Germany
Glass bottles: 250, 500, 1000 ml	Fischer, Germany
GS-800 <sup>TM</sup> Calibrated Densitometer	Bio-Rad, USA
Laser microbeam system	Palm, Germany
Light microscope; LEICA DMIL	Leica, Germany
Mini spin centrifuge	Eppendorf, Germany
Multifuge centrifuge, 3 s-R	Heraeus, Germany
Nanodrop®	Peqlab, Germany
Olympus BX51 microscope	Olympus, Germany
PCR-thermocycler	MJ Research, USA
Pipetboy	Eppendorf, Germany
Pipetmans: P10, P20, P100, P200, P1000	Gilson, France

---

Power Supply; Power PAC 300	Bio-Rad, USA
Petri dish with vents	Greiner Bio-One, Germany
Pipette tip: 200, 1000 $\mu$ l,	Sarstedt, Germany
Pipette tip 10 $\mu$ l	Gilson, USA
Quantity One software	Bio-Rad, USA
Radiographic film X-Omat LS	Sigma-Aldrich, Germany
Serological pipette: 5, 10, 25, 50 ml	Falcon, USA
Test tubes: 15, 50 ml	Greiner Bio-One, Germany
Tissue culture chamber slides	BD Falcon, USA
Tissue culture dish 100 mm	Greiner Bio-One, Germany
Tissue culture flask 250 ml	Greiner Bio-One, Germany
Tissue culture plates: 6, 24, 48 well	Greiner Bio-One, Germany
Vortex machine	Eppendorf, Germany
Western blot chambers:	
Mini Trans-Blot	Bio-Rad, USA
Mini-Protean 3 Cell	Bio-Rad, USA

### 3.1.2 Reagents

Acetic acid	Merck, Germany
Acrylamide solution, Rotiphorese Gel 30	Roth, Germany
Agarose	Invitrogen, UK
Ammonium persulfate	Promega, Germany
Ammonium sulfate	Sigma-Aldrich, Germany
Ampicillin sodium	Sigma-Aldrich, Germany
$\beta$ -glycerophosphate	Sigma-Aldrich, Germany
$\beta$ -mercaptoethanol	Sigma-Aldrich, Germany
Bromophenol blue	Sigma-Aldrich, Germany
Calcium chloride	Sigma-Aldrich, Germany
Complete <sup>TM</sup> Protease inhibitor	Roche, Germany
DEPC water	Roth, Germany

---

D-(+)-Glucose	Sigma-Aldrich, Germany
Dimethyl sulfoxide (DMSO)	Sigma-Aldrich, Germany
Dispase	BD Biosciences, USA
Dithiothreitol (DTT)	Promega, USA
D-MEM medium	Gibco BRL, Germany
DNA Ladder (1 kb)	Promega, USA
DNase	BD Biosciences, USA
Dulbecco's phosphate buffered saline 10×	PAA Laboratories, Austria
Dulbecco's phosphate buffered saline 1×	PAA Laboratories, Austria
Ethylendinitrilo-N, N, N', N', -tetra-acetic-acid (EDTA)	Promega, USA
Ethanol absolute	Riedel-de Haën, Germany
ECL Plus Western Blotting Detection System	Amersham Biosciences, UK
Ethidium bromide	Roth, Germany
Fetal calf serum (FCS)	Gibco BRL, Germany
Gel extraction kit	Qiagen, Germany
Glycine	Roth, Germany
Glycerol	Merck, Germany
GoTaq <sup>®</sup> Flexi DNA Polymerase	Promega, USA
Heparin	Merial GmbH, Germany
Hydrochloric acid	Sigma-Aldrich, Germany
2-(-4-2-hydroxyethyl)-piperazinyl-1-ethansulfonate (HEPES)	Sigma-Aldrich, Germany
Lipofectamine	Invitrogen, UK
Isotonic sodium chloride solution	Delta Select, Germany
Luria-Bertani Medium	Invitrogen, UK
Magnesium chloride	Sigma-Aldrich, Germany
Magnesium sulfate	Sigma-Aldrich, Germany
Methanol	Fluka, Germany
MiniElute Gel Extraction Kit	Qiagen, Germany
M-MLV reverse transcriptase	Promega, USA
Narcoren	Merial GmbH, Germany



---

<i>N,N,N',N'</i> -tetramethyl-ethane-1,2-diamine (TEMED)	Bio-Rad, USA
Nitro-cellulose membrane	Bio-Rad, USA
Non-fat dry milk powder	Roth, Germany
Oligo(dT) <sub>15</sub> Primer	Promega, USA
Opti-MEM medium	Gibco BRL, Germany
PCR Nucleotide Mix	Promega, USA
Penicillin-streptomycin	PAA Laboratories, Austria
Platinum <sup>®</sup> SYBR <sup>®</sup> Green qPCR SuperMix UDG	Invitrogen, UK
Potassium acetate	Sigma-Aldrich, Germany
Potassium chloride	Merck, Germany
Potassium phosphate	Sigma-Aldrich, Germany
Precision Plus Protein <sup>™</sup> Standards	Bio-Rad, USA
2-Propanol	Merck, Germany
Pure Yield Plasmid Midiprep System	Promega, Germany
QIAprep Spin Miniprep Kit	Qiagen, Germany
Quick Start <sup>™</sup> Bradford Dye Reagent	Bio-Rad, USA
Restriction endonucleases	Promega, Germany
RNasin inhibitor	Promega, Germany
RNaseZAP	Sigma-Aldrich, Germany
RNeasy Midi Kit	Qiagen, Germany
Select agar	Invitrogen, UK
Sodium acetate	Sigma-Aldrich, Germany
Sodium chloride	Merck, Germany
Sodium dodecyl sulfate (SDS)	Promega, USA
Sodium <i>ortho</i> vanadate	Sigma-Aldrich, Germany
Sodium phosphate	Sigma-Aldrich, Germany
Sodium sulfate	Merck, Germany
SuperSignal <sup>®</sup> West Pico Chemiluminescent Substrate	Pierce, USA
<i>Taq</i> DNA polymerase	Invitrogen, Germany
T4 DNA ligase	Promega, Germany

---

TGF- $\beta$ 1	R&D Systems, USA
Tris	Roth, Germany
Triton X-100	Promega, USA
Trypsin/EDTA	Gibco BRL, Germany
Tween 20	Sigma-Aldrich, Germany
Histostain-SP Kit	Zymed, USA

## 3.2 Animal Tissues

All animal studies were performed in accordance with the guidelines of the Ethic Committee of University of Giessen School of Medicine and approved by the local authorities (Regierungspräsidium Giessen, no. II25.3–19c20–15; GI20/10-Nr.22/2000). All animal studies utilized pathogen-free adult male C57BL/6N mice (18-20 g). After administration of bleomycin or saline, all mouse tissues were surgically excised, washed in ice-cold 1 x PBS and frozen in liquid nitrogen for further analyses. AT2 cells were also isolated from mice treated with or without bleomycin.

## 3.3 Human Tissues

Lung tissue biopsies were obtained from twelve patients with IPF (mean age  $51 \pm 11$  years; six females, six males) and nine control subjects (mean age  $48 \pm 14$  years; five females, four males). The study protocol was approved by the Ethics Committee of the University of Giessen School of Medicine (AZ 31/93). Informed consent was obtained from each subject for the study protocol.

## 3.4 Methods

### 3.4.1 Mammalian cell culture

#### 3.4.1.1 A549 cells

The human lung carcinoma alveolar epithelial cell line A549 (ATCC CCL-185; Manassas, VA, USA) was propagated in tissue culture flasks in D-MEM medium

supplemented with 10% (v/v) heat-inactivated FCS at 37 °C, 5% CO<sub>2</sub>, 95-100% humidity. The cell line was passaged when it attained 80-90% confluence. During passaging, cells were washed with 1 × PBS and incubated with 3 ml of Trypsin/EDTA solution for 3 min at 37 °C, after which 7 ml of D-MEM medium was added. Cells were transferred to new tissue culture flasks after 1:5 dilution with medium.

#### **3.4.1.2 Isolation of alveolar epithelial type II (AT2) cells**

Primary mouse alveolar epithelial type II (AT2) cells were isolated from adult male C57BL/6N mice, by dispase disaggregation followed by differential adherence on IgG coated petriplates and cultured as previously described (M. Corti, et al., 1996, I. Vadasz, et al., 2005).

Briefly, mice were sacrificed by intraperitoneal injection of a mixture of narcorin and heparin (1:1:1 - Narcorin:heparin:saline in a final volume of 200 µl). The thoracic cavity was opened carefully to avoid puncturing the lung. The trachea was exposed by a midline neck incision and a catheter was inserted and ligated. The abdomen was opened, the renal artery was separated and pneumothorax was drawn. Afterwards, lungs were perfused with saline and lavaged. Next, the proteolytic enzyme dispase (1.2 ml) was instilled via trachea to release AT2 cells. This was followed by low-melting-point agarose instillation (0.4 ml), maintained in liquid form at 55 °C. Agarose solution was allowed to solidify for 2 min inside the lungs and the respiratory organs were then separated from the thorax and incubated in 1.5 ml Dispase solution for 45 min at room temperature. After this incubation period, lung tissue was transferred into Petri dish with DNase containing Plus Medium and was gently teased with forceps to aid cell separation. This was followed by subsequent washes with Plus Medium and filtration through 100 µm, 20 µm and 10 µm nylon mesh filters and centrifuged at 130 g for 10 min to collect cells and exclude debris. The resulting pellets were dispersed with Minus Medium.

##### **Minus Medium**

500 ml D-MEM

10 mM HEPES

1% Pen-strep

1.8 g Glucose

2% L-Glutamine

### **Plus Medium**

Minus Medium with 0.04 mg/ml DNase

Following dispase disaggregation, a purification method based on the differential adherence of immune cells and other contaminating cells to IgG-coated Petri dishes was performed. Petri dishes were coated with a mixture of CD45 (20  $\mu$ l/dish) and CD16/32 (15  $\mu$ l/dish) antibodies diluted in Minus Medium, and incubated overnight at 4 °C, to allow the antibodies to adhere to the Petri dishes. The cell suspension was first incubated on mouse IgG-coated dishes for 45 min for attachment of contaminating cells bearing Fc receptors. This was followed by a 30 min incubation of the cell suspension, containing unattached cells, on uncoated Petri dishes for the attachment of fibroblasts. The unattached cells, mainly comprising of AT2 cells, were then collected and a cell count was performed using Nile Red staining, which identifies lamellar bodies, a characteristic organelle in AT2 cells. Briefly, the Nile Red staining was performed as follows: 20  $\mu$ l of cell suspension was dispensed in 500  $\mu$ l D-MEM containing a 1:20 dilution of Nile Red solution. The mix then was vortexed and incubated for 5 min at room temperature. Stained cells were counted under UV-light.

Freshly isolated cells were immunocytochemically tested for contaminating cells. Macrophages, lymphocytes and endothelial cells were not detected upon immunofluorescence analysis using CD45 and vWF antibodies. Such cultures were used for subsequent experiments. The AT2 pneumocytes were plated either on dishes (1 X 10<sup>6</sup> cells/ml) or on chamber slides (90,000 cells/well) in Minus Medium supplemented with 10% FCS. Cells were subjected to serum starvation before treatment with TGF- $\beta$ 1. Only AT2 cells up to day 3 were used in this study. All cultures were maintained in humidified atmosphere with 5% CO<sub>2</sub> at 37 °C, the media was changed every other day.

### **3.4.2 RNA isolation**

In order to isolate RNA from cell culture and tissue samples, two alternative methods were applied.

#### 3.4.2.1 RNA isolation from cultured cells

Using RNeasy Mini Kit, RNA was isolated from A549 cells and freshly isolated AT2 cells according to the manufacturer's instructions.

#### 3.4.2.2 RNA isolation from lung homogenates

Human and mouse lung tissue were ground to powder under liquid nitrogen with a mortar and pestle, and total RNA was extracted using Roti-Quick Kit. Guanidinium isothiocyanate was added to the tissue to isolate RNA, which was separated from the sheared DNA and proteins by adding phenol/chloroform, and precipitated overnight with isopropanol. Further steps were performed according to the manufacturer's protocol.

#### 3.4.3 Determining RNA and DNA concentration

The concentration of isolated RNA or DNA was determined according to a protocol from Peqlab by applying 1.5  $\mu$ l of the sample to a Nanodrop<sup>®</sup> spectrophotometer.

#### 3.4.4 Reverse transcription reaction

Reverse Transcription Polymerase Chain Reaction (RT-PCR) is a reverse transcriptase (RT)-driven enzymatic reaction, which generates complementary DNA (cDNA) using mRNA as a template.

In order to perform RT-PCR, 500 ng of total RNA was added to 1  $\mu$ l of oligo-(dT)<sub>15</sub> (100  $\mu$ g/ml) primers, and mixed with RNase free water to a final volume of 10  $\mu$ l in a PCR tube. The mix was heated at 70 °C for 5 min. The reaction was cooled on ice for 5 min to allow annealing of Oligo(dT)<sub>15</sub> to the poly A tail of the mRNA and the master-mix of the following RT-reaction reagents were added.

The reaction was performed at 42 °C for 60 min and completed at 70 °C for 5 min. The resulting complementary DNA (cDNA) was further used for polymerase chain reaction or stored at -20 °C.

**Table 3.1 RT reaction master mix**

Components	Volume	Final concentration
5× RT Buffer	5 µl	1 ×
10 mM dNTP mix	0.5 µl	0.2 mM
RNAsin inhibitor (1 U/µl)	0.5 µl	0.5 U
MMLV Reverse transcriptase (1 U/µl)	0.5 µl	0.5 U
RNase free water	8.5 µl	not applicable

### 3.4.5 Polymerase chain reaction

Polymerase chain reaction (PCR) is a DNA polymerase driven enzymatic reaction, which permits the amplification of selected fragments of genomic DNA. Product specificity is determined by the DNA primers used in the reaction.

#### 3.4.5.1 Semi-quantitative PCR

The reaction was performed according manufacturer's protocol from Go Taq® Flexi DNA polymerase kit, and all components were combined as follows and the final volume was adjusted with distilled, autoclaved water upto 50 µl.

**Table 3.2 PCR reaction master mix**

Components	Volume	Final concentration
5× PCR Buffer (free MgCl <sub>2</sub> free)	10 µl	1 ×
10 mM dNTP mix	1 µl	0.2 mM
25 mM MgCl <sub>2</sub>	2 µl	1 mM
10 µM forward primer	1 µl	0.2 mM
10 µM reverse primer	1 µl	0.2 mM
DNA template	1 µl	not applicable
GoTaq® Flexi DNA polymerase (5U/µl)	0.25 µl	1.25 U

This reaction mix is transferred to a PCR thermal cycler and denatured for 5 min at 95 °C. The PCR process was carried out for appropriate cycle numbers as indicated in Table 6.1 and 6.2 with appropriate primers. Each PCR cycle consists of three steps: denaturation (separation of double-stranded DNA), annealing (binding of primers to specific region of DNA), and elongation (extending of generated product). The steps were carried out as follows:

**Table 3.3 PCR program**

Step	Temperature	Duration
First denaturation	95 °C	5 min
Second denaturation	95 °C	45 s
Annealing	58-62 °C	30 s
Extension	72 °C	1 min
Final extension	72 °C	10 min

The reaction was completed by a final extension step at 72 °C for 10 min. The sample was further analyzed by DNA gel electrophoresis or stored at -20 °C.

#### 3.4.5.2 Real-time PCR

Real-time RT-PCR is a variation of the conventional PCR and allows the simultaneous amplification and quantification of specific DNA fragments. The reaction mix of real-time RT-PCR includes a fluorescent dye (e.g. Syber Green) that intercalates with the newly synthesized double-stranded DNA during the PCR reaction, resulting in increased fluorescence intensity detected after each cycle. The level of fluorescence is proportional to the amount of amplified DNA.

The reaction was performed according to a protocol from the Syber<sup>®</sup> Green PCR kit using a Sequence Detection System 7500 Fast from Applied Biosystems. All components were combined as follows and the final volume was adjusted to 25 µl with distilled, autoclaved water and the real-time PCR was performed for 45 cycles as follows, using the appropriate primers indicated in Table 6.3 and 6.4.

**Table 3.4 Real-time PCR master mix:**

Components	Valume	Final concentration
Platinum® Syber® Green qPCR SuperMix-UDG	13 µl	1 ×
50 mM MgCl <sub>2</sub>	1 µl	2 mM
10 µM forward primer	0.5 µl	0.2 mM
10 µM reverse primer	0.5 µl	0.2 mM
DNA template	1 µl	not applicable

**Table 3.5 Real-time PCR program**

Step	Temperature	Duration
Activation of polymerase enzyme	50 °C	2 min
First denaturation	95 °C	5 min
Second denaturation	95 °C	5 s
Annealing	59 °C	5 s
Extension	72 °C	30 s
Dissociation step 1	95 °C	15 s
Dissociation step 2	60 °C	1 min
Dissociation step 3	95 °C	15 s
Dissociation step 4	60 °C	15 s

The gene expression was analyzed by 7500 Fast System Software. All results were normalized to the relative expression of the constitutively-expressed porphobilinogen deaminase (PBGD) gene. The relative transcript abundance of the target gene is expressed in  $\Delta C_t$  values ( $\Delta C_t = C_t \text{ reference} - C_t \text{ target}$ ). Relative changes in transcript levels compared to controls are expressed as  $\Delta\Delta C_t$  values ( $\Delta\Delta C_t = \Delta C_t \text{ treated} - \Delta C_t \text{ control}$ ). All  $\Delta\Delta C_t$  values correspond approximately to the binary logarithm of the fold-change. The specific amplification of the PCR products was confirmed by melting curve analysis and gel electrophoresis.



### 3.4.6 Protein isolation

In order to isolate proteins from cell culture and tissue samples, two alternative methods were applied.

#### 3.4.6.1 Protein isolation from cell culture

In order to isolate proteins, confluent monolayers of cells were washed twice with ice-cold 1 × PBS. PBS buffer was applied to cell monolayers (100 µl/cm<sup>2</sup>), and cells were detached by scraping, and transferred to 1.5 ml tubes. After centrifugation for 3 min at 3000 g, the pellet was resuspended in 100 µl of cell-lysis buffer. The cell lysate was incubated for 30 min on ice and centrifuged at 16000 g for 15 min. The resulting supernatant was used as a crude cell extract, and stored at -20 °C.

**1 × PBS, pH 7.4:**

0.02% (w/v) KCl

0.115% (w/v) Na<sub>2</sub>HPO<sub>4</sub> · 2H<sub>2</sub>O

0.02% (w/v) KH<sub>2</sub>PO<sub>4</sub> · 2H<sub>2</sub>O

**Cell-lysis buffer:**

20 mM Tris-HCl, pH 7.5

150 mM NaCl

1 mM EDTA

1 mM EGTA

0.5% Igepal CA-630

2 mM Na<sub>3</sub>VO<sub>4</sub> \*

Complete™, protease inhibitor mix \*

\* Added immediately prior to homogenization

#### 3.4.6.2 Protein isolation from tissue

Human or mouse tissue was homogenized in liquid nitrogen and ice-cold tissue lysis buffer was added. Tissue lysate was then passed three times through a 0.9 mm needle fitted to a RNase-free syringe. Homogenized tissue was incubated for 1 h on ice and centrifuged for 15 min at 16000 g. The resulting supernatant was used as a crude tissue extract and stored at -20 °C.

**Tissue lysis buffer:**

20 mM Tris-HCl, pH 7.5

150 mM NaCl

1 mM EDTA

1 mM EGTA

1% (v/v) Triton X-100

2 mM Na<sub>3</sub>VO<sub>4</sub> \*

Complete™, protease inhibitor mix \*

\* Added immediately prior to homogenization

### 3.4.7 Gel electrophoresis

The length and purity of nucleic acids (DNA, RNA) is routinely determined accurately by gel electrophoresis method. This method also allows separation of proteins based on their physical properties such as, size and electric charge.

#### 3.4.7.1 DNA gel electrophoresis

For preparation of 1% agarose gels, agarose was dissolved in 1 × Tris-acetate-EDTA (TAE) buffer containing 0.5 µg/ml ethidium bromide, a fluorescent intercalating dye. DNA samples were mixed 5:1 with 6 × agarose gel-loading buffer and loaded onto the gel. Electrophoresis was performed for 1 h at 100 V, in 1 × TAE buffer. Separated nucleic acids were visualized with short wavelength UV-light ( $\lambda$  257 nm).

**1 × TAE buffer:**

40 mM Tris acetate, pH 8.0

1 mM EDTA, pH 8.0

**6 × agarose gel-loading buffer:**

0.025% (w/v) bromophenol blue

40% (w/v) sucrose

#### 3.4.7.2 Protein gel electrophoresis

The denaturing SDS polyacrylamid gel electrophoresis (SDS-PAGE) was used to separate proteins electrophoretically according to their molecular weight. The 10% resolving gel mixture was poured between two glass plates with spacers between, and

allowed to polymerize. The stacking gel was poured on top of the resolving gel, and a comb was inserted into the gel to form wells. Prior to loading on the gel, samples were mixed with 10 × SDS gel-loading buffer and heated at 95 °C for 7 min. Electrophoresis was carried out in 1 × SDS-running buffer at 120 V for 1 h.

**5% stacking gel:**

5% acrylamide/bisacrylamide

125 mM Tris-HCl, pH 6.8

0.1% SDS (w/v)

0.1% APS (w/v)

0.1% TEMED (v/v)

**10% resolving gel:**

10% acrylamide/bisacrylamide

375 mM Tris-HCl, pH 8.8

0.1% SDS (w/v)

0.1% APS (w/v)

0.1% TEMED (v/v)

**10 × SDS-loading buffer:**

625 mM Tris-HCl, pH 6.8

50% (v/v) glycerol

20% (w/v) SDS

9% (v/v) β-mercaptoethanol

0.3% (w/v) bromophenol blue

**1 × SDS running buffer:**

25 mM Tris

250 mM Glycine

0.1% (w/v) SDS

0.08% (w/v) NaCl

### 3.4.8 Western blot analysis

Western blotting is a protein detection method and allows identification of specific proteins by exposing all proteins present on gel to a specific antibody.

### 3.4.8.1 Western blotting

Proteins resolved by SDS-PAGE were transferred from a polyacrylamide gel to a polyvinylidene difluoride (PVDF) or nitrocellulose membrane. In case of PVDF, it was first activated in 100% methanol. Protein transfer was performed in transfer buffer at 100 V for 1 h.

**Transfer buffer (pH 7.4):**

24 mM Tris  
193 mM glycine  
10% (v/v) methanol

### 3.4.8.2 Protein visualization

The membrane was incubated in blocking solution for 1 h at room temperature followed by incubation with appropriate primary antibodies in blocking buffer at 4 °C overnight. The membrane was then washed three times with washing buffer and incubated with horseradish peroxidase (HRP) labeled secondary antibodies for 1 h at room temperature. The membrane was washed five times for 10 min. Proteins were detected using chemiluminescence by Enhanced Chemiluminescent Immunoblotting System and membrane was exposed to radiographic film.

**Blocking buffer:**

5% (w/v) non-fat dry milk  
1 × PBS  
0.1% (v/v) Tween 20

**Washing buffer:**

1 × PBS  
0.1% (v/v) Tween 20

**Stripping buffer:**

62.5 mM Tris-HCl, pH 6.8  
2% (w/v) SDS  
100 mM β-mercaptoethanol

For subsequent applications of different secondary antibodies, the membrane was incubated in stripping buffer for 10 min and washed repeatedly and protein visualization

was performed as previously described. Primary and secondary antibodies are listed in Tables 6.6 and 6.7.

### 3.4.9 Immunohistochemistry

To localize and assess the expression of particular proteins in human and mouse lung sections, immunohistochemical analysis was performed using a standardized avidin/biotin detection system (Histostain-SP Kit). At first, formalin-fixed paraffin-embedded tissue sections (3  $\mu\text{m}$  thickness) were incubated overnight at 48 °C and deparaffinized in xylene. After rehydration, using a stepwise decreasing ethanol concentration gradient (100% to 70%), antigen retrieval was performed in citrate buffer (pH 6.0) for 20 min at 100 °C. Slides were washed two times for 5 min in 1  $\times$  PBS. Endogenous peroxidase activity was quenched with 1% (v/v)  $\text{H}_2\text{O}_2$  for 20 min. Slides were blocked with serum blocking solution for 1 h at room temperature and incubated with the respective primary antibody (Table 6.6) at desired concentration overnight at 4 °C. The following day slides were incubated with biotinylated secondary antibody (Table 6.7) for 10 min at room temperature and subsequently 100  $\mu\text{l}$  of a substrate chromogen mixture was added to each section. Slides were developed for 5 min with AEC and counterstained with Mayers hematoxylin. Finally, sections were covered in glycergel and cover-slide was mounted and evaluated using an Olympus BX51 microscope.

### 3.4.10 Immunofluorescence

This method identified localization of particular proteins in cells by using fluorescent dyes. Cells were plated on 8-well chamber slides, incubated in the absence or presence of TGF- $\beta$ 1 (2 ng/ml) for 24 h, and fixed with ice-cold methanol. After blocking nonspecific binding sites with 5% FBS in PBS, cells were incubated with primary antibodies (Table 6.6) at 4 °C overnight, washed three times in PBS and incubated with Fluorescein isothiocyanate (FITC) and or Alexa Fluor 546-labelled secondary antibodies (Table 6.7). Cells were washed again five times with PBS. The plastic border of the slide was removed and slides were covered with mounting medium and a cover slide. Nuclei

were visualized by 4',6-diamidino-2-phenylindole staining (DAPI). The staining was analyzed by deconvolution fluorescence microscope.

### 3.4.11 Laser-assisted microdissection

In brief, 10  $\mu\text{m}$  cryosections were mounted on glass slides, stained with hemalaun for 45 s, immersed in 70% and 96% ethanol, and stored in 100% ethanol until use. Alveolar septae were selected and microdissected with a sterile 30 G needle under optical control using the Laser Microbeam System. Microdissected tissues were transferred into reaction tubes containing 200  $\mu\text{l}$  RNA lysis buffer and samples were processed for RNA analysis.

### 3.4.12 Cloning and transfection of human SNAI1 and SNAI2

The human SNAI1 expression construct was generated by amplifying full-length SNAI1 cDNA from total A549 RNA by PCR. SNAI1 cDNA was cloned into a mammalian expression vector, pcDNA3.1(-). SNAI2 expression construct was obtained from Origene, USA. SNAI1 and SNAI2 were transiently transfected into A549 cells and the effect of their ectopic expression were analysed.

#### 3.4.12.1 PCR product purification

To subclone SNAI gene into an expression vector, the DNA template was analysed for the appropriate restriction sites (BamH1 and Xho1) using the DNA Star software and appropriate primers were designed. Full-length SNAI1 cDNA was amplified from total lung RNA by PCR using the forward and reverse primers 5'- CAG TGC CTC ACC ACT ATG C-3' and 5'- AGG ATC CTC GAG GGT CAG-3', respectively. The amplified DNA fragment was analyzed and separated by agarose gel electrophoresis, excised and gel-purified using a commercially available gel extraction kit according to the manufacturer's protocol.

#### 3.4.12.2 Ligation of PCR products into pGEM-T Easy vector

The purified PCR product was ligated into pGEM-T Easy vector using the following ligation mix:

**Table 3.6 Ligation mix**

Components	Volume
2 X rapid ligation buffer	5 $\mu$ l
pGEMT-T Easy Vector (50 ng)	1 $\mu$ l
Purified PCR product	Depends on DNA concentration
T4 DNA ligase	1 $\mu$ l
Autoclaved, deionized water	up to 10 $\mu$ l

This reaction mix was incubated overnight at 4°C.

#### 3.4.12.3 Transformation and amplification of plasmids

After ligation, plasmids were transformed in competent *E. coli* DH5 $\alpha$  for further amplification. 1  $\mu$ g of plasmid DNA was added to 50  $\mu$ l of competent bacteria and the samples were incubated on ice for 30 min. Cells were then subjected to heat shock for 1 min in a 42 °C water bath, and snap chilled for 2 min on ice. 400  $\mu$ l of LB medium was added and the tube was shaken for 15 min at 37 °C at 250 rpm. X-Gal and IPTG were added to the LB medium and then plated on LB plates (LB medium plus 1.5% agar) containing appropriate antibiotics. After overnight incubation of the plates at 37 °C, individual bacterial colonies were picked from the plate on the following day and inoculated in LB medium containing the appropriate antibiotics. The bacterial tubes were shaken overnight at 37 °C at 250 revolutions per minute (rpm). Plasmids were subsequently isolated using Qiagen plasmid isolation kit.

#### 3.4.12.4 Subcloning into mammalian expression vectors

In order to subclone SNAI1 from pGEM-T Easy vector into a mammalian expression vector, pcDNA3.1(-), both empty expression vector and pGEM-T Easy plasmid, containing the human SNAI1 PCR product, were digested with the same restriction enzymes for 1-3 h at 37 °C, separated by agarose gel electrophoresis and gel-purified. The purified PCR product and the linearized purified vector were ligated in the ratio 3:1 with T4 DNA ligase and incubating 30 min at room temperature. The following

steps were performed as described in the previous chapter (3.4.12.3). All the SNAI1 constructs used were verified by sequencing.

#### **3.4.12.5 Transfection of A549 cells**

Transient transfection of plasmids is a technique to transfer DNA into eukaryotic cells. This method is transient as the transfected DNA is not integrated into the host chromosomes. SNAI1 and SNAI2 were transiently transfected into A549 cells using Lipofectamine<sup>TM</sup>2000 reagent. Briefly, Lipofectamine was added to OptiMEM, vortexed for 30 s, and incubated at room temperature for 5 min. Two micrograms of SNAI plasmids were added at a 1:3 DNA:Lipofectamine ratio in OptiMEM, incubated for 30 min at room temperature and added to the cells. 24 h and 48 h post-transfection, cells were harvested and RNA and protein was isolated for further analysis.

#### **3.4.13 siRNA transfection**

The siRNA oligonucleotides specific for human SNAI1 and SNAI2 mRNA (Table 6.5) were obtained from Dharmacon Inc. (Lafayette, USA). A549 cells were transiently transfected with 100 nM SNAI or non-specific siRNA using Lipofectamine<sup>TM</sup>2000 reagent. Briefly, Lipofectamine was added to OptiMEM and incubated for 15 min. siSNAI or non-specific siRNA was added to OptiMEM, and this mix was transferred into Lipofectamine and OptiMEM mix after 15 min. The mix was incubated for another 15 min at room temperature with constant shaking. Afterwards the siRNA mix was added to the cells and 4 h post transfection, cells were treated with TGF- $\beta$ 1. Cells were lysed after 24 h and efficiency of gene knockdown was monitored.

#### **3.4.14 Migration assay**

Cell migration was determined using Boyden chamber assay (ThinCerts<sup>TM</sup> Tissue Culture Inserts, 24 well, pore size 3.0  $\mu$ m from Kremsmunster, Austria). A549 cells were transfected with SNAI1, SNAI2 or non-specific siRNA at a total concentration of 75 nM, detached, and  $5 \times 10^4$  cells were seeded into Boyden chamber insert. Cells were cultured for 8 h to allow their attachment to the membrane and migration was induced by adding TGF- $\beta$ 1 (2 ng/ml) to the media in the lower wells. After 24 h, cells were fixed and



stained using crystal violet solution, and non-migrated cells were removed by cotton swabbing. The membranes were carefully separated from the insert wall, and optical densities of migrated cells were measured with a GS-800 Calibrated Densitometer and analysed with the Quantity One software.

### 3.4.15 Experimental model of idiopathic pulmonary fibrosis

Bleomycin is an anticancer agent and a single administration in mice, causes pathologic alterations in the lung that mimicks human IPF. The bleomycin mouse model of IPF is one of the most widely used animal models of IPF.

Bleomycin sulfate was dissolved in sterile saline solution and was applied to adult male C57Bl/6 mice as a single dose (0.08 mg/mouse in a total volume of 200  $\mu$ l) by intratracheal instillation using a microsyringe. Control mice received 200  $\mu$ l saline. Mice were sacrificed after 7, 14, or 21 days, as indicated. AT2 cells were isolated from these mice lungs or lungs were inflated with 4% (w/v) paraformaldehyde in phosphate buffered saline at 21 cm H<sub>2</sub>O pressure and processed for histological analyses, or excized, snap frozen in liquid nitrogen, and processed for molecular biological analyses.

### 3.4.16 Experimental model of renal fibrosis

This experiment was performed in collaboration with Sperandio et al., (B. Lange-Sperandio, et al., 2007) and animal experiments were performed in Heidelberg and RNA samples from kidney was provided for EMT marker analysis. Briefly, two-day-old wild-type mice (C57BL/6) were distributed into four groups ( $n = 16$  in each group) receiving subcutaneous injections of either BX471 (Berlex Biosciences, Richmond, CA) at 100 mg/kg body weight per day dissolved in propylene glycol (vehicle) for 5 (days 2 to 7 of life) or 12 (days 2 to 14 of life) days, or vehicle, once daily. BX471 was dissolved in propylene glycol (no. 39,803-9, 1,2-propanediol; Aldrich, Seelze, Germany) at a concentration of 25 mg/ml. Mice were subjected to complete left ureteral obstruction or sham operation under general anesthesia with isoflurane and oxygen at the second day of life. After recovery, neonatal mice were returned to their mothers until sacrificed 5 and 12 days after surgery (at days 7 and 14 of life;  $n = 8$  per group). The experimental

protocol was approved by the Committee for Animal Experimentation of the University of Heidelberg.

#### 3.4.17 Statistical analysis of data

Values are presented as mean  $\pm$  SEM. The mean of indicated groups were compared using two-tailed Student's *t*-test or a 1-way analysis of variance (ANOVA) with Tukey HSD post hoc test for studies with more than two groups. A level of  $p < 0.05$  was considered statistically significant. All experiments were performed at least three times.

## 4 Results

### 4.1 Analysis of EMT *in vitro*

#### 4.1.1 Estimation of the purity of primary mouse AT2 cells

Various cellular markers were used to assess the purity of isolated mouse AT2 cells. Freshly isolated, as well as primary AT2 cells cultured for up to three days routinely exhibited a purity of >95%, as assessed by immunofluorescence analysis of cells positive for the AT2 cell marker proSP-C, epithelial marker Tjp1 and fibroblast marker  $\alpha$ -SMA.

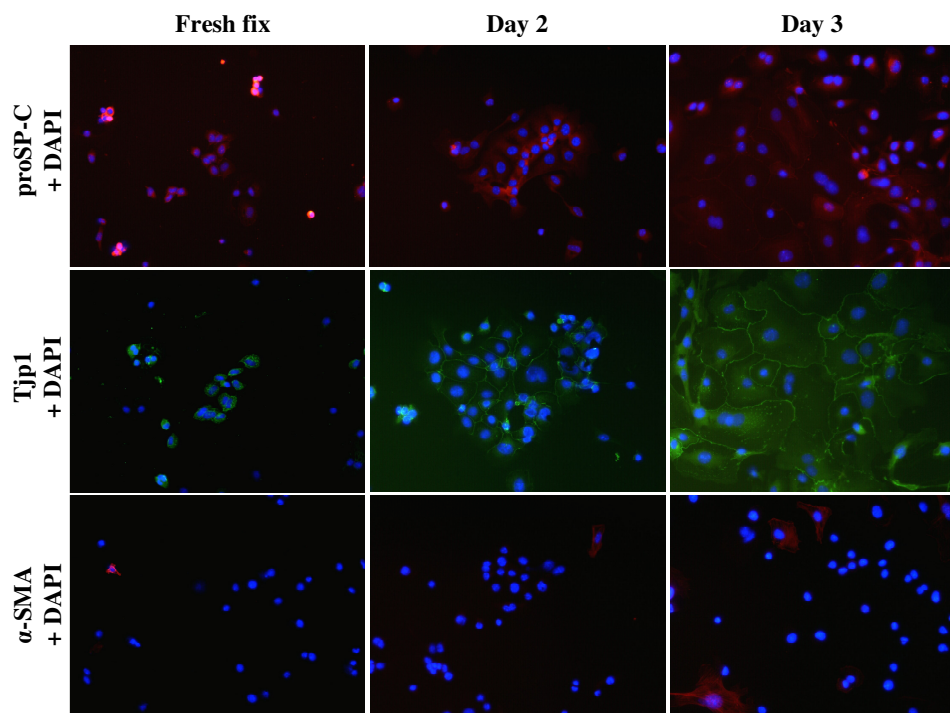


**Figure 4.1 Purity of primary alveolar epithelial type II (AT2) cells.** Expression and localization of proSP-C, Tjp1 and  $\alpha$ -SMA in freshly isolated mouse AT2 cells and two and three days after plating was determined by immunofluorescence analysis. Nuclei were analyzed by 4'6-diamidino-2-phenylindole (DAPI) staining. Original magnification is 20 $\times$ .

A large number of cells stained positive for proSP-C and Tjp1 immediately after isolation and plating, as well as two and three days after plating, whereas very few cells stained positive for  $\alpha$ -SMA as depicted in Figure 4.1.

#### 4.1.2 Expression of TGF- $\beta$ 1 signaling components in primary mouse AT2 cells

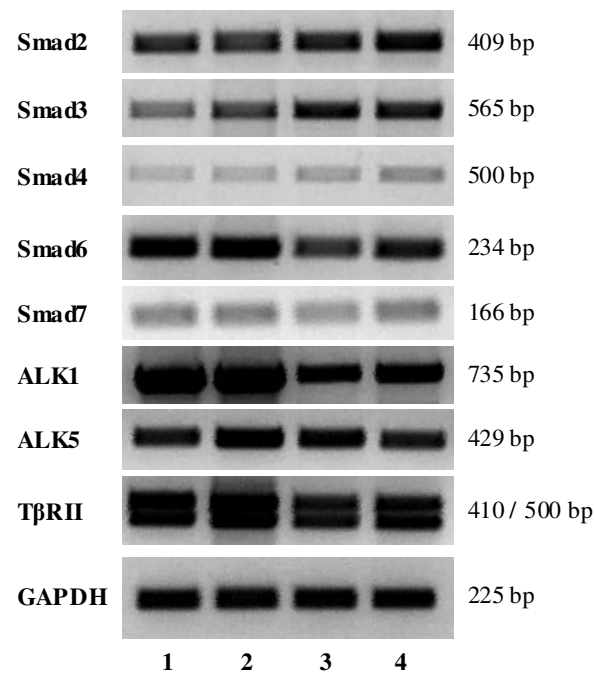


**Figure 4.2 Expression of TGF- $\beta$ 1 signaling components in AT2 cells.** Expression analysis of Smad2-4, Smad6-7, ALK1, ALK5, T $\beta$ RII, and GAPDH was performed by RT-PCR on whole lung RNA derived from two different mice (lanes 1, 2), and from two different primary AT2 cell preparations (lanes 3, 4). T $\beta$ RII amplification reveals the two known isoforms of this receptor. Product sizes are indicated to the right of the PCR panel.

To analyze whether TGF- $\beta$ 1 treatment of primary AT2 cells resulted in EMT, initially the expression of various TGF- $\beta$  signaling components was assessed. The TGF- $\beta$  signaling components, namely the TGF- $\beta$  type I receptors (ALK1, ALK5), TGF- $\beta$  type II receptor (T $\beta$ RII), TGF- $\beta$ -activated Smads (Smad2, Smad3, and the common

Smad4), and inhibitory Smads (Smad6 and Smad7) were examined by semi-quantitative RT-PCR analysis in RNA from isolated AT2 cells, as well as total mouse lungs.

When comparing RNA levels in total mouse lung homogenates (Figure 4.2, lanes 1, 2) with primary mouse AT2 cells (Figure 4.2, lanes 3, 4), a lower expression level of ALK1 in AT2 cells compared with homogenates was observed. All other genes were expressed and exhibited equal expression in total mouse lung homogenates and AT2 cells. Glyceraldehyde-3-phosphate dehydrogenase (GAPDH) served as a loading control.

#### 4.1.3 EMT marker localization in primary mouse AT2 cells

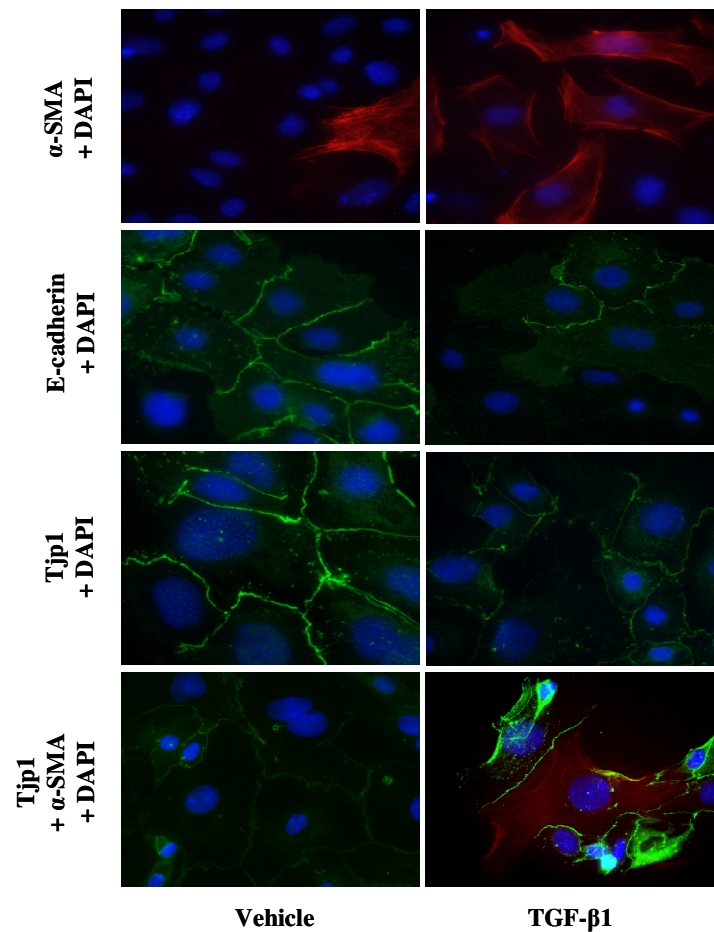


**Figure 4.3 EMT marker localization and expression in primary AT2 cells.** Immunofluorescence detection of  $\alpha$ -SMA, E-cadherin, and Tjp1 was performed after treatment with TGF- $\beta$ 1 (2 ng/ml) or vehicle for 24 h. Co-localization of  $\alpha$ -SMA (red) and Tjp1 (green) was assessed by immunofluorescence in AT2 cells treated with TGF- $\beta$ 1 for 24 h. Nuclei were visualized by 4'6-diamidino-2-phenylindole (DAPI) staining. Original magnification is 63 $\times$ .

As depicted in Figure 4.3, TGF- $\beta$ 1 treatment in AT2 cells for 24 h induced changes in  $\alpha$ -SMA, E-cadherin, and Tjp1 (zona occludens-1) expression and/or localization indicative of EMT. Epithelial markers, E-cadherin and Tjp1 staining decreased in TGF- $\beta$ 1-treated cells. In contrast, the mesenchymal marker  $\alpha$ -SMA staining increased in TGF- $\beta$ 1-treated cells compared with vehicle treated cells. While these changes in EMT marker staining strongly suggested the occurrence of EMT in primary mouse AT2 cells, this was unequivocally demonstrated by  $\alpha$ -SMA and Tjp1 double-positive cells in TGF- $\beta$ 1-treated, but not vehicle-treated cells (Figure 4.3, bottom panels).

#### 4.1.4 Mesenchymal marker expression in primary mouse AT2 cells

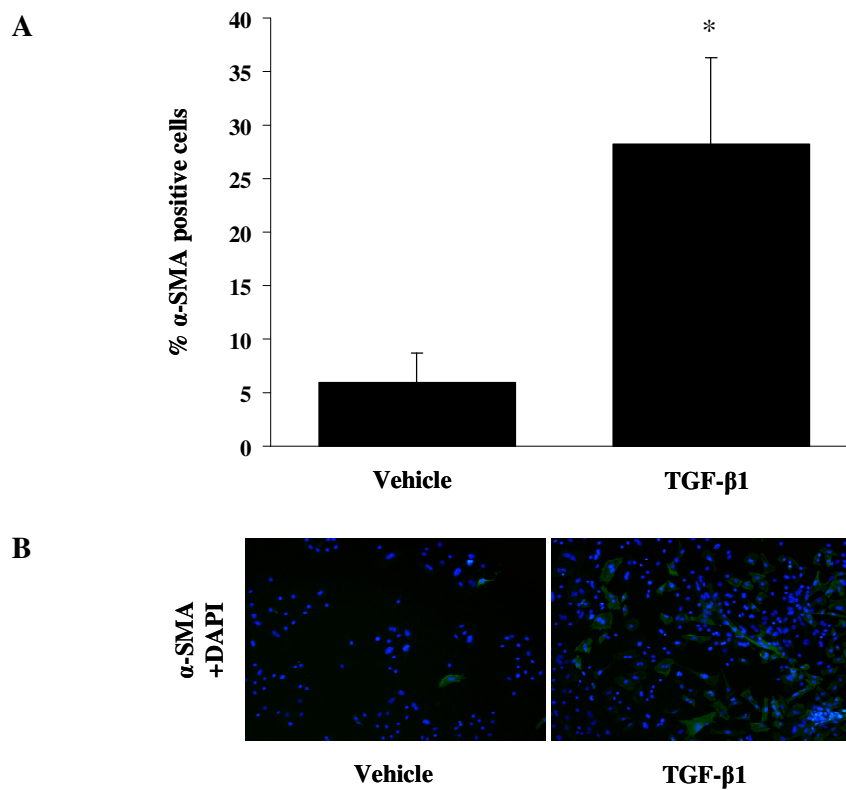


**Figure 4.4 Expression of mesenchymal marker  $\alpha$ -SMA in AT2 cells.** Panel (A) depicts the quantification of the percentage of  $\alpha$ -SMA-positive cells 24 h after TGF- $\beta$  treatment (2 ng/ml). (B) Original magnification of the representative figure showing immunofluorescence detection of  $\alpha$ -SMA with TGF- $\beta$ 1 (2 ng/ml) or vehicle for 24 h is 10 $\times$ . Data are expressed as mean  $\pm$  SE; \*  $p < 0.05$ ,  $n = 10$ .

Subsequently, the increase in mesenchymal marker  $\alpha$ -SMA expressing cells 24 h post TGF- $\beta$ 1 treatment was quantified. The number of  $\alpha$ -SMA-positive cells clearly increased in TGF- $\beta$ 1-treated cells from  $5.9 \pm 2.8$  % to  $28.2 \pm 8.1$ % in untreated and TGF- $\beta$ 1-treated cells, respectively (Figure 4.4).

#### 4.1.5 EMT marker gene expression in primary mouse AT2 cells

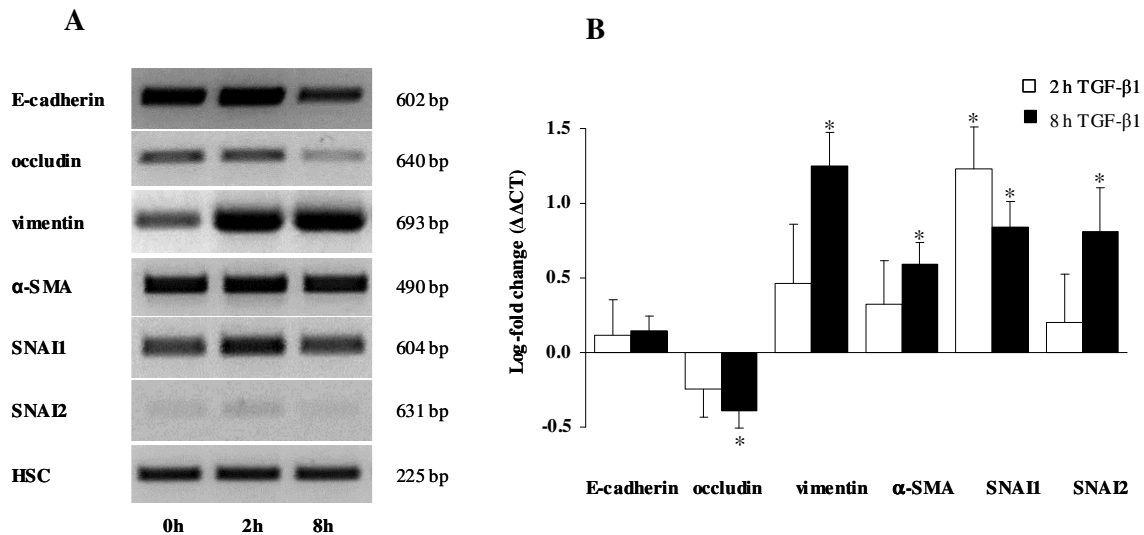


**Figure 4.5 EMT marker gene expression in primary AT2 cells.**

Using semi-quantitative (A) and real-time RT-PCR (B) analysis, the expression patterns of the indicated EMT markers was detected in primary mouse AT2 cells, after TGF- $\beta$ 1 treatment for 2 and 8 h, as indicated. Data are expressed as mean  $\pm$  SEM; \*  $p < 0.05$ ,  $n = 5$ .

Next, the mRNA expression patterns of several EMT marker genes were evaluated by semi-quantitative and real-time RT-PCR analysis, with the aim of identifying crucial mediators of EMT that, if depleted by experimental manipulation, could lead to a reduction in EMT. As depicted by semi-quantitative RT-PCR, (Figure 4.5A), when primary mouse AT2 cells were grown in the presence of TGF- $\beta$ 1 for 2 and 8 h, a decrease in the expression of the epithelial markers E-cadherin and occludin, and an increase in mesenchymal marker vimentin was observed. No change in the expression of  $\alpha$ -SMA was detected. An increase in SNAIL1 and SNAIL2 expression was also detected. A significant increase in SNAIL1 and SNAIL2 gene expression was evident in AT2 cells

(Figure 4.5B) treated with TGF- $\beta$ 1 for 2 and 8 h. An increase in the expression of vimentin and  $\alpha$ -SMA and concomitant decrease in the expression of E-cadherin and occludin mRNA was observed by real-time RT-PCR.

#### 4.1.6 EMT marker gene expression in the human A549 cell line

Immortalized A549 cells are a model cell-line routinely used in place of primary AT2 cells. In order to confirm the occurrence of TGF- $\beta$ 1-mediated EMT in A549 cells, the mRNA expression patterns of several EMT marker genes was investigated using semi-quantitative and real-time RT-PCR analysis. As depicted in Figure 4.6, downregulation of occludin and upregulation of  $\alpha$ -SMA, SNAI1 and SNAI2 was observed by semi-quantitative PCR, upon TGF- $\beta$ 1 stimulation for 2 and 8 h. No changes in E-cadherin and vimentin expression were detected. Real-time RT-PCR demonstrated a significant increase in SNAI1 and SNAI2 gene expressions in A549 cells (Figure 4.6B), grown in the presence of TGF- $\beta$ 1. A decrease in the expression of E-cadherin and occludin and a concomitant increase in the expression of vimentin and  $\alpha$ -SMA were observed by real-time RT-PCR in A549 cells after TGF- $\beta$ 1 stimulation.

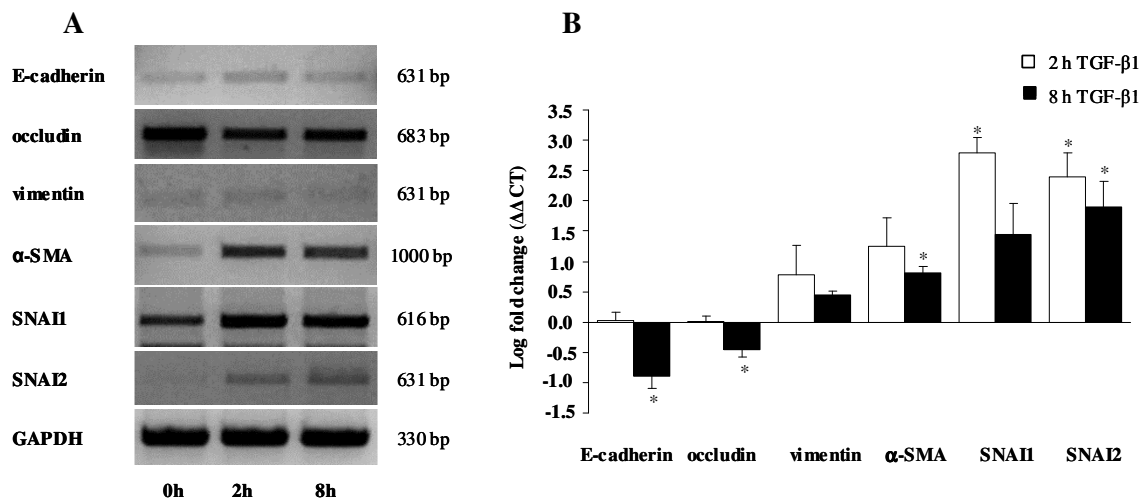


**Figure 4.6 EMT marker gene expression in A549 cells.** Using semi-quantitative (A) and real-time RT-PCR (B) analysis, the expression patterns of the indicated EMT markers was detected in A549 cells, after TGF- $\beta$ 1 treatment for 2 and 8 h, as indicated. Data are expressed as mean  $\pm$  SEM; \*  $p < 0.05$ ,  $n = 5$ .



#### 4.1.7 SNAI1 and SNAI2 protein localization in A549 and primary mouse AT2 cells

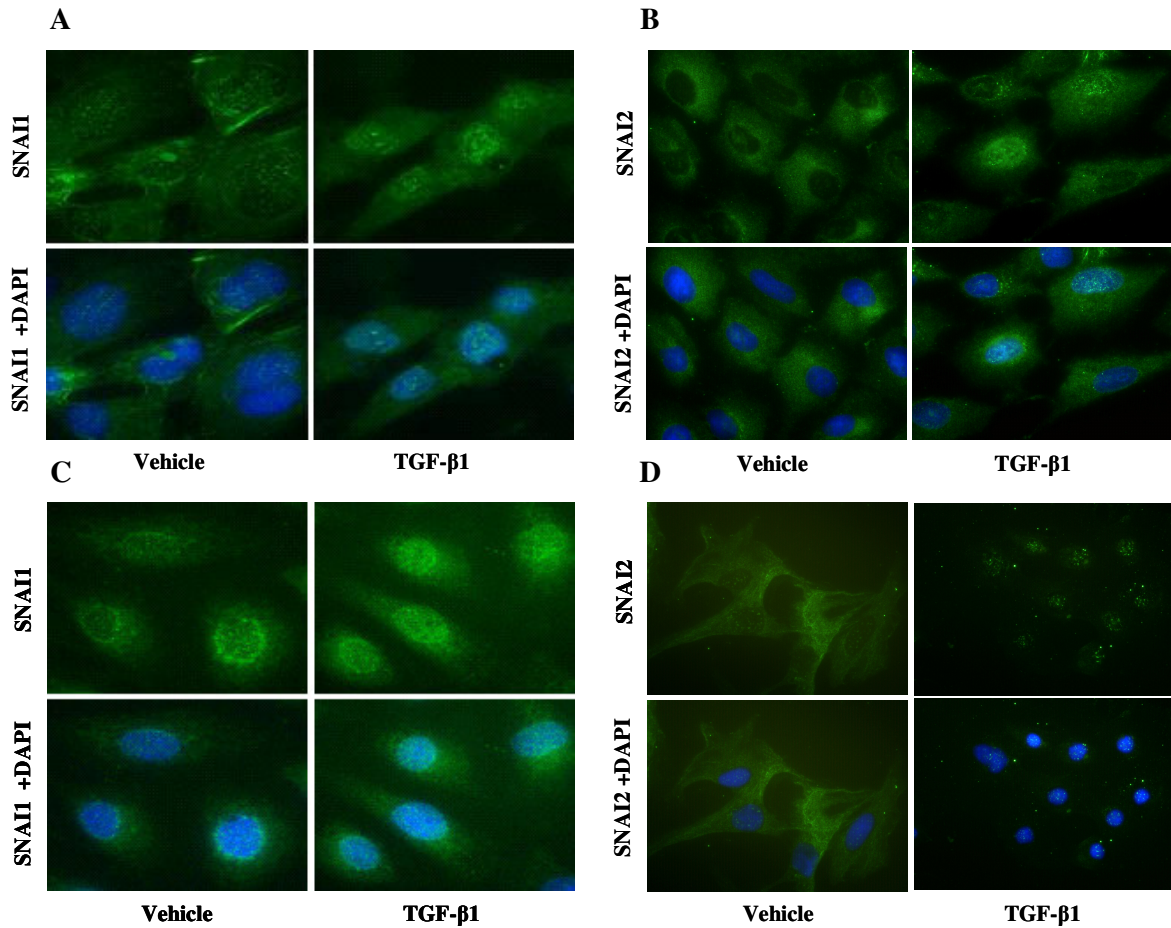


**Figure 4.7 SNAI localization in A549 and mouse AT2 cells.** Immunofluorescence analysis was performed using a primary antibody directed against goat anti-SNAI1 (A) and SNAI2 (B) in A549 cells. Localization of SNAI1 (C) and SNAI2 (D) was also performed in AT2 cells. Nuclei were visualized by 4'6-diamidino-2-phenylindole (DAPI) staining. Original magnification is 63 $\times$ .

Since the SNAI transcription factors were regulated at the mRNA level in both A549 and in primary mouse AT2 cells, immunofluorescence analysis was performed to determine whether their cellular localization was also influenced by TGF- $\beta$ 1 treatment. Immunofluorescence analysis revealed increased nuclear localization of endogenous

---

SNAI1 (A) and SNAI2 (B) upon TGF- $\beta$ 1 treatment for 24 h in A549 cells (Figure 4.7). A similar increase in nuclear localization of SNAI1 (C) and SNAI2 (D) was observed in AT2 cells (Figure 4.7) after 24 h of TGF- $\beta$ 1 treatment.

## 4.2 Analysis of EMT marker expression in an experimental model of pulmonary fibrosis

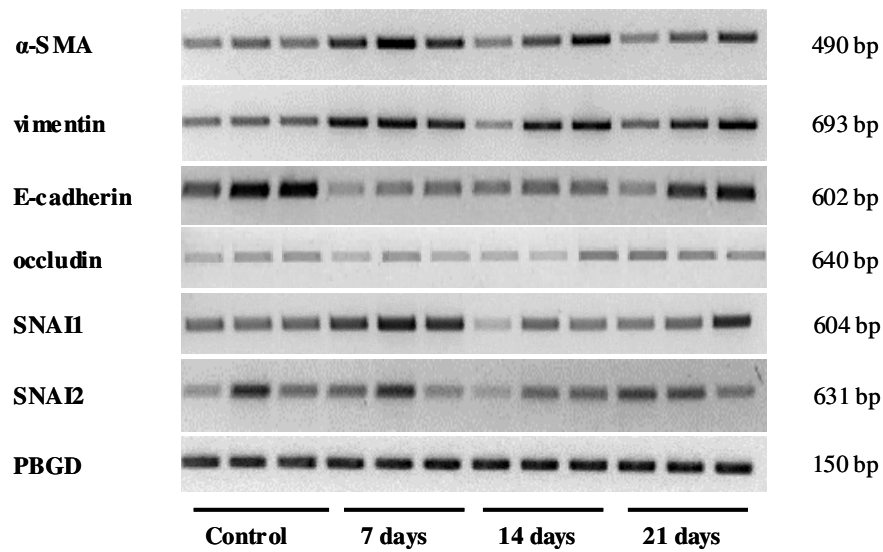
### 4.2.1 EMT marker expression in bleomycin-induced pulmonary fibrosis

To analyze whether EMT occurred in a mouse model of bleomycin-induced pulmonary fibrosis and to determine whether the expression of SNAI transcription factors were regulated during experimental pulmonary fibrosis, mice were subjected to bleomycin treatment for 7, 14, or 21 days.

As depicted in Figure 4.8 (A), in total lung homogenates, semi-quantitative RT-PCR revealed decrease in the expression of the epithelial marker E-cadherin as early as day 7 after bleomycin treatment compared to controls. At day 7, a concomitant increase in the expression of mesenchymal markers vimentin and  $\alpha$ -SMA was observed. No changes in occludin levels were noted. In total lung homogenates, elevated levels of SNAI1 but not SNAI2 were observed 7 days after bleomycin administration. Prominent changes in gene expression were evident only at day 7 post bleomycin treatment, compared to saline-treated controls.

Real-time RT-PCR revealed elevated levels of  $\alpha$ -SMA 7, 14 and 21 days post bleomycin treatment compared to saline-treated controls. A decline in the expression of E-cadherin and occludin were not seen. Elevated SNAI1 gene expression in total lung homogenates was seen 7, 14 and 21 days after bleomycin administration compared to control mice, while an increase in SNAI2 mRNA levels was evident at 14 and 21 days after bleomycin treatment.

A



B

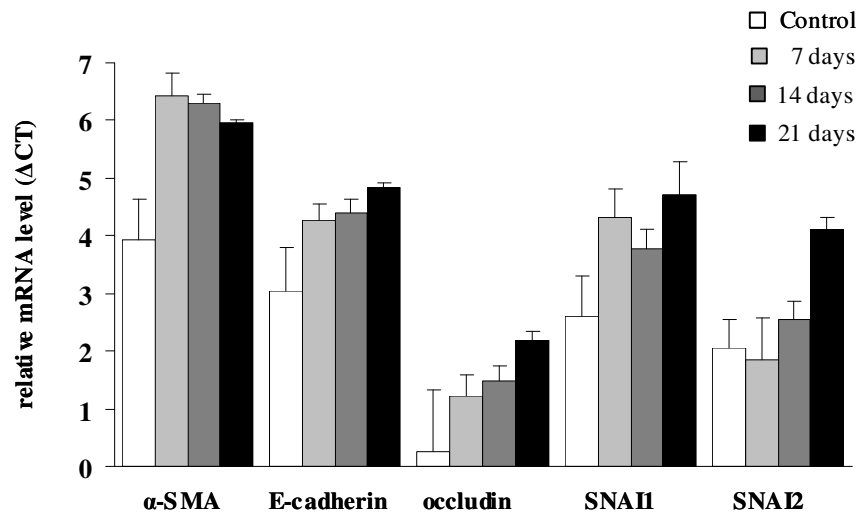


**Figure 4.8 Expression of EMT markers in total lung homogenates from bleomycin treated mice.** Mice were exposed to bleomycin and lungs were harvested after 7, 14, or 21 days, as indicated. RNA was isolated from lungs 7, 14 or 21 days after bleomycin challenge or saline treatment and semi-quantitative (A) and real-time RT-PCR (B) was performed for EMT marker genes. Data are expressed as mean  $\pm$  SEM,  $n = 3$ .

#### 4.2.2 EMT marker expression in AT2 cells of bleomycin-treated mice

To evaluate whether alveolar epithelial cells contributed to EMT in the experimental model of lung fibrosis, and to further determine if alveolar epithelial cells served as a source of SNAI, AT2 cells isolated from mice treated with bleomycin for 7, 14, were tested for EMT marker expression. In Figure 4.9, real-time PCR revealed significantly elevated levels of both SNAI1 and SNAI2 in AT2 cells isolated from bleomycin treated mouse lungs as early as seven days after treatment compared with saline treated control. Significantly elevated levels of  $\alpha$ -SMA was observed at both day 7 and 14 after bleomycin treatment, whereas increase in vimentin was seen at day 14. Significant repression in E-cadherin and occludin expression was observed in AT2 cells at day 7 after bleomycin treatment.

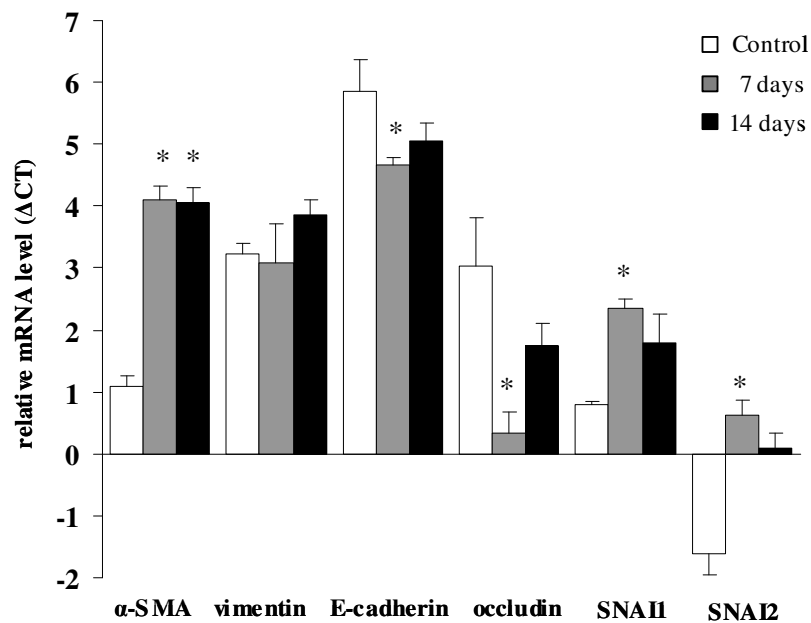


**Figure 4.9** Expression of EMT markers in AT2 cells from the lungs of bleomycin treated mice. EMT marker gene expression was quantified by real-time RT-PCR in AT2 cells isolated from lungs 7 or 14 days after bleomycin challenge or saline treatment. Data are expressed as mean  $\pm$  SEM; \*  $p < 0.05$ ,  $n = 3$ .

### 4.2.3 SNAI protein localization in lungs of bleomycin treated mice

Using immunohistochemistry, the localization of  $\alpha$ -SMA, SNAI1, and SNAI2 in bleomycin-treated lungs was investigated. As depicted in Figure 4.10,  $\alpha$ -SMA was primarily localized in airway and vascular smooth muscle cells in saline-treated control mouse lungs, but was also localized in the lung interstitium after bleomycin treatment.

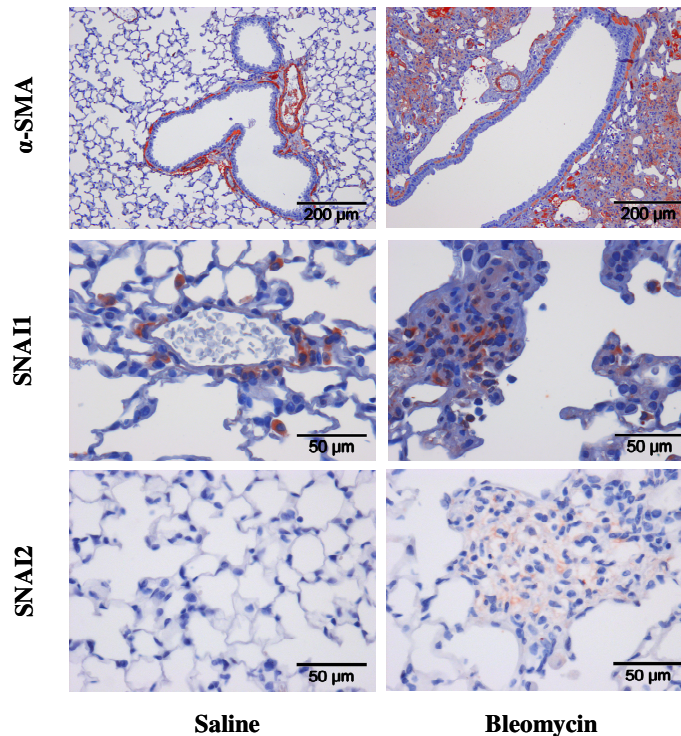


**Figure 4.10 Localization of SNAI in mice lungs treated with bleomycin.** Immunohistochemical analysis of  $\alpha$ -SMA, SNAI1, and SNAI2 localization was performed in paraffin-embedded lung specimen from mice treated with saline or bleomycin for 14 days.

While SNAI1 was predominantly localized to perivascular mesenchymal cells and alveolar macrophages in saline-treated lungs, it also localized in the lung interstitium, particularly in subepithelial areas, after bleomycin treatment. Although little or no staining for SNAI2 was detectable in saline-treated mouse lungs, SNAI2 localization was detected in the lung interstitium after bleomycin treatment.

### 4.3 Analysis of EMT marker expression in lungs of patients with idiopathic pulmonary fibrosis

#### 4.3.1 Expression of EMT markers in idiopathic pulmonary fibrosis

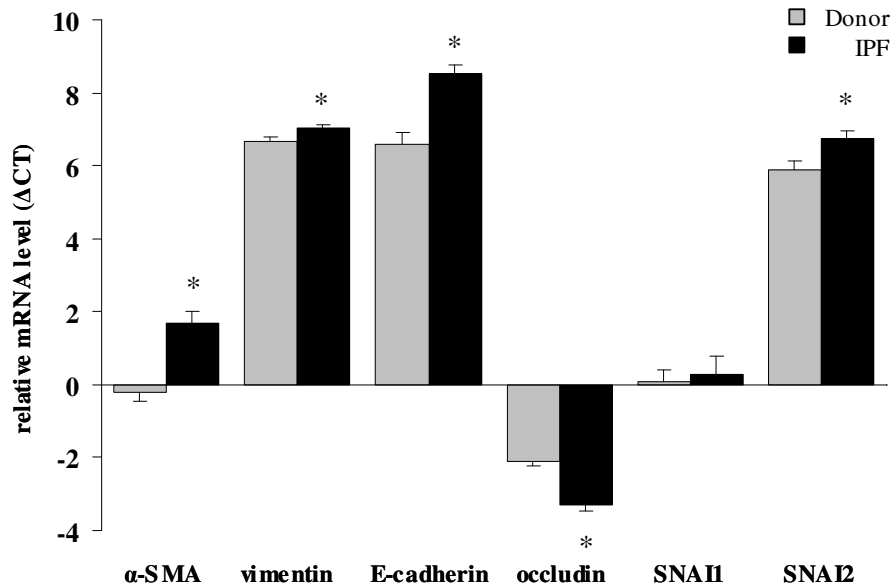


**Figure 4.11 Expression of EMT markers in IPF.** Expression analysis of EMT marker genes was performed by real-time RT-PCR analysis of total RNA derived from lung biopsies of twelve patients with IPF or nine control subjects. Data are expressed as mean  $\pm$  SEM; \*  $p < 0.05$ .

In order to investigate the occurrence of EMT in IPF, real-time RT-PCR was performed and expression profiles of various EMT markers in lung homogenates obtained from nine control subjects and twelve IPF lungs (UIP pattern) were compared. As depicted in Figure 4.11, real-time RT-PCR revealed significant upregulation of  $\alpha$ -SMA and vimentin in total lung homogenates from IPF patients compared with control subjects. Significant downregulation of occludin in IPF patients compared to control subjects was also observed. However an increase in E-cadherin expression in IPF patients was detected.

To gain additional insight into the possible role of SNAI1 and SNAI2 in EMT during IPF, SNAI gene expression was investigated in IPF by comparing mRNA expression in lung homogenates obtained from nine control subjects and twelve IPF lungs (UIP pattern). Real-time RT-PCR showed significant increased levels of SNAI2 gene expression in total lung homogenates from IPF patients compared with control subjects. No significant changes were noted in SNAI1 gene expression levels between IPF and control subject lung homogenates.

#### 4.3.2 SNAI gene expression in the lungs of patients with idiopathic pulmonary fibrosis

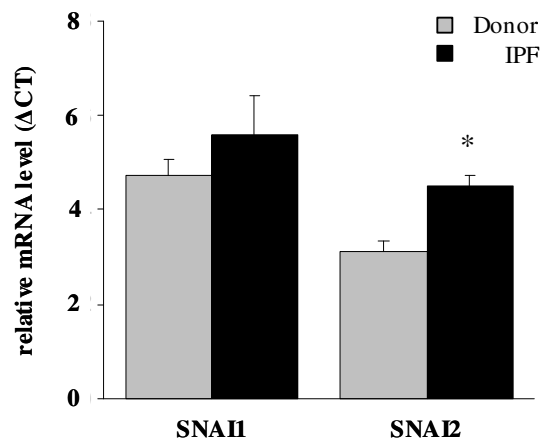


**Figure 4.12 Expression of SNAI genes in IPF.** Expression analysis of EMT marker genes was performed by real-time RT-PCR analysis of RNA derived from microdissected alveolar septae from lung biopsies of twelve patients with IPF or nine control subjects. Data are expressed as mean ± SEM; \* p<0.05.

To determine if alveolar epithelial cells served as the main source of elevated SNAI levels in total lung homogenates of IPF patients, microdissected alveolar epithelial cells were obtained from nine control subjects and twelve IPF lungs (UIP pattern).

Real-time RT-PCR in Figure 4.12, showed elevated levels of SNAI1 and SNAI2 mRNA in the alveolar septae of IPF patients compared to control subjects, however, only expression of SNAI2 was significantly elevated.

### 4.3.3 SNAI protein localization in lungs of patients with idiopathic pulmonary fibrosis

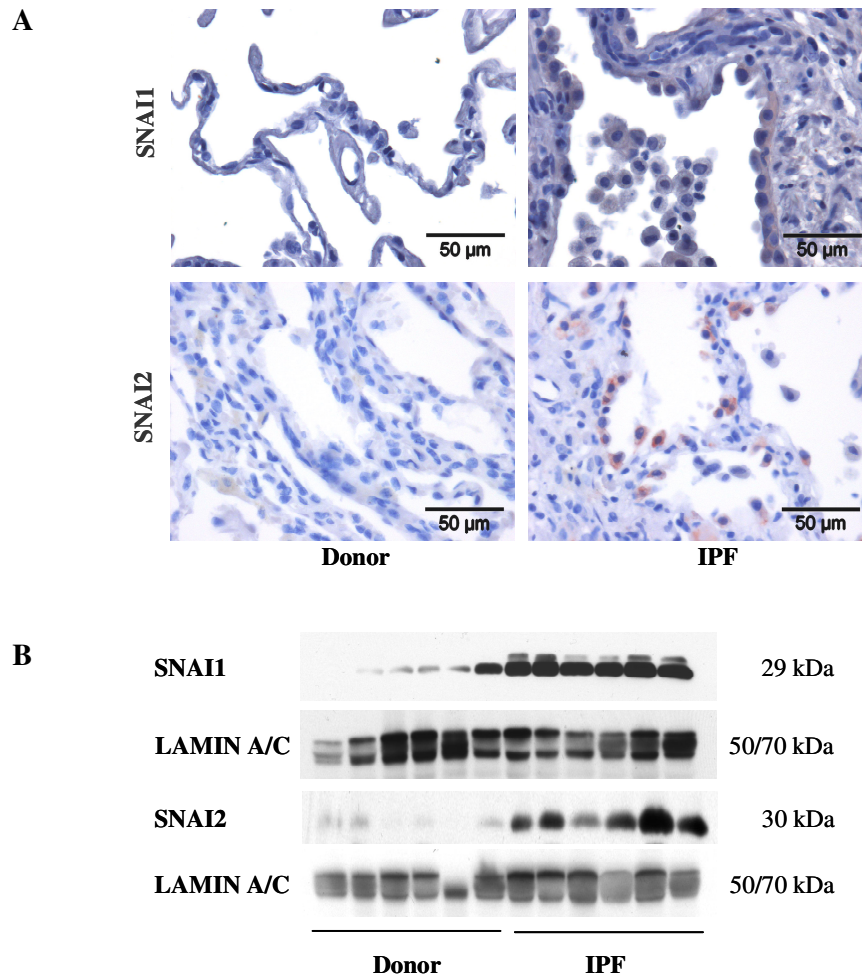


**Figure 4.13 Expression of SNAI protein in IPF.** (A) Immunohistochemical analysis of SNAI1 and SNAI2 localization was performed on paraffin-embedded lung specimens from IPF patients or control subjects. (B) Western blot analysis of SNAI1 and SNAI2 was performed with total lung homogenates obtained from IPF patients and control subjects. Lamin A/C served as the loading control.

In order to analyze the localization pattern of SNAI proteins in IPF, immunohistochemistry was performed. As depicted in Figure 4.13, immunohistochemistry determined localization of SNAI1 and SNAI2 predominantly in



alveolar epithelial cells in IPF lungs. In contrast, the control subject lungs showed very little or no localization of SNAI1 and SNAI2 in alveolar epithelial cells. Subsequently, the expression of SNAI was analyzed at the protein level. Western blot analysis revealed elevated protein levels of both SNAI1 and SNAI2 in total lung homogenates obtained from six IPF patients compared with six control subjects. Lamin A/C served as a loading control.

## 4.4 Functional studies in A549 cells

### 4.4.1 Effect of ectopically-expressed human SNAI1 on EMT marker gene expression in A549 cells

It has been suggested that SNAI transcription factors mediate the transcriptional repression of epithelial markers such as E-cadherin and occludin and thereby triggers EMT. To further investigate whether SNAI1 has a functional role in inducing EMT, the full-length SNAI1 cDNA was cloned into a mammalian expression vectors and A549 cells were transiently transfected for 24 and 48 h.

Next the expression pattern of different epithelial and mesenchymal markers were examined. Real-time RT-PCR revealed downregulation of epithelial markers including E-cadherin and occludin and upregulation of  $\alpha$ -SMA evident 48 h after transfection (Figure 4.14A). Similarly upon SNAI1 overexpression, Western blot analysis indicated a decrease in the protein expression of E-cadherin and occludin and increase in the protein expression of  $\alpha$ -SMA compared to empty vector-transfected control (Figure 4.14B).  $\alpha$ -Tubulin served as a loading control.

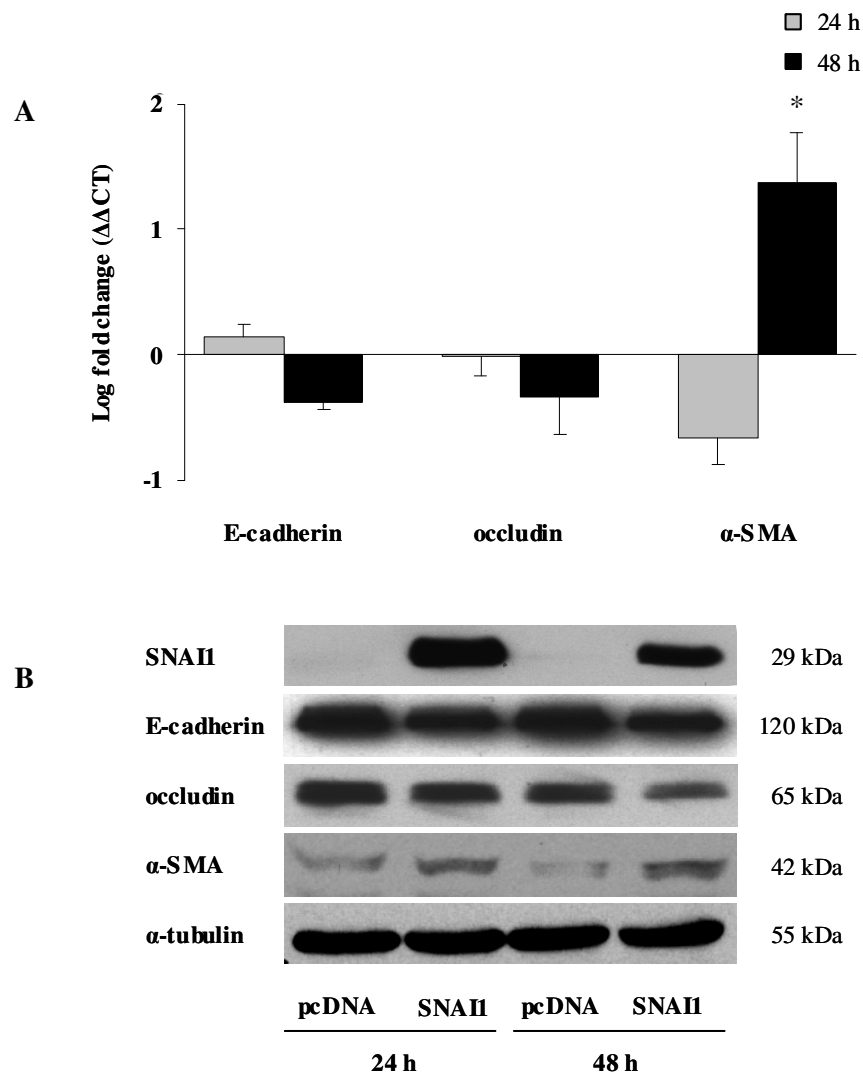


**Figure 4.14 Effect of SNAI1 overexpression on EMT in A549 cells.** EMT marker expression was analyzed by real-time RT-PCR (A) and western blot (B) in A549 cells overexpressing human SNAI1 protein for 24 and 48 h compared to the empty vector control.  $\alpha$ -Tubulin served as the loading control. Data are expressed as mean  $\pm$  SEM; \*  $p < 0.05$ ,  $n = 3$ .

#### 4.4.2 Effect of ectopically-expressed human SNAI2 on EMT marker gene expression in A549 cells

To further test whether SNAI2 induces EMT and also to determine if SNAI2 has a functional role similar to SNAI1 in inducing EMT, the full-length SNAI2 cDNA was

cloned into a mammalian expression vector and A549 cells were transiently transfected for 24 and 48 h. The expression patterns of various epithelial and mesenchymal markers were then evaluated.

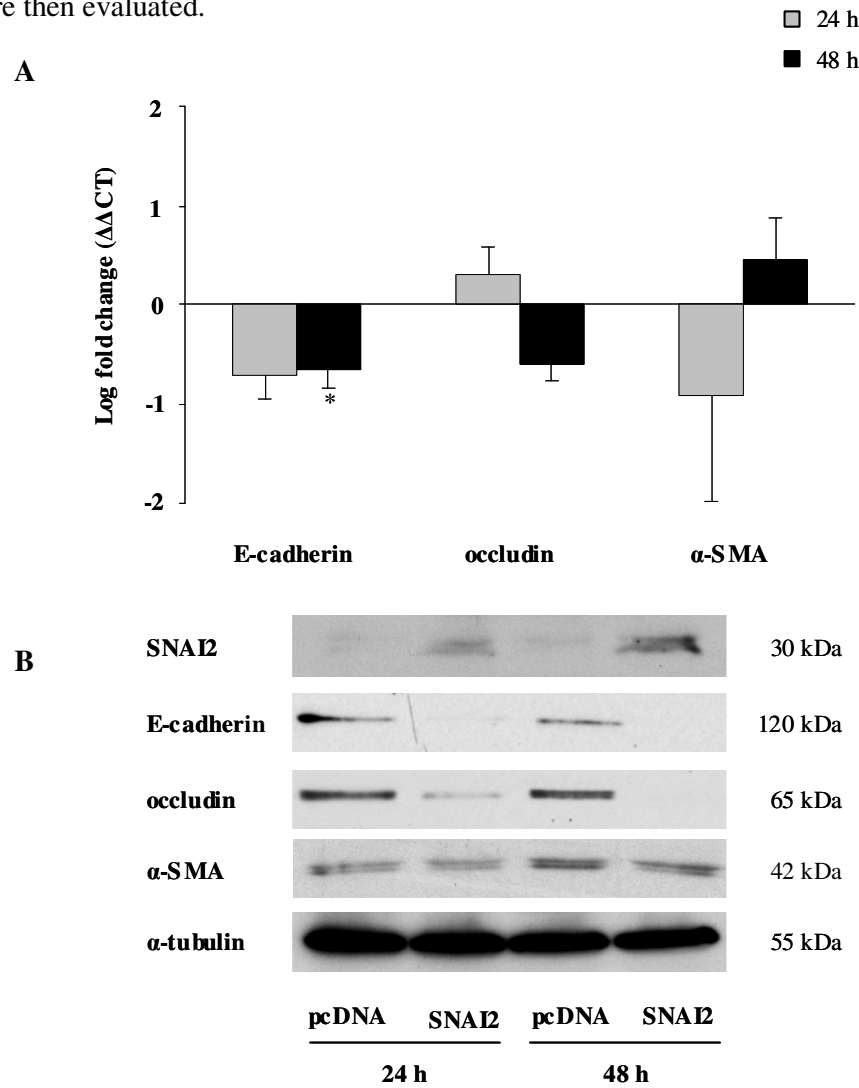


**Figure 4.15 Effect of SNAI2 overexpression on EMT in A549 cells.** EMT marker expression was analyzed by real-time RT-PCR (A) and western blot (B) in A549 cells overexpressing human SNAI2 protein for 24 and 48 h compared to the empty vector control.  $\alpha$ -Tubulin served as the loading control. Data are expressed as mean  $\pm$  SEM; \*  $p < 0.05$ ,  $n = 3$ .

Upon SNAI2 overexpression, real-time RT-PCR revealed downregulation of epithelial markers including E-cadherin and occludin and upregulation of  $\alpha$ -SMA (Figure 4.15A). Decline in E-cadherin level was significant after 48 h of SNAI2 overexpression.

Western blot analysis indicated decrease in the protein expression of E-cadherin and occludin compared to empty vector control (Figure 4.15B). However, no increase in the protein expression of  $\alpha$ -SMA was detected.  $\alpha$ -Tubulin served as the loading control.

#### 4.4.3 siRNA-mediated downregulation of SNAI1 and SNAI2

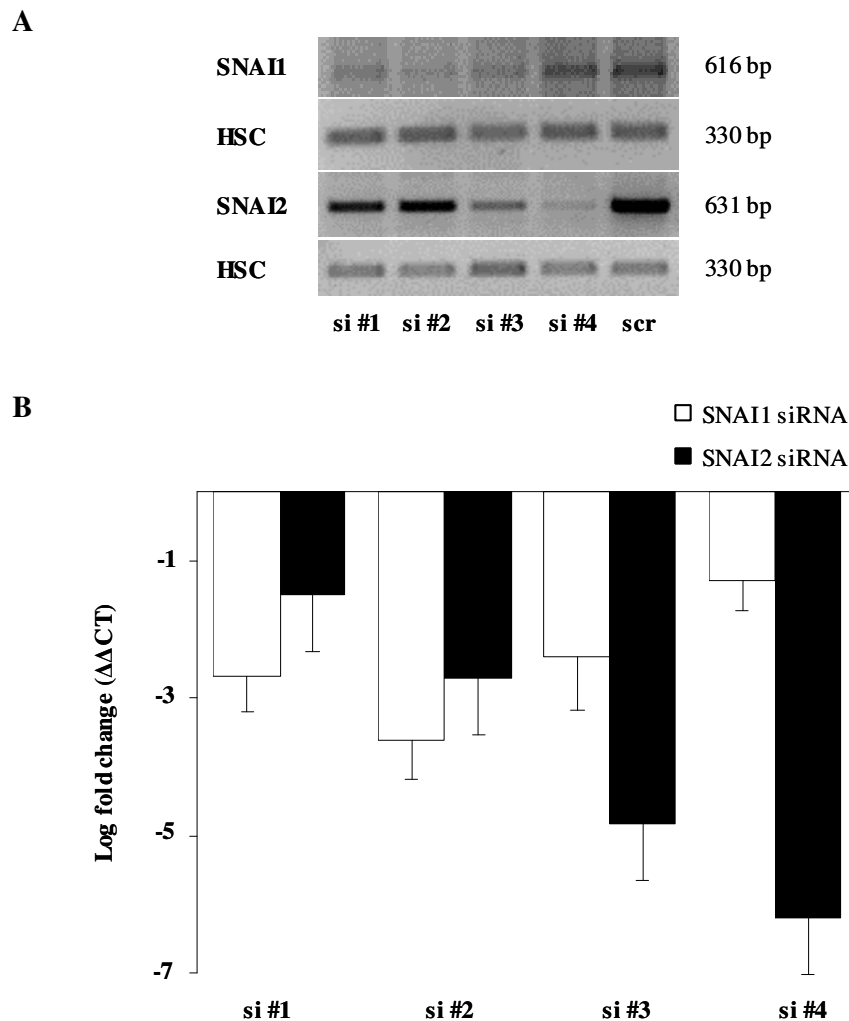


**Figure 4.16** siRNA-mediated downregulation of SNAI1 and SNAI2 expression in A549 cells. (A, B). The mRNA knockdown of four different SNAI1 and SNAI2 siRNA oligonucleotides was assayed by semi-quantitative (A) and real-time (B) RT-PCR. In B, the relative expression of SNAI1 and SNAI2 was normalized for PBGD and expressed as log fold change. scr; scrambled siRNA oligonucleotide.

Whether a direct causal relationship existed between upregulation of SNAI1 or SNAI2 and the process of EMT in A549 cells was next examined. To do so, four different sequences of siRNA oligonucleotides targeting SNAI1 and SNAI2 were initially characterized (Figure 4.16A and B).

Quantitative as well as semi-quantitative RT-PCR analysis revealed that three out of four SNAI1 and SNAI2 siRNA oligonucleotides were effective in reducing the respective mRNA levels in response to TGF- $\beta$ 1 treatment (Figure 4.16A and B). The most effective siRNA oligonucleotides targeting SNAI1 and SNAI2 were then used to examine the effect of SNAI depletion on EMT.

#### 4.4.4 Effect of siRNA-mediated downregulation of SNAI1 on EMT marker gene expression in A549 cells

As depicted in Figure 4.17, SNAI1 depletion effectively inhibited TGF- $\beta$ 1-induced EMT. This was assessed by attenuation of the increase in mesenchymal markers as well as the decrease in epithelial markers. Semi-quantitative RT-PCR (Figure 4.17A) showed that in SNAI1-depleted A549 cells treated with TGF- $\beta$ 1, there was an increase in mRNA levels of E-cadherin and occludin, with a concomitant decrease in the expression of  $\alpha$ -SMA compared to the cells transfected with control non-specific scrambled siRNA. HSC-70 served as the loading control. These observations were confirmed by real-time RT-PCR (Figure 4.17B), which indicated a decline in  $\alpha$ -SMA and vimentin, as well as increase in E-cadherin, occludin and Tjp1 mRNA levels in SNAI1-depleted A549 cells treated with TGF- $\beta$ 1, compared to the control non-specific scrambled siRNA-treated cells.

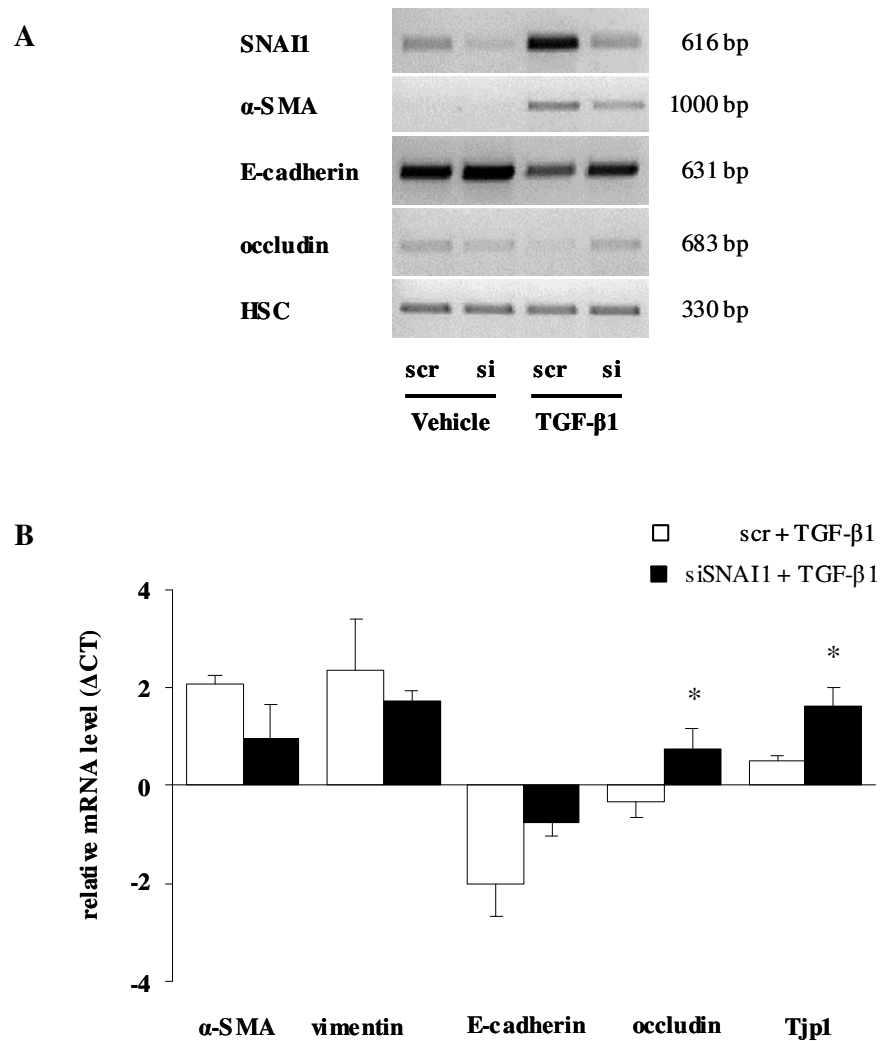


**Figure 4.17 Effect of siRNA-mediated downregulation of SNAI1 expression on TGF- $\beta$ -mediated EMT.** Using semi-quantitative (A) and real-time (B) RT-PCR analysis, the expression patterns of EMT marker genes were assessed in A549 cells after siRNA treatment against SNAI1 with or without TGF- $\beta$  exposures for 24 h. scr, scrambled siRNA oligonucleotide. Data are expressed as mean  $\pm$  SEM; \*  $p < 0.05$ ,  $n = 3$ .

#### 4.4.5 Effect of siRNA-mediated downregulation of SNAI2 on EMT marker gene expression in A549 cells

Next, to evaluate whether silencing of SNAI2 attenuated TGF- $\beta$ 1-mediated EMT, siRNA-mediated knockdown of SNAI2 was performed in A549 cells. The expression of

EMT markers was then assessed. Increases in  $\alpha$ -SMA and vimentin, as well as a decrease in E-cadherin, occludin, and Tjp1 mRNA levels were indicated by both semi-quantitative and real-time RT-PCR (Figure 4.18A and B).

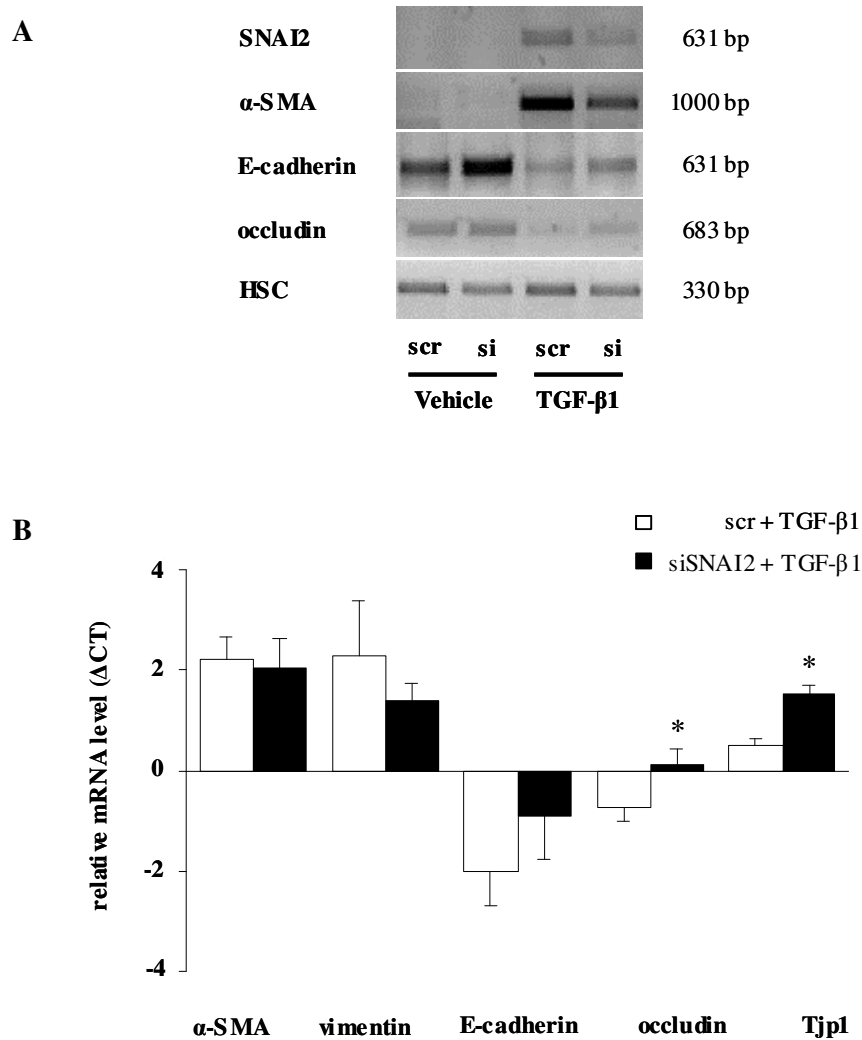


**Figure 4.18 Effect of siRNA-mediated downregulation of SNAI2 expression on TGF- $\beta$ -mediated EMT.** Using semi-quantitative (A) and real-time (B) RT-PCR analysis, the expression patterns of EMT marker genes were assessed in A549 cells after siRNA treatment against SNAI2 with or without TGF- $\beta$  exposures for 24 h. Scr, scrambled siRNA oligonucleotide. Data are expressed as mean  $\pm$  SEM; \*  $p < 0.05$ ,  $n = 3$ .

#### 4.4.6 Role of SNAI1 and SNAI2 in TGF- $\beta$ 1-induced cell migration

One of the consequences of transition from an epithelial to a mesenchymal phenotype is the acquisition of migratory properties. Thus, the migratory potential of A549 cells was measured by performing an *in vitro* migration assay. Twenty four hours of TGF- $\beta$ 1 treatment to cells transfected with non-specific siRNA, led to a four-fold induction of cell migration (Figure 4.19). Silencing of SNAI1 and SNAI2 by siRNA significantly reduced TGF- $\beta$ 1-induced migration in these cells.

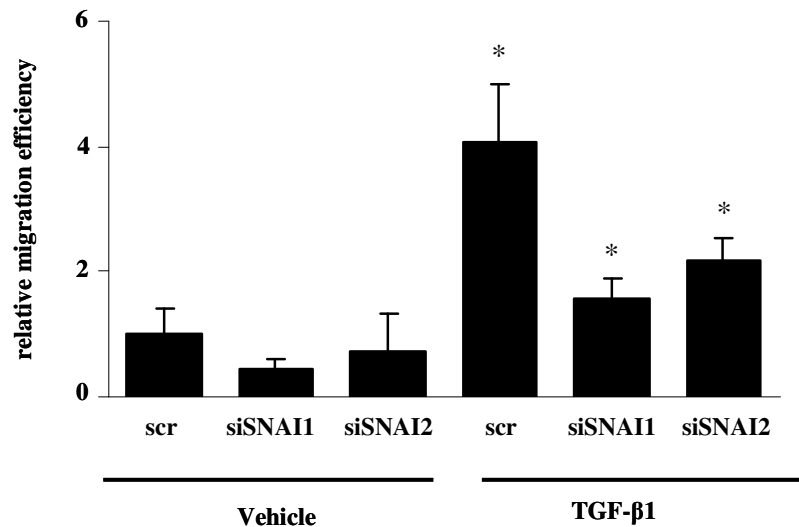


**Figure 4.19 Effect of SNAI1 and SNAI2 on TGF- $\beta$ -induced cell migration.** siRNA-treated A549 cells were treated with or without TGF- $\beta$ 1 for 24 h and the relative migration potential of A549 cells was assessed. scr, scrambled siRNA oligonucleotide. Data are expressed as mean  $\pm$  SEM; \*  $p < 0.05$ ,  $n = 3$ .

### 4.5 Analysis of EMT in unilateral ureteral obstruction model of renal fibrosis

#### 4.5.1 EMT marker expression in a unilateral ureteral model of renal fibrosis

Sperandio et al., investigated the role of inflammatory leukocytes in EMT in neonatal obstructive nephropathy (B. Lange-Sperandio, et al., 2007). The authors



demonstrated that UUO in neonatal mice enhanced leukocyte infiltration, tubular apoptosis and caused EMT in renal fibrosis. Furthermore, they also reported that treatment with BX471, a leukocyte receptor inhibitor, reduced leukocyte infiltration into the obstructed kidney, inhibited tubular apoptosis, atrophy and also decreased interstitial collagen deposition. In collaboration with Sperandio et al., the following experiment was performed: to examine whether EMT occurs in UUO model of renal fibrosis in neonatal mice, EMT markers were assessed, including SNAI transcription factors. To further investigate whether leukocyte recruitment regulated EMT, neonatal mice with UUO were treated with leukocyte receptor blocker BX471.

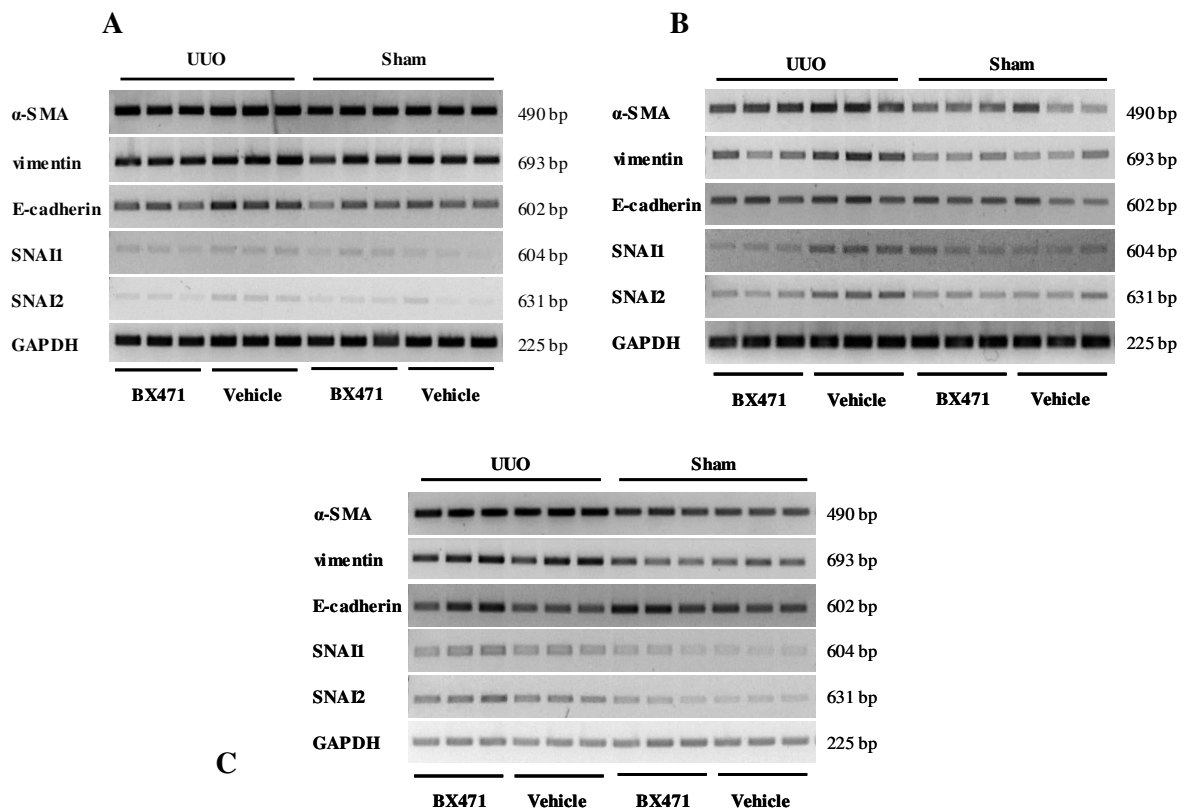


**Figure 4.20 Effect of BX471 on UUO-induced EMT marker expression.** Neonatal mice were subjected to unilateral ureteral obstruction (UUO) or sham operation and treated with BX471 or vehicle, as indicated. Whole kidney extracts were prepared, total RNA isolated, and RT-PCR for the indicated genes performed. RNA profiles were obtained in cohorts that were harvested at days 1 (A), 5 (B) and 14 (C) after UUO or sham operation, respectively.

---

As depicted in Figure 4.20, SNAI1 and SNAI2 expression levels were rapidly increased in obstructed kidneys, as early as day 1 after UUO, compared with sham-treated control. In the presence of BX471, this increase in SNAI1 and SNAI2 mRNA was completely attenuated. Increased expression of  $\alpha$ -SMA and vimentin became evident at day 5 and at day 14 after UUO. Expression of both these mesenchymal markers was attenuated upon BX471 treatment. SNAI1 and SNAI2 expression preceded the induction of  $\alpha$ -SMA and vimentin. Total E-cadherin mRNA abundance in the kidney remained unchanged by BX471 treatment and UUO surgery.

## 5 Discussion

### 5.1 Assessment of EMT in alveolar epithelial cells

#### 5.1.1 TGF- $\beta$ 1 as a potent inducer of EMT

In many organs such as the kidney, liver, and skin, TGF- $\beta$ 1 has been identified as a major inducer of EMT (E.P. Bottinger, et al., 2002, J. Zavadil, et al., 2007, M. Zeisberg, et al., 2007). TGF- $\beta$ 1-driven EMT in AECs is currently the subject of intense research. Initially, the ability of TGF- $\beta$ 1 to promote EMT in AECs was reported *in vitro*, in primary AT2 cell from SD rats (H.W. Yao, et al., 2004). Subsequently, a growing number of studies have demonstrated the occurrence of EMT in TGF- $\beta$ 1-treated AECs from both human and rat origins (H. Kasai, et al., 2005, B.C. Willis, et al., 2005). To date, very little is known concerning the molecular mediators involved in EMT in the lungs. Elucidation of the molecular mediators as well as the underlying mechanism that regulate EMT both *in vitro* and *in vivo* in lungs, is an active area of research.

At the onset of this study, the highest possible purity of freshly-isolated primary mouse AT2 cells could be demonstrated. These cells were responsive to TGF- $\beta$ 1 as they expressed all necessary TGF- $\beta$  signaling components. Upon exposure to TGF- $\beta$ 1, AT2 cells demonstrated an increase in the expression of mesenchymal markers ( $\alpha$ -SMA) with a corresponding decrease in epithelial markers (E-cadherin, and Tjp1), suggestive of EMT. The occurrence of EMT was ultimately reinforced by the presence of  $\alpha$ -SMA and Tjp1 double-positive cells in TGF- $\beta$ 1-treated, but not in untreated cells. Upon TGF- $\beta$ 1 exposure, the expression of epithelial markers was repressed, conversely the expression of mesenchymal markers was induced in AT2 cells. These results in AT2 cells was confirmed in alveolar epithelial A549 cell line, free of fibroblast contamination. Data from the current study indicates that AECs undergo EMT. These findings are in agreement with recent studies reported in A549 cells and primary murine AT2 cells, highlighting the role of TGF- $\beta$ -mediated EMT in alveolar epithelial cells (S. Ando, et al.,

2007, H. Kasai, et al., 2005, J.H. Kim, et al., 2007, K.K. Kim, et al., 2006, B.C. Willis, et al., 2005, H.W. Yao, et al., 2004). Another study previously described that 5 ng/ml of TGF- $\beta$ 1 induced EMT at late time point, 72 h, in primary mouse AT2 cells (S. Ando, et al., 2007). In addition to these previous reports, the current study demonstrates that a low dose of TGF- $\beta$ 1 (2 ng/ml) was sufficient to induce EMT in A549 and primary mouse AT2 cells, and that EMT is an early phenomenon, observed as early as 24 h at the protein level and 2 h at the RNA level, after TGF- $\beta$ 1 stimulation. Real-time RT-PCR illustrated a decline in E-cadherin and an increase in  $\alpha$ -SMA levels in A549 and AT2 cells, respectively. However, these changes were not detectable by semi-quantitative RT-PCR. A possible explanation for this discrepancy in data may be that semi-quantitative RT-PCR is not as sensitive as real-time RT-PCR in detection of gene expression. Recently, TGF- $\beta$ 1-induced EMT has also been demonstrated in triple transgenic mouse model *in vivo* in AECs (K.K. Kim, et al., 2006). Kasai et al., identified that TGF- $\beta$ 1 mediates EMT via Smad2-dependent pathways in A549 cells (H. Kasai, et al., 2005). Further studies will be required to define the mechanism of EMT in AECs.

### 5.1.2 Implication of SNAI in EMT of alveolar epithelial cells

EMT is a complex process involving restructuring the cell cytoskeleton, cell membrane, and cell-cell junction (E.D. Hay, et al., 1995). Previous studies have implicated several regulatory molecules in EMT (M.A. Huber, et al., 2005, J.P. Thiery, et al., 2006). In the present study, a comparison of the gene expression profile of EMT markers in mouse primary AT2 and human A549 cells revealed that TGF- $\beta$ 1 triggered an immediate transcriptional activation of the zinc finger transcription factors SNAI1 and SNAI2 in both cells. TGF- $\beta$ 1 treatment also increased nuclear localization of the zinc finger transcription factors in both cell types.

#### 5.1.2.1 Processes regulating SNAI nuclear localization

The distribution of SNAI1 and SNAI2 are not homogeneous in the nucleus. This is in accordance with previous studies demonstrating the presence of SNAI1 and SNAI2 in discrete foci in the nucleus (D. Dominguez, et al., 2003, K. Hemavathy, et al., 2000).

Nuclear speckles have been identified as sites of active RNA splicing on the basis of their costaining with factor U2AF65 (D. Dominguez, et al., 2003). SNAI1 nuclear translocation is aided by the presence of nuclear export signal. SNAI2 lacks this NES. The SLUG domain, whose function has yet to be identified and may regulate its nuclear translocation.

A recent study suggests that SNAI1 function may be regulated by its intracellular location, as serine phosphorylation-dependent cytoplasmic redistribution of SNAI1 inhibits its activity as a transcriptional repressor (D. Dominguez, et al., 2003). Another study showed that GSK-3 $\beta$  phosphorylation of SNAI1, promotes its degradation and may be another mode of SNAI1 regulation (B.P. Zhou, et al., 2004). SNAI1 is regulated by GSK-3 $\beta$ , which results in either destruction or subcellular localization, depending on which of the two phosphorylation motifs within SNAI1 is targeted. Pak1 phosphorylation also promotes SNAI1's nuclear accumulation and consequently its repressor activity in the nucleus (Z. Yang, et al., 2005). In zebrafish embryos, nuclear localization of SNAI1 is mediated by zinc transporter LIV1 (S. Yamashita, et al., 2004). The stability of SNAI1 is not only controlled by its phosphorylation state but also by its oxidative state, as demonstrated by interaction with LOXL2 and LOXL3 (H. Peinado, et al., 2005). To date, less is known about post-translational regulation of SNAI2. Recently, in *Xenopus*, partner of paired (Ppa) protein has shown to regulate SNAI2 stability and degradation (A.E. Vernon, et al., 2006). Further investigations of SNAI regulation may provide a novel approach for disease prevention and treatment.

#### **5.1.2.2 SNAI transcription factors in TGF- $\beta$ 1-induced EMT**

A direct effect of TGF- $\beta$ 1 signaling on the induction of SNAI1 and SNAI2 was recently demonstrated in MDCKII and MDCK cells, which are canine renal epithelial cell lines (T. Morita, et al., 2007, H. Peinado, et al., 2003). These studies reported that TGF- $\beta$ 1 directly induced SNAI1 or SNAI2 expression by interacting with TGF- $\beta$ 1 response elements located in SNAI promoters. This is in line with the observed elevated expression levels of SNAI upon TGF- $\beta$ 1 stimulation in the current study. Furthermore, SNAI1 and SNAI2 are known to play an important role in the disassembly of cell-cell

junctions namely, adherens junctions, tight junctions and desmosomes, and separation of cells induced by TGF- $\beta$ . In accordance with the present study, elevated levels of SNAI1 were also demonstrated at the RNA level in A549 cells treated with TGF- $\beta$ 1 (J.H. Kim, et al., 2007).

## 5.2 Evidence of EMT in bleomycin mouse model of pulmonary fibrosis

Bleomycin induces peribronchial fibrosis in the mouse, and this recapitulates histological features of human IPF. This disease model has been widely-used as a tool for the study of the pathogenetic mechanisms of IPF. The current study demonstrates the occurrence of EMT in this animal model, with AT2 cells being the key contributors of EMT. Monitoring the expression profile of EMT markers in total lung homogenates by semi-quantitative RT-PCR indicates the occurrence of EMT as early as day 7 post bleomycin administration. However, semi-quantitative RT-PCR failed to detect the elevated levels of mesenchymal markers at days 14 and 21 after bleomycin treatment as observed by real-time RT-PCR. Furthermore, increases in mesenchymal marker were not significant by real-time RT-PCR, and no repression of epithelial markers was observed after bleomycin treatment. Thus, the occurrence of EMT in total lung homogenates of bleomycin-treated mice was not conclusive.

A recent study was unable to detect evidence of EMT by immunohistochemistry in four week and twelve day bleomycin-treated rat and mouse lungs, respectively (K. Barth, et al., 2005). This is consistent with another study, where the authors were also unable to detect EMT by dual-immunohistochemistry in bleomycin-treated mouse lungs (M. Yamada, et al., 2008). These studies suggest that EMT may be a transient phenomenon. Furthermore, the possibility that cells undergoing EMT are rarely found in this animal model cannot be excluded.

However, Wu Z et al., demonstrated that a small subset of bronchiolar and alveolar epithelial cells could convert into myofibroblasts *in vivo*, using an  $\alpha$ -SMA-Cre transgenic mouse treated with bleomycin (Z. Wu, et al., 2007). In agreement with this

---

report, in the present study, isolated AT2 cells were more promising than total lung homogenates from animals treated with bleomycin and provided clear evidence for the occurrence of EMT in the experimental model of lung fibrosis.

### 5.2.1 Implication of SNAI in bleomycin-induced lung fibrosis

Significant changes in SNAI gene expression were observed in the bleomycin model, thereby confirming the importance of these transcription factors in this disease model *in vivo*, as evident *in vitro*, in AECs. In total mouse lung homogenates, elevated levels of both SNAI1 and SNAI2 were demonstrated after bleomycin treatment. Significant elevation in SNAI1 and SNAI2 levels in AT2 cells isolated from bleomycin treated lungs, as early as day 7, as well as increased localization of these key transcription factors in bleomycin treated lung sections implicate SNAI1 and SNAI2 in EMT in this experimental model of fibrosis, early in the disease process.

## 5.3 Assessment of EMT marker expression in idiopathic pulmonary fibrosis

IPF is the most common form of idiopathic interstitial pneumonias, which exhibits a distortion of normal tissue architecture and a loss of lung function. IPF exhibits a poor prognosis and unresponsiveness to currently available therapies, reflecting our limited understanding of the basic mechanisms and mediators implicated in the pathogenesis of this progressive and fatal fibrotic disease (W.D. Travis and T.E. King, Jr, 2002, T.J. Gross, et al., 2001). The typical histological appearance of IPF is called UIP and includes the heterogeneous transformation of normal lung tissue by coexisting emphysematous and fibrotic lesions, as evident by honeycomb cysts and fibroblast foci (A.L. Katzenstein, et al., 1998). These processes lead to an increase in total lung collagen levels with the inability of the lung to properly facilitate gas exchange.

The hallmark lesions of IPF are the fibroblast foci, which are aggregates of activated myofibroblasts promoting excessive ECM deposition. The presence of fibroblast foci is an important prognostic factor and their number has been shown to correlate with survival in IPF (T.E. King, Jr., et al., 2001). Fibroblast foci consistently

occur in the subepithelial layer between areas of collagen deposition and normal alveoli, close to areas demonstrating alveolar epithelial cell injury and repair. In lungs of patients with IPF, these activated myofibroblasts are thought to represent the key cell-type responsible for the enhanced secretion and deposition of ECM. While historically, inflammatory processes were thought to trigger and facilitate the progression of IPF (T.J. Gross, et al., 2001). This monocausal view has recently been questioned, primarily due to the ineffectiveness of anti-inflammatory therapy in IPF (F. Chua, et al., 2005, J. Gauldie, et al., 2002, M. Selman, et al., 2001). Key pathophysiological events in IPF that are currently discussed include local growth factor-dependent fibroproliferation, repetitive alveolar epithelial cell injury with subsequent EMT and fibroblast activation, and trans-differentiation of circulating precursor cells into myofibroblasts, which migrate to the diseased lung (B. Hinz, et al., 2007, B.C. Willis, et al., 2006).

A key question in IPF pathogenesis that remains to be answered is: what is the origin of the activated myofibroblast? Due to the spatio-temporal heterogeneity of IPF, many studies have focused on the analysis of local profibrotic growth factor/cytokine release in the lung, in an attempt to elucidate regulatory factors able to generate activated cell types. In this respect, TGF- $\beta$ 1 has emerged as one of the key profibrotic growth factors in the lung (G.C. Blobe, et al., 2000).

In this current study, significantly elevated levels of  $\alpha$ -SMA and vimentin and a concomitant decline in occludin mRNA levels in total lung homogenates from IPF patients compared with control subjects, suggests the occurrence of EMT in IPF. In agreement with this observation, a recent report by B.C. Willis et al., demonstrated the colocalization of  $\alpha$ -SMA and pro-SP-B or TTF-1 in AECs of IPF patient lung sections (B.C. Willis, et al., 2005). A study by K.K. Kim et al., revealed costaining of pro-SPC and N-cadherin in cells near sites of alveolar collapse and AEC clustering in lung biopsies from IPF patients (K.K. Kim, et al., 2006). These studies provide evidence of EMT in lung tissue biopsies, raising the possibility that this process may contribute to the increased pool of myofibroblasts in lung fibrosis. However, a more recent study failed to identify EMT in pulmonary fibrosis by dual-immunohistochemistry (M. Yamada, et al., 2008). Possible explanations for this apparently discordant observation are that EMT is a



---

very transient process and it is a possibility that epithelial cells in transition may rapidly lose expression of epithelial markers below the level of detection before mesenchymal markers expression is above the level of detection. Thus, the incidence of cells co-expressing epithelial and mesenchymal markers may be underestimated by double immunohistochemistry (M. Yamada, et al., 2008).

Loss of E-cadherin expression is a primal molecular event that contributes to tumor invasion and metastasis (E.M. Fish, et al., 1994). In contrast to the anticipated decrease in expression levels of E-cadherin in IPF patients compared to control subjects, an elevated expression of E-cadherin in IPF patient lung homogenates was observed. A possible explanation is that E-cadherin may be a very robust epithelial cell marker and fibroblast retain the expression of this marker. It will be of interest to examine E-cadherin expression in microdissected alveolar septae from IPF patients.

Does EMT constitute a relevant mechanism for the observed increase in activated myofibroblasts in IPF and other forms of lung fibrosis? This is an essential question of therapeutic relevance, and this study suggests that SNAI-mediated EMT indeed represents an early event of pathophysiological relevance.

### 5.3.1 Implication of SNAI in idiopathic pulmonary fibrosis

Previously, it has been shown that SNAI1-deficient mice die at the gastrulation stage (E.A. Carver, et al., 2001), because of the inability to undergo EMT, reinforcing the importance of the SNAI transcription factors in the process of embryonic development. While the importance of SNAI-mediated EMT has been unequivocally demonstrated in embryonic development and organogenesis, its importance in pathophysiological conditions such as cancer and tissue fibrosis are less well substantiated and require further investigation. In cancer, SNAI family members have been shown to facilitate the delamination of cells from the primary tumor and their metastatic potential (H. Peinado, et al., 2007). Extensive analyses of tumor cell lines and biopsies obtained from primary tumors from the breast, colon, liver, and stomach have confirmed that SNAI plays a pivotal role in progression of cancer (V. Dasari, et al., 2006). Recently, high SNAI expression has been associated with poor prognosis and tumor recurrence in lung cancer

patients (M.L. Lee, et al., 2005, N.K. Kurrey, et al., 2005, T.A. Martin, et al., 2005, J.Y. Shih, et al., 2005). Increasing evidence supports the idea that the *in vivo* action of different SNAI family members in epithelial marker repression can be modulated by their relative concentrations, as well as by specific cellular or tumoral contexts (T.A. Martin, et al., 2005). In tissue fibrosis, SNAI-mediated EMT is suggested to play an important role, wherein SNAI1 is activated in epithelial cells that undergo EMT in renal fibrosis (M. Sato, et al., 2003) and lens cataract formation (S. Saika, et al., 2004), whereas SNAI2 is activated during skin wound healing (P. Savagner, et al., 2005).

However, *in vivo* evidence in lung fibrosis remains modest. The present study, points out a crucial role for SNAI transcription factors in the development of IPF, as elevated levels of SNAI2 were detected both at the RNA and protein levels in total lung homogenates and microdissected alveolar septae from IPF patients compared to control subjects. Elevated protein levels of SNAI1 in homogenates of lung from patients with IPF was also observed, whereas no significant changes were detected at RNA level. However, increased protein expression of both SNAI1 and SNAI2 were detected in the IPF patient lungs compared to control donor lungs. It remains to be seen if these SNAI transcription factors play a specific or redundant role in EMT during IPF.

## 5.4 Analysis of SNAI mediated transcriptional control of EMT in alveolar epithelial cells

By applying both loss-of-function and gain-of-function approaches, the role of these transcription factors in EMT from perspective of carcinogenesis and development, have been extensively examined (E. Batlle, et al., 2000, A. Cano, et al., 2000). However, to date, the role of these transcription factors in AECs is not known and the current study offers new insight into the functional role of SNAI in EMT in AECs.

The data presented here are consistent with the notion that SNAI1 and SNAI2 are essential mediators involved in the initiation and perpetuation of TGF- $\beta$ 1-mediated EMT in the lung. Since EMT could be inhibited in cell culture with siRNA targeting the two key transcription factors SNAI1 and SNAI2, it will have to be demonstrated whether *in vivo* interference with these factors may lead to an attenuation of fibrosis. The current

study offers evidence that SNAI1 and SNAI2 endow cells with capacity to migrate. Previously, our group has determined that TGF- $\beta$  induces migration in AECs (H. Yu, et al., 2008). Recently, SNAI1 RNAi based loss of function studies in A549 cells showed SNAI1 increases chemoresistance of cancer cells to anti-cancer agents (W. Zhuo, et al., 2008). This study did not examine the effect of SNAI silencing on EMT markers. The current study also presents evidence that SNAI1 and SNAI2 induces EMT even in the absence of TGF- $\beta$ 1, hence recapitulating their role as potent inducers of EMT. In accordance to these observations, SNAI1 and SNAI2 have previously been implicated in a central role in the process of EMT in both developmental, as well as in tumoral context in various cultured epithelial cells. In the present study, ectopically-expressed SNAI1 induces complete EMT, whereas, SNAI2 overexpression induces partial EMT by repression of E-cadherin and Occludin expression and no induction in  $\alpha$ -SMA expression. This data suggest that SNAI family members may use different mechanisms to induce EMT, and also suggest the existence of functional differences between SNAI1 and SNAI2 as previously described (H. Peinado, et al., 2005). Further functional analyses *in vivo* may yield diagnostic markers as well as therapeutic approaches.

## 5.5 EMT in a unilateral ureteral obstruction model of renal fibrosis

Tubulo-interstitial fibrosis is a constant feature of chronic renal failure and it is suspected to contribute to the deterioration of renal function. Renal fibrosis is also characterized by exaggerated accumulation and replication of fibroblasts. EMT as a key contributor of myofibroblasts has been well document in kidney fibrosis (R. Kalluri, et al., 2003). Further, using the classical UUO mouse model of renal fibrosis, Iwano et al., demonstrated that the epithelial cells contribute 36% to EMT (M. Iwano, et al., 2002). The current focus is to identify new therapeutics in reversing EMT and thereby attenuating kidney fibrosis. Using the UUO model, another group has also demonstrated reverse MET, the reverse process of EMT by treatment with BMP-7 (M. Zeisberg, et al., 2005).

### 5.5.1 SNAI transcription factors in unilateral ureteral obstruction model of renal fibrosis

Role of SNAI transcription factors have been demonstrated in the kidney. In the current collaborative study, both SNAI1 and SNAI2, key regulators of EMT, rapidly increases in neonatal UUO. These data suggest a close relationship between the degree of leukocyte infiltration and EMT, due to the attenuation in levels of SNAI1 and SNAI2 after leukocyte receptor blocker, (BX471) treatment. Furthermore, detection of high SNAI levels as early as day 1 after UUO indicates that SNAI1 and SNAI2 are early markers of EMT. While elevated levels of mesenchymal markers were evident on day 5 and day 14 after UUO, no changes in the expression of the epithelial marker, E-cadherin were detected at any stage investigated after UUO. However, using immunofluorescence, E-cadherin expression was observed in the intercellular junction area of renal tubules. After UUO, E-cadherin expression strongly decreased in the obstructed kidney over time. Furthermore, treatment with BX471 reduced the loss of E-cadherin in UUO kidneys. The data presented here suggest that EMT occurs in neonatal UUO mice and infiltrating leukocytes induce EMT in neonatal model of renal fibrosis. This study argues for a significant role of infiltrating leukocytes in the induction of EMT and the progression of interstitial fibrosis in congenital obstructive nephropathy.

## 5.6 Conclusions and future perspectives

The key finding of the present study is that TGF- $\beta$ 1 is a potent inducer of EMT in primary mouse alveolar epithelial type II cells and in the human alveolar epithelial A549 cell line. Transcription factors of the SNAI family are key regulators of TGF- $\beta$ 1-induced-EMT, and depletion of SNAI1 and SNAI2 by siRNA technology inhibited EMT in response to TGF- $\beta$ 1. Further, silencing of SNAI transcription factors abrogates the TGF- $\beta$ 1-induced migratory potential of A549 cells. Ectopic expression of SNAI promotes EMT even in the absence of TGF- $\beta$ 1. Elevated expression of SNAI1 and SNAI2 were initially observed *in vitro* and later substantiated *in vivo*, in the bleomycin model of pulmonary fibrosis, early in disease. An increase of SNAI transcription factors

---

was also corroborated in IPF patient lungs compared to control lungs. In sum, this study presents clear *in vitro* and *in vivo* evidence demonstrating that EMT occurs in primary AT2 cells in response to a major profibrogenic cytokine, TGF- $\beta$ 1. It may be speculated that EMT is an early event in tissue fibrosis such as IPF and that activation and nuclear localization of SNAI transcription factors constitutes an important aspect in EMT of alveolar epithelial cells and thus, these findings may be of significance to the field. Furthermore, the detection of SNAI transcription factors early in EMT in a UUO model of renal fibrosis and the inhibition of EMT by leukocyte blocker treatment further emphasizes the significance of SNAI transcription factors in EMT as a causal factor in disease mechanism and also as a potential target to provide either preventive or therapeutic efficacy. This pathway has implications for several active fields of research and may be considered as a potential target of therapeutic interventions.

In the future, using a microarray approach, novel EMT markers in AECs have to be screened. Furthermore, to identify mode of SNAI regulation, a comprehensive investigation of downstream targets and interaction partners of these zinc finger proteins is required. Few post-translational modifications have been reported to regulate SNAI factors and a comprehensive study on SNAI post-translational modifications is an avenue that deserves further examination. The screening and identification of other SNAI family members as causal factors in EMT in lung fibrosis is of immense interest. It is of particular interest to clarify whether SNAI transcription factors are involved in EMT in other animal models of pulmonary fibrosis and also to detect whether lung fibrosis can be induced in conditional SNAI mouse knockout models. It is also essential to elucidate whether TGF- $\beta$ 1 activates SNAI in a Smad-dependent or independent manner. In the near future, it will be imperative to determine whether EMT can be reversed and if so, identification of molecules inhibiting or modulating the SNAI transcription factors may prove to be potentially beneficial in the treatment of IPF.

## 6 Appendix

**Table 6.1 Human RT-PCR primers**

Gene Bank Accession Number	Forward primer (5'-3')	Reverse primer (5'-3')	Annealing Temp. (°C)	Cycle Number	Amplicon Size (bp)
SNAI1 NM_005985	TTTACCTTCCAGCAG CCCTA	TGACATCTGAGTGGG TCTGG	55	28	616
SNAI2 NM_003068	CCATGCCTGTCATAC CACAA	TTGGAGCAGTTTTTG CACTG	55	28	631
$\alpha$ -SMA NM_001613	AGTTATGGTGGGTAT GGGTCAGAA	GAGGGAAGGTGGTTT GGGAGA	62	30	1000
vimentin NM_003380	CGAAAACACCTGCA ATCTT	TCCAGCAGCTTCCTG TAGGT	55	28	693
E-cadherin NM_004351	GGTTCAAGCTGCTGA CCTTC	CTCAAAATCCTCCCT GTCCA	55	28	631
occludin NM_002538	TATGGAGGAAGTGGC TTTGG	TCATTCACCTTGCCA TTGGA	62	30	683
HSC-70 NM_006597	TTACCCGTCCCGATT TGAAGAAC	TGTGTCTGCTTGGA GGAATGGTGGTA	55	22	330

**Table 6.2 Mouse RT-PCR primers**

Gene Bank Accession Number	Forward primer (5'-3')	Reverse primer (5'-3')	Annealing Temp. (°C)	Cycle Number	Amplicon Size (bp)
Smad2 NM_010754	CTCCGGCTGAACTGT CTCCTACT	TTACAGCCTGGTGGG ATCTTACA	60	25	409
Smad3 NM_016769	AGAACGGGCAGGAG GAGAAGTGGT	GGATTTCGGGGAGAGG TTTGAGA	60	25	565
Smad4 NM_008540	ACAGAGAACATTGGA TGGAC	AGTAGCTGGCTGAGC AGTAA	55	28	500
Smad6 NM_008542	GAGCACCCCATCTT CGTCAA	AACAGGGGCAGGAGG TGATG	60	25	234

Smad7 NM_001042660	CCTCCTCCTTACTCC AGATA	ACGCACCAGTGTGAC CGATC	60	28	166
ALK1 NM_009612	AGGGCCGATATGGTG AGGTGTGG	GCCGGTTAGGGATGG TGGGTGTC	58	24	735
ALK5 NM_009370	AGAGCGTTCATGGTT CCGAGAG	GGGGCCATGTACCTT TTAGTGC	59	25	429
TβRII NM_031132	GAGAGGGCGAGGGCG AGGAGTAAAGG	GTGGTAGGTGAGCTT GGGGT	60	24	410/500
SNAI1 NM_011427	CACCCATCTGTTGGA CTCTC	GCCAGACTCTTGGTG CTTGT	58	30	604
SNAI2 NM_011415	AACATTTCAACGCCT CCAAG	CAGTGAGGGCAAGAG AAAGG	58	32	631
α-SMA NM_007392	CTGACAGAGGCACCA CTGAA	CTTCTGCATCCTGTC AGCAA	60	25	490
vimentin NM_0117013	CGCAGCCTCTATTCC TCATC	AGCCACGCTTTCATA CTGCT	58	30	693
E-cadherin NM_009864	AGTTTACCCAGCCGG TCTTT	AGGGTTCCTCGTTCT CCTT	58	30	602
occludin NM_008756	GCTCTCTCAGCCAGC GTACT	AATCATGAACCCAG GACAA	58	30	640
GAPDH NM_008084	ACACATTGGGGGTAG GAACA	AACTTTGGCATTGGA AGG	60	21	225
PBGD NM_001110251	GGTACAAGGCTTTCA CGATCGC	ATGTCCGGTAACGGC GGC	58	23	150

**Table 6.3 Human real-time RT-PCR primers**

Gene Bank Accession Number	Forward primer (5' - 3')	Reverse primer (5' - 3')
SNAI1 NM_005985	TGGGCGCTCCGTA CAC	ACGAGGGAAACGCAC ATCA
SNAI2 NM_003068	GGCAAGGCGTTTCC AGAC	CTCTGTTGCAGTGAG GGCAA
α-SMA NM_001613	CGAGATCTCACTGAC TACCTCATGA	AGAGCTACATAACAC AGTTTCTCCTTGA
vimentin NM_003380	GAGAACTTTGCCGTT GAAGC	TCCAGCAGCTTCCTG TAGGT
E-cadherin NM_004351	ATACACTCTCTTCTC TCACGCTGTGT	ATACACTCTCTTCTC TCACGCTGTGT
occludin NM_002538	GCCGAGGAGCCGGTC TAG	CAGGATGAGCAATGC CCTTT

Tjp1 NM_003257	GAGGAAACAGCTATA TGGGAACAAC	TGACGTTTCCCCACT CTGAAA
PBGD NM_000190	CCCACGCGAATCACT CTCAT	TGTCTGGTAACGGCA ATGCG

**Table 6.4 Mouse real-time RT-PCR primers**

Gene Bank Accession Number	Forward primer (5' - 3')	Reverse primer (5' - 3')
SNAI1 NM_011427	AGCCCAACTATAGCG AGCTG	GGGGTACCAGGAGAG AGTCC
SNAI2 NM_011415	GAAGCCCAACTACAG CGAAC	AGGAGAGTGGAGTGG AGCTG
$\alpha$ -SMA NM_007392	GCTGGTGATGATGCT CCCA	GCCATTCCAACCAT TACTCC
vimentin NM_0117013	TGAAGGAAGAGATGG CTCGT	TCCAGCAGCTTCCTG TAGGT
E-cadherin NM_009864	CCATCCTCGGAATCC TTGG	TTGACCACCGTTCT CCTCC
occludin NM_008756	CCGCCAAGGTTGCT TATC	TCAGGTCTGTAAGGA GGTGGACTT
Tjp1 NM_009386	ACTATGACCATCGCC TACGG	GGGGATGCTGATTCT CAAAA
PBGD NM_001110251	GGTACAAGGCTTTCA CGATCGC	ATGTCCGGTAACGGC GGC

**Table 6.5 Human siRNA sequences**

Gene name	Sense Sequence	Antisense Sequence
SNAI1-si#1	ACUCAGAUGUCAAGAAGUAUU	PUACUUCUUGACAUCUGAGUUU
SNAI1-si#2	GCAAAUACUGCAACAAGGAUU	PUCCUUGUUGCAGUAUUUGCUU
SNAI1-si#3	GCUCGGACCUUCUCCGAAUU	PUUCGGGAGAAGGUCCGAGCUU
SNAI1-si#4	GCUUGGGCCAAGUGCCCAAUU	PUUGGGCACUUGGCCCAAGCUU
SNAI2-si#1	GGACACACAUACAGUGAUUUU	PAAUCACUGUAUGUGUGUCCUU



SNAI2-si#2	UAAAUACUGUGACAAGGAAU	PUCCUUGUCACAGUAUUUAU
SNAI2-si#3	GAAUGUCUCUCCUGCACA AU	PUUGUGCAGGAGAGACAUUCU
SNAI2-si#4	GAAUCUGGCUGCUGUGUAGU	PCUACACAGCAGCCAGAUUCU

**Table 6.6 Primary antibodies used for western blotting (WB), immunohistochemistry (IHC) and immunofluorescence (IF)**

Primary	Host	Dilution			Company	Catalog number
		WB	IHC	IF		
SNAI1	Rat	1:50	1:20		K.F. Becker, et al., 2006	Technical University of Munich
SNAI1	Rabbit	1:100		1:100	Santa Cruz	sc-28199
SNAI2	Mouse	1:300			Cell Signaling	L40C6
SNAI2	Goat		1:100	1:100	Santa Cruz	sc-10437
$\alpha$ -SMA	Mouse	1:300	1:500	1:500	Sigma-Aldrich	A5228
E-cadherin	Mouse	1:500		1:300	BD Biosciences	610181
occludin	Rabbit	1:1000		1:100	Zymed	40-4700
Tjp1	Rabbit			1:100	Zymed	61-7300
proSP-C	Rabbit			1:100	Chemicon	AB3786
lamin A/C	Mouse	1:5000			Santa Cruz	sc-20681
$\alpha$ -tubulin	Mouse	1:5000			Santa Cruz	sc-5286

**Table 6.7 Secondary antibodies used for western blotting, immunohistochemistry and immunofluorescence**

Secondary	Host	Dilution	Company	Catalog number
<b>Western blotting</b>	Rabbit	1:3000	Pierce	31450
HRP-conjugated anti-mouse IgG				

HRP-conjugated anti-rabbit IgG	Goat	1:3000	Pierce	31460
HRP-conjugated anti-rat IgG	Rabbit	1:3000	Pierce	31420
<b>Immunofluorescence</b>	Rabbit	1:300	Zymed	811611
FITC-conjugate anti-goat IgG				
FITC-conjugate anti-mouse IgG	Goat	1:300	Zymed	816511
FITC-conjugate anti-rabbit IgG	Goat	1:300	Zymed	816111
Alexa Fluor 546 anti-mouse IgG	Goat	1:300	Invitrogen	A11030
<b>Immunohistochemistry</b>		Ready to use	Invitrogen	956543B
Biotinylated anti-mouse IgG				
Biotinylated anti-goat IgG				
Broad spectrum		Ready to use	Invitrogen	959743

---

## 7 References

- S. Ando, H. Otani, Y. Yagi, K. Kawai, H. Araki, S. Fukuhara and C. Inagaki. (2007). Proteinase-activated receptor 4 stimulation-induced epithelial-mesenchymal transition in alveolar epithelial cells. *Respir Res.* 8(31).
- K. Ask, P. Bonniaud, K. Maass, O.Eickelberg, P.J. Magetts, D. Warburton, J.Groffen, J. Gauldie and M. Kolb. (2008). Progressive pulmonary fibrosis is mediated by TGF-beta isoform 1 but not TGF-beta 3. *Int J Biochem Cell Biol.* 40(3):484-95.
- A. Barrallo-Gimeno and M.A. Nieto. (2005). The Snail genes as inducers of cell movement and survival: implications in development and cancer. *Development.* 132(14):3151-61.
- K. Barth, J. Reh, A. Sturrock and M. Kasper. (2005). Epithelial vs myofibroblast differentiation in immortal rat lung cell lines--modulating effects of bleomycin. *Histochem Cell Biol.* 124(6):453-64.
- E. Battle, E. Sancho, C. Franci, D. Dominguez, M. Monfar, J. Baulida and A. Garcia De Herreros. (2000). The transcription factor snail is a repressor of E-cadherin gene expression in epithelial tumour cells. *Nat Cell Biol.* 2(2):84-9.
- K. Blechschmidt, I. Mylonas, D. Mayr, B. Schiessl, S. Schulze, K.F. Becker and U. Jeschke. (2006). Expression of E-cadherin and its repressor Snail in placental tissue of normal, preclamptic and HELLP pregnancies. *Virchows Arch.* 450(2):195-202.
- G.C. Blobe, W.P. Schieman and H.F. Lodish. (2000). Role of transforming growth factor beta in human disease. *N Engl J Med.* 342(18):1350-8.
- E.P. Bottinger and M. Bitzer. (2002). TGF-beta signaling in renal disease. *J Am Soc Nephrol.* 13(10):2600-10.
- B. Boyer, A.M. Valles and N. Edme. (2000). Induction and regulation of epithelial-mesenchymal transitions. *Biochem Pharmacol.* 60(8):1091-9.
- T.J. Broekelmann, A.H. Limper, T.V. Colby and J.A. McDonald. (1991). Transforming growth factor beta 1 is present at sites of extracellular matrix gene expression in human pulmonary fibrosis. *Proc Natl Acad Sci U S A.* 88(15):6642-6.

- A. Cano, M.A. Perez-Moreno, I. Rodrigo, A. Locascio, M.J. Blanco, M.G. del Barrio, F. Portillo and M.A. Nieto. (2000). The transcription factor snail controls epithelial-mesenchymal transitions by repressing E-cadherin expression. *Nat Cell Biol.* 2(2):76-83.
- E.A. Carver, R. Jiang, Y. Lan, K.F. Oram and T. Gridley. (2001). The mouse snail gene encodes a key regulator of the epithelial-mesenchymal transition. *Mol Cell Biol.* 21(23):8184-8.
- F. Chua, J. Gauldie and G.J. Laurent. (2005). Pulmonary fibrosis: searching for model answers. *Am J Respir Cell Mol Biol.* 33(1):9-13.
- R.K. Coker, G.J. Laurent, P.K. Jeffery, R.M. du Bois, C.M. Black and R.J. McAnulty. (2001). Localisation of transforming growth factor beta1 and beta3 mRNA transcripts in normal and fibrotic human lung. *Thorax.* 56(7):549-56.
- M. Corti, A.R. Brody and J.H. Harrison. (1996). Isolation and primary culture of murine alveolar type II cells. *Am J Respir Cell Mol Biol.* 14(4):309-15.
- V. Dasari, M. Gallup, H. Lemjabbar, I. Maltseva and N. McNamara. (2006). Epithelial-mesenchymal transition in lung cancer: is tobacco the "smoking gun"? *Am J Respir Cell Mol Biol.* 35(1):3-9.
- R. Derynck and Y.E. Zhang. (2003). Smad-dependent and Smad-independent pathways in TGF-beta family signaling. *Nature.* 425(6958):577-84.
- D. Dominguez, B. Montserrat-Sentis, A. Virgos-Soler, S. Guaita, J. Grueso, M. Porta, I. Puig, J. Baulida, C. Franci and A. Garcia de Herreros. (2003). Phosphorylation regulates the subcellular location and activity of the snail transcriptional repressor. *Mol Cell Biol.* 23(14):5078-89.
- O.Eickelberg and R.E. Morty. (2007). Transforming growth factor beta/bone morphogenic protein signaling in pulmonary arterial hypertension: remodeling revisited. *Trends Cardiovasc Med.* 17(8):263-9.
- E.M. Fish and B.A. Molitoris. (1994). Alterations in epithelial polarity and the pathogenesis of disease states. *N Engl J Med.* 330(22):1580-8.
- C.A. Frolik, L.L. Dart, C.A. Meyers, D.M. Smith and M.B. Sporn. (1983). Purification and initial characterization of a type beta transforming growth factor from human placenta. *Proc Natl Acad Sci U S A.* 80(12):3676-80.

- J. Gauldie, M. Kolb and P.J. Sime. (2002). A new direction in the pathogenesis of idiopathic pulmonary fibrosis? *Respir Res.* 3(1).
- L. Gilboa, R.G. Wells, H.F. Lodish and Y.I. Henis. (1998). Oligomeric structure of type I and type II transforming growth factor beta receptors: homodimers form in the ER and persist at the plasma membrane. *J Cell Biol.* 140(4):767-77.
- G. Greenburg and E.D. Hay. (1982). Epithelia suspended in collagen gels can lose polarity and express characteristics of migrating mesenchymal cells. *J Cell Biol.* 95(1):333-9.
- T.J. Gross and G.W. Hunninghake. (2001). Idiopathic pulmonary fibrosis. *N Engl J Med.* 345(7):517-25.
- A.M. Hales, M.W. Schulz, C.G. Chamberlain and J.W. McAvoy. (1994). TGF-beta 1 induces lens cells to accumulate alpha-smooth muscle actin, a marker for subcapsular cataracts. *Curr Eye Res.* 13(12):885-90.
- S. Harari and A. Caminati. (2005). Idiopathic pulmonary fibrosis. *Allergy.* 60(4):421-35.
- E.D. Hay and A. Zuk. (1995). Transformations between epithelium and mesenchyme: normal, pathological, and experimentally induced. *Am J Kidney Dis.* 26(4):678-90.
- K. Hemavathy, S.I. Ashraf and Y.T. Ip. (2000). Snail/slug family of repressors: slowly going into the fast lane of development and cancer. *Gene.* 257(1):1-12.
- K. Hemavathy, S.C. Guru, J. Harris, J.D. Chen and Y.T. Ip. (2000). Human Slug is a repressor that localizes to sites of active transcription. *Mol Cell Biol.* 20(14):5087-95.
- B. Hinz, S.H. Phan, V.J. Thannickal, A. Galli, M.L. Bochaton-Piallat and G. Gabbiani. (2007). The myofibroblast: one function, multiple origins. *Am J Pathol.* 170(6):1807-16.
- M.A. Huber, N. Kraut and H. Beug. (2005). Molecular requirements for epithelial-mesenchymal transition during tumor progression. *Curr Opin Cell Biol.* 17(5):548-58.
- G.W. Hunninghake, D.A. Lynch, J.R. Galvin, B.H. Gross, N. Muller, D.A. Schwartz, T.E. King, Jr., J.P. Lynch, 3rd, R. Hegele, J. Waldron, T.V. Colby and J.C. Hogg. (2003). Radiologic findings are strongly associated with a pathologic diagnosis of usual interstitial pneumonia. *Chest.* 124(4):1215-23.
- M. Iwano, D. Plieth, T.M. Danoff, C. Xue, H. Okada and E.G. Neilson. (2002). Evidence that fibroblasts derive from epithelium during tissue fibrosis. *J Clin Invest.* 110(3):341-50.

- R. Kalluri and E.G. Neilson. (2003). Epithelial-mesenchymal transition and its implications for fibrosis. *J Clin Invest.* 112(12):1776-84.
- H. Kasai, J.T. Allen, R.M. Mason, T. Kamimura and Z. Zhang. (2005). TGF-beta1 induces human alveolar epithelial to mesenchymal cell transition (EMT). *Respir Res.* 6(56).
- M. Kasper and G. Haroske. (1996). Alterations in the alveolar epithelium after injury leading to pulmonary fibrosis. *Histol Histopathol.* 11(2):463-83.
- A.L. Katzenstein and J.L. Myers. (1998). Idiopathic pulmonary fibrosis: clinical relevance of pathologic classification. *Am J Respir Crit Care Med.* 157(4 Pt 1):1301-15.
- A.L. Katzenstein, D.A. Zisman, L.A. Litzky, B.T. Nguyen and R.M. Kotloff. (2002). Usual interstitial pneumonia: histologic study of biopsy and explant specimens. *Am J Surg Pathol.* 26(12):1567-77.
- M. Kelly, M. Kolb, P. Bonniaud and J. Gauldie. (2003). Re-evaluation of fibrogenic cytokines in lung fibrosis. *Curr Pharm Des.* 9(1):39-49.
- N. Khalil and R. O'Connor. (2004). Idiopathic pulmonary fibrosis: current understanding of the pathogenesis and the status of treatment. *CMAJ.* 171(2):153-60.
- N. Khalil, R.N. O'Connor, K.C. Flanders and H. Unruh. (1996). TGF-beta 1, but not TGF-beta 2 or TGF-beta 3, is differentially present in epithelial cells of advanced pulmonary fibrosis: an immunohistochemical study. *Am J Respir Cell Mol Biol.* 14(2):131-8.
- J.H. Kim, Y.S. Jang, K.S. Eom, Y.I. Hwang, H.R. Kang, S.H. Jang, C.H. Kim, Y.B. Park, M.G. Lee, I.G. Hyun, K.S. Jung and D.G. Kim. (2007). Transforming growth factor beta1 induces epithelial-to-mesenchymal transition of A549 cells. *J Korean Med Sci.* 22(5):898-904.
- K.K. Kim, M.C. Kugler, P.J. Wolters, L. Robillard, M.G. Galvez, A.N. Brumwell, D. Sheppard and H.A. Chapman. (2006). Alveolar epithelial cell mesenchymal transition develops in vivo during pulmonary fibrosis and is regulated by the extracellular matrix. *Proc Natl Acad Sci U S A.* 103(35):13180-5.
- T.E. King, Jr., M.I. Schwarz, K. Brown, J.A. Tooze, T.V. Colby, J.A. Waldron, Jr., A. Flint, W. Thurlbeck and R.M. Cherniack. (2001). Idiopathic pulmonary fibrosis:

- relationship between histopathologic features and mortality. *Am J Respir Crit Care Med.* 164(6):1025-32.
- T.E. King, Jr. (2000). American Thoracic Society. Idiopathic pulmonary fibrosis: diagnosis and treatment. International consensus statement. American Thoracic Society (ATS), and the European Respiratory Society (ERS). *Am J Respir Crit Care Med.* 161(2 Pt 1):646-64.
- N.K. Kurrey, A. K and S.A. Bapat. (2005). Snail and Slug are major determinants of ovarian cancer invasiveness at the transcription level. *Gynecol Oncol.* 97(1):155-65.
- B. Lange-Sperandio, A. Trautmann, O. Eickelberg, A. Jayachandran, S. Oberle, F. Schmidutz, B. Rodenbeck, M. Homme, R. Horuk and F. Schaefer. (2007). Leukocytes induce epithelial to mesenchymal transition after unilateral ureteral obstruction in neonatal mice. *Am J Pathol.* 171(3):861-71.
- T.A. Martin, A. Goyal, G. Watkins and W.G. Jiang. (2005). Expression of the transcription factors snail, slug, and twist and their clinical significance in human breast cancer. *Ann Surg Oncol.* 12(6):488-96.
- J. Massague. (1996). TGFbeta signaling: receptors, transducers, and Mad proteins. *Cell.* 85(7):947-50.
- J. Massague and R.R. Gomis. (2006). The logic of TGFbeta signaling. *FEBS Lett.* 580(12):2811-20.
- B.B. Moore, L. Murray, A. Das, C.A. Wilke, A.B. Herrygers and G.B. Toews. (2006). The role of CCL12 in the recruitment of fibrocytes and lung fibrosis. *Am J Respir Cell Mol Biol.* 35(2):175-81.
- T. Morita, T. Mayanagi and K. Sobue. (2007). Dual roles of myocardin-related transcription factors in epithelial mesenchymal transition via slug induction and actin remodeling. *J Cell Biol.* 179(5):1027-42.
- S.A. Murray and T. Gridley. (2006). Snail family genes are required for left-right asymmetry determination, but not neural crest formation, in mice. *Proc Natl Acad Sci U S A.* 103(27):10300-4.
- M.A. Nieto. (2002). The snail superfamily of zinc-finger transcription factors. *Nat Rev Mol Cell Biol.* 3(3):155-66.

- H. Peinado, M. Del Carmen Iglesias-de la Cruz, D. Olmeda, K. Csiszar, K.S. Fong, S. Vega, M.A. Nieto, A. Cano and F. Portillo. (2005). A molecular role for lysyl oxidase-like 2 enzyme in snail regulation and tumor progression. *EMBO*. 24(19):3446-58.
- H. Peinado, D. Olmeda and A. Cano. (2007). Snail, Zeb and bHLH factors in tumour progression: an alliance against the epithelial phenotype? *Nat Rev Cancer*. 7(6):415-28.
- H. Peinado, F. Portillo and A. Cano. (2004). Transcriptional regulation of cadherins during development and carcinogenesis. *Int J Dev Biol*. 48(5-6):365-75.
- H. Peinado, M. Quintanilla and A. Cano. (2003). Transforming growth factor beta-1 induces snail transcription factor in epithelial cell lines: mechanisms for epithelial mesenchymal transitions. *J Biol Chem*. 278(23):21113-23.
- S.H. Phan. (2002). The myofibroblast in pulmonary fibrosis. *Chest*. 122(6 Suppl):286S-289S.
- R.J. Phillips, M.D. Burdick, K. Hong, M.A. Lutz, L.A. Murray, Y.Y. Xue, J.A. Belperio, M.P. Keane and R.M. Strieter. (2004). Circulating fibrocytes traffic to the lungs in response to CXCL12 and mediate fibrosis. *J Clin Invest*. 114(3):438-46.
- D.C. Radisky. (2005). Epithelial-mesenchymal transition. *J Cell Sci*. 118(Pt 19):4325-6.
- A.B. Roberts. (1998). Molecular and cell biology of TGF-beta. *Miner Electrolyte Metab*. 24(2-3):111-9.
- S. Saika, S. Kono-Saika, Y. Ohnishi, M. Sato, Y. Muragaki, A. Ooshima, K.C. Flanders, J. Yoo, M. Anzano, C.Y. Liu, W.W. Kao and A.B. Roberts. (2004). Smad3 signaling is required for epithelial-mesenchymal transition of lens epithelium after injury. *Am J Pathol*. 164(2):651-63.
- M. Sato, Y. Muragaki, S. Saika, A.B. Roberts and A. Ooshima. (2003). Targeted disruption of TGF-beta1/Smad3 signaling protects against renal tubulointerstitial fibrosis induced by unilateral ureteral obstruction. *J Clin Invest*. 112(10):1486-94.
- P. Savagner. (2001). Leaving the neighborhood: molecular mechanisms involved during epithelial-mesenchymal transition. *Bioessays*. 23(10):912-23.
- P. Savagner, D.F. Kusewitt, E.A. Carver, F. Magnino, C. Choi, T. Gridley and L.G. Hudson. (2005). Developmental transcription factor slug is required for effective re-epithelialization by adult keratinocytes. *J Cell Physiol*. 202(3):858-66.



- B. Schmierer and C.S. Hill. (2007). TGFbeta-SMAD signal transduction: molecular specificity and functional flexibility. *Nat Rev Mol Cell Biol.* 8(12):970-82.
- C.J. Scotton, R.C. Chambers. (2007). Molecular targets in pulmonary fibrosis: the myofibroblast in focus. *Chest.* 132(4):1311-21.
- M. Sefton, S. Sanchez and M.A. Nieto. (1998). Conserved and divergent roles for members of the Snail family of transcription factors in the chick and mouse embryo. *Development.* 125(16):3111-21.
- M. Selman, T.E. King and A. Pardo. (2001). Idiopathic pulmonary fibrosis: prevailing and evolving hypotheses about its pathogenesis and implications for therapy. *Ann Intern Med.* 134(2):136-51.
- M. Selman and A. Pardo. (2003). The epithelial/fibroblastic pathway in the pathogenesis of idiopathic pulmonary fibrosis. *Am J Respir Cell Mol Biol.* 29(3 Suppl):S93-7.
- M. Selman and A. Pardo. (2002). Idiopathic pulmonary fibrosis: an epithelial/fibroblastic cross-talk disorder. *Respir Res.* 3(3).
- M. Selman and A. Pardo. (2006). Role of epithelial cells in idiopathic pulmonary fibrosis: from innocent targets to serial killers. *Proc Am Thorac Soc.* 3(4):364-72.
- J.Y. Shih, M.F. Tsai, T.H. Chang, Y.L. Chang, A. Yuan, C.J. Yu, S.B. Lin, G.Y. Liou, M.L. Lee, J.J. Chen, T.M. Hong, S.C. Yang, J.L. Su, Y.C. Lee and P.C. Yang. (2005). Transcription repressor slug promotes carcinoma invasion and predicts outcome of patients with lung adenocarcinoma. *Clin Cancer Res.* 11(22):8070-8.
- P.J. Sime, Z. Xing, F.L. Graham, K.G. Csaky and J. Gauldie. (1997). Adenovector-mediated gene transfer of active transforming growth factor-beta1 induces prolonged severe fibrosis in rat lung. *J Clin Invest.* 100(4):768-76.
- R.M. Strieter. (2005). Pathogenesis and natural history of usual interstitial pneumonia: the whole story or the last chapter of a long novel. *Chest.* 128(5 Suppl 1):526S-532S.
- P. ten Dijke and C.S. Hill. (2004). New insights into TGF-beta-Smad signalling. *Trends Biochem Sci.* 29(5):265-73.
- V.J. Thannickal, G.B. Toews, E.S. White, J.P. Lynch, 3rd and F.J. Martinez. (2004). Mechanisms of pulmonary fibrosis. *Annu Rev Med.* 55(395-417).
- J.P. Thiery. (2003). Epithelial-mesenchymal transitions in development and pathologies. *Curr Opin Cell Biol.* 15(6):740-6.

- J.P. Thiery and J.P. Sleeman. (2006). Complex networks orchestrate epithelial-mesenchymal transitions. *Nat Rev Mol Cell Biol.* 7(2):131-42.
- W.D. Travis and T.E. King, Jr. (2000). American Thoracic Society/European Respiratory Society International Multidisciplinary Consensus Classification of the Idiopathic Interstitial Pneumonias. This joint statement of the American Thoracic Society (ATS), and the European Respiratory Society (ERS) was adopted by the ATS board of directors, June 2001 and by the ERS Executive Committee, June 2001. *Am J Respir Crit Care Med.* 165(2):277-304.
- I. Vadasz, R.E. Morty, A. Olschewski, M. Konigshoff, M.G. Kohstall, H.A. Ghofrani, F. Grimminger and W. Seeger. (2005). Thrombin impairs alveolar fluid clearance by promoting endocytosis of Na<sup>+</sup>,K<sup>+</sup>-ATPase. *Am J Respir Cell Mol Biol.* 33(4):343-54.
- A.E. Vernon and C. LaBonne. (2006). Slug stability is dynamically regulated during neural crest development by the F-box protein Ppa. *Development.* 133(17):3359-70.
- F. Verrecchia and A. Mauviel. (2007). Transforming growth factor-beta and fibrosis. *World J Gastroenterol.* 13(22):3056-62.
- E.S. White, M.H. Lazar and V.J. Thannickal. (2003). Pathogenetic mechanisms in usual interstitial pneumonia/idiopathic pulmonary fibrosis. *J Pathol.* 201(3):343-54.
- B.C. Willis and Z. Borok. (2007). TGF-beta-induced EMT: mechanisms and implications for fibrotic lung disease. *Am J Physiol Lung Cell Mol Physiol.* 293(3):L525-34.
- B.C. Willis, R.M. duBois and Z. Borok. (2006). Epithelial origin of myofibroblasts during fibrosis in the lung. *Proc Am Thorac Soc.* 3(4):377-82.
- B.C. Willis, J.M. Liebler, K. Luby-Phelps, A.G. Nicholson, E.D. Crandall, R.M. du Bois and Z. Borok. (2005). Induction of epithelial-mesenchymal transition in alveolar epithelial cells by transforming growth factor-beta1: potential role in idiopathic pulmonary fibrosis. *Am J Pathol.* 166(5):1321-32.
- J.L. Wrana and L. Attisano. (2000). The Smad pathway. *Cytokine Growth Factor Rev.* 11(1-2):5-13.
- Z. Wu, L. Yang, L. Cai, M. Zhang, X. Cheng, X. Yang and J. Xu. (2007). Detection of epithelial to mesenchymal transition in airways of a bleomycin induced pulmonary fibrosis model derived from an alpha-smooth muscle actin-Cre transgenic mouse. *Respir Res.* 8(1).

- M. Yamada, K. Kuwano, T. Maeyama, N. Hamada, M. Yoshimi, Y. Nakanishi and M. Kasper. (2008). Dual-immunohistochemistry provides little evidence for epithelial-mesenchymal transition in pulmonary fibrosis. *Histochem Cell Biol.* 129(4):453-62.
- S. Yamashita, C. Miyagi, T. Fukada, N. Kagara, Y.S. Che and T. Hirano. (2004). Zinc transporter LIV1 controls epithelial-mesenchymal transition in zebrafish gastrula organizer. *Nature.* 429(6989):298-302.
- Z. Yang, S. Rayala, D. Nguyen, R.K. Vadlamudi, S. Chen and R. Kumar. (2005). Pak1 phosphorylation of snail, a master regulator of epithelial-to-mesenchyme transition, modulates snail's subcellular localization and functions. *Cancer Res.* 65(8):3179-84.
- H.W. Yao, Q.M. Xie, J.Q. Chen, Y.M. Deng and H.F. Tang. (2004). TGF-beta1 induces alveolar epithelial to mesenchymal transition in vitro. *Life Sci.* 76(1):29-37.
- H. Yu, M. Königshoff, A. Jayachandran, D. Handley, W. Seeger, N. Kaminski, and O. Eickelberg. (2008). Transgelin is a direct target of TGF-beta/Smad3-dependent epithelial cell migration in lung fibrosis. *FASEB J.* 22(6):1778-89.
- J. Zavadil and E.P. Bottinger. (2005). TGF-beta and epithelial-to-mesenchymal transitions. *Oncogene.* 24(37):5764-74.
- J. Zavadil, M. Narasimhan, M. Blumenberg and R.J. Schneider. (2007). Transforming growth factor-beta and microRNA:mRNA regulatory networks in epithelial plasticity. *Cells Tissues Organs.* 185(1-3):157-61.
- M. Zeisberg, A.A. Shah and R. Kalluri. (2005). Bone morphogenic protein-7 induces mesenchymal to epithelial transition in adult renal fibroblasts and facilitates regeneration of injured kidney. *J Biol Chem.* 280(9):8094-100.
- M. Zeisberg, C. Yang, M. Martino, M.B. Duncan, F. Rieder, H. Tanjore and R. Kalluri. (2007). Fibroblasts derive from hepatocytes in liver fibrosis via epithelial to mesenchymal transition. *J Biol Chem.* 282(32):23337-47.
- B.P. Zhou, J. Deng, W. Xia, J. Xu, Y.M. Li, M. Gunduz and M.C. Hung. (2004). Dual regulation of Snail by GSK-3beta-mediated phosphorylation in control of epithelial-mesenchymal transition. *Nat Cell Biol.* 6(10):931-40.
- W. Zhuo, Y. Wang, X. Zhuo, Y. Zhang, X. Ao and Z. Chen. (2008). Knockdown of Snail, a novel zinc finger transcription factor, via RNA interference increases A549 cell

---

sensitivity to cisplatin via JNK/mitochondrial pathway. *Lung Cancer*. (Epub ahead of print) PMID:18372076.

F. Zuo, N. Kaminski, E. Eugui, J. Allard, Z. Yakhini, A. Ben-Dor, L. Lollini, D. Morris, Y. Kim, B. DeLustro, D. Sheppard, A. Pardo, M. Selman and R.A. Heller. (2002). Gene expression analysis reveals matrilysin as a key regulator of pulmonary fibrosis in mice and humans. *Proc Natl Acad Sci U S A*. 99(9):6292-7.

## **8 Declaration**

I declare that I have completed this dissertation single-handedly without the unauthorized help of a second party and only with the assistance acknowledged therein. I have appropriately acknowledged and referenced all text passages that are derived literally from or are based on the content of published or unpublished work of others, and all information that relates to verbal communications. I have abided by the principles of good scientific conduct laid down in the charter of the Justus Liebig University of Giessen in carrying out the investigations described in the dissertation.

## 9 Curriculum vitae

PERSONAL DATA:	
First name:	Aparna
Surname:	Jayachandran
Date of birth:	21 <sup>st</sup> November 1980
Place of birth:	Kozhikode, Kerala, India
Nationality:	Indian
Sex:	Female
Status:	Unmarried
Address:	858-Haus 65, Unterhof 35392 Giessen, Germany
Telephone:	+(49) 17626191571
E-mail:	<a href="mailto:Aparna.Jayachandran@innere.med.uni-giessen.de">Aparna.Jayachandran@innere.med.uni-giessen.de</a> <a href="mailto:aparnajc@gmail.com">aparnajc@gmail.com</a>
Present position:	PhD student (supervisor: Dr. O. Eickelberg) Zentrum für Innere Medizin Medizinische Klinik und Poliklinik II Justus Liebig University Giessen
Institute address:	University of Giessen School of Medicine Department of Medicine II Aulweg 123, Room 6-11, 35392 Giessen, Germany
Telephone:	+(49) 641 9942303

EDUCATION:	
2005 – to date	PhD Student (Supervisor: Dr. O. Eickelberg), PhD programme of the Faculties of Veterinary Medicine and Medicine, Justus Liebig University Giessen
2006 - 2004	International Graduate Program: “Molecular Biology and Medicine of the Lung (MBML)”, “Signaling Mechanisms in Lung Physiology and Disease (SMLPD)” University of Giessen School of Medicine
2004 - 2003	R&D Assistant (Supervisor: Dr. A. Anand), Jawaharlal Nehru Centre for Advanced Scientific Research, Bangalore, India
2003 - 2001	Master of Science Biotechnology, Jnanabharathi Bangalore University Campus, India
2001 - 1998	Bachelor of Science (Biotechnology, Botany, Chemistry), B.M.S. College, Bangalore University, India
1998 - 1996	Pre-University (Physics, Chemistry, Biology, Computer Science), St. Anne’s PU College, Bangalore University, India
1996 - 1986	Matriculation (10 <sup>th</sup> Standard), St. Francis Xaviers Girls’ High School, ICSE, Bangalore, India

PUBLICATIONS:	
1) Lange-Sperandio B, Trautmann A, Eickelberg O, <b>Jayachandran A</b> , Oberle S, Schmidutz F, Rodenbeck B, Hömmer M, Horuk R, and Schaefer F. “Leukocytes induce epithelial to mesenchymal transition after unilateral ureteral obstruction in neonatal	

mice.” <i>Am J Pathol.</i> 2007 Sep; 171(3):861-71
2) Yu H, Königshoff M, <b>Jayachandran A</b> , Handley D, Seeger W, Kaminski N, and Eickelberg O. “Transgelin is a direct target of TGF-beta/Smad3-dependent epithelial cell migration in lung fibrosis.” <i>FASEB J.</i> 2008 Feb; 22(6): 1778-89
3) <b>Jayachandran A</b> , Königshoff M, Yu H, Rupniewska E, Hecker M, Klepetko W, Seeger W, and Eickelberg O. “SNAI Transcription Factors are Key Mediators of Epithelial-to-Mesenchymal Transition in Lung Fibrosis.” (In preparation).
4) Milosevic J, Königshoff M, <b>Jayachandran A</b> , and Eickelberg O. “Rapid loss of the alveolar epithelial cell phenotype during primary culture in a matrix-independent fashion.” (In preparation).

ORAL PRESENTATIONS:
---------------------

- |   |
|---|
| 1) Section Cell Biology DGP Congress 2007: “SNAI transcription factors in epithelial-to-mesenchymal transitions: Comparative analysis of experimental and idiopathic pulmonary fibrosis.”   |
| 2) ATS International Conference 2007: “The zinc finger transcription factor Snail is sufficient to induce Epithelial-to-Mesenchymal Transition: Relevance to Pulmonary Fibrosis.” This abstract was highlighted in the ATS 2007 Conference Final Program as an example of the focus and quality of the original research presented at the conference. |
| 3) Section Cell Biology DGP Congress 2006: “Role of TGF- $\beta$ 1 in epithelial-to-mesenchymal transitions in alveolar epithelial cells.”  |

POSTER PRESENTATIONS:
-----------------------

- |   |
|---|
| 1) <b>Jayachandran A</b> , Königshoff M, Yu H, Rupniewska E, Hecker M, Yu H, Klepetko |
|---|



W, Seeger W, and Eickelberg O. "SNAI transcription factors in epithelial-to-mesenchymal transition: Comparative analysis of experimental and idiopathic pulmonary fibrosis." ECCPS, 29-2 July 2008, Bad Nauheim, Germany.

2) Milosevic J, Königshoff M, **Jayachandran A**, and Eickelberg O. "Rapid loss of the alveolar epithelial cell phenotype during primary culture in a matrix-independent fashion." ATS International Conference, 18-23 May 2007, San Francisco, USA

3) **Jayachandran A**, Königshoff M, Yu H, Rupniewska E, Hecker M, Klepetko W, Seeger W, and Eickelberg O. "The zinc finger transcription factor Snail is sufficient to induce Epithelial-to-Mesenchymal Transition: Relevance to Pulmonary Fibrosis." ICLF, 7-10 September 2006, Mainz, Germany

4) Rupniewska E, Sevilla-Perez J, **Jayachandran A**, Yu H, Dumitrascu R, Seeger W, Grimminger F, Schermuly RT and Eickelberg O. "TGF- $\beta$ -dependent inhibitor of DNA protein (Id) expression in lung fibrosis." European Respiratory Society, 2-6 September 2006, Munich, Germany.

5) **Jayachandran A**, Königshoff M, Yu H, Rupniewska E, Hecker M, Klepetko W, Seeger W, and Eickelberg O. "SNAI transcription factors are key mediators of Epithelial-to-Mesenchymal Transition in lung fibrosis." ATS International Conference, 19-24 May 2006 San Diego, USA

6) **Jayachandran A**, Königshoff M, Yu H, Rupniewska E, Hecker M, Yu H, Klepetko W, Seeger W, and Eickelberg O. "SNAI transcription factors are key mediators of Epithelial-to-Mesenchymal Transition in lung fibrosis." 112<sup>th</sup> Annual Meeting of the German Society of Internal Medicine, 2006, Wiesbaden, Germany

#### SCHOLARSHIPS:

1) Respiratory Cell and Molecular Biology (RCMB) travel grant, American Thoracic Society International Conference (May 2007)

2) Poster travel award, 14th International Colloquium on Lung Fibrosis ICLF

---

(September 2006)
3) Merit Prize for having secured highest grades in MBML Graduate School (2006)
4) Qualified Council of Scientific and Industrial Research, Junior Research Fellow (December 2003)
5) Sir Ratan Tata Merit Scholarship for Post-Graduates (February 2002)
6) Merit Prize for having secured highest grades in Botany, B.M.S. Endowment Trust (1998 - 99)

---

## 10 Acknowledgements

I would like to express my sincere gratitude to my supervisor Dr. Oliver Eickelberg for giving me the opportunity to work in his laboratory and for introducing me to the exciting world of EMT research. I thank him for sharing with me a lot of his expertise and research insights. I appreciate his constant guidance, encouragement, and especially his patience during the entire course of present investigation. During this time, Dr. Eickelberg has helped widen my scientific horizon by given me the opportunity to participate in various international conferences, in collaborative research work, as well as in the transatlantic SMLPD student exchange program. It has been a privilege to be Dr. Eickelberg's student.

I am also very grateful to Prof. Dr. Werner Seeger, for accepting me into the MBML program. I thank my MBML mentors: Dr. O. Eickelberg, Dr. R.E. Morty, Dr. M. Königshoff and Dr. G. Kwapiszewska for their excellent training and effort. I also thank the International PhD program. I am indebted to postdoctoral fellows Dr. M. Königshoff and Dr. H. Yu for their advices regarding scientific problems, generous assistance and active participation in this research work. I also thank M. Hecker and E. Rupniewska for their help in this project. I thank Dr. K.F. Becker for the generous gift of Snail antibody. Special thanks to Dr. R.E. Morty for proof-reading of dissertation. I am grateful to N. Balsara and S. Becker for the German part of my dissertation. I thank all the dedicated molecular biologists at the Eickelberg laboratory and MBML program with whom I have worked and interacted during my four years of research. Special thanks to my lab-friends Darek, Iza and Simone for support and constant entertainment. I am also thankful to all my friends who have made Giessen a special place over all these years.

I thank my family and friends in India for all their love and support. Particularly, thanks to Vijay for enormous amount of faith in me and lots of wise words. I thank Soumya for all emotional support. I thank little Adu for her love and prayers. I express my gratitude to my parents Thankam and Jayan for allowing me to follow my dreams and encouraging me to do my best in all matters of life. To them I dedicate this thesis.